UNIVERSITY OF CALIFORNIA
RIVERSIDE

The Phenology, Biology, Ecology and Genetic Profiling of the Invasive Avocado Lace Bug *Pseudacysta perseae* populations (Hemiptera: Tingidae)

A Thesis submitted in partial satisfaction
of the requirements for the degree of

Master of Science

in

Entomology

by

Lakshmi Paloma Dadlani

June 2024

Thesis Committee:
- Dr. Mark Hoddle, Chairperson
- Dr. Kerry Mauck
- Dr. Thomas Perring
- Dr. Houston Wilson

The Thesis of Lakshmi Paloma Dadlani is approved:

_____

_____

_____

_____

Committee Chairperson

University of California, Riverside

Acknowledgements

I would like to acknowledge the California Avocado Commission (CAC) for providing research and academic funding under Research Agreement number: CAC-65131-00-000.

I am deeply grateful to my principal advisor, Dr. Mark Hoddle, for welcoming me into his laboratory and offering unwavering support throughout my graduate program at UCR. Under his guidance, I have evolved as a researcher and enhanced my skills in science communication. I extend my sincere gratitude to my thesis committee members, Dr. Kerry Mauck, Dr. Thomas Perring, and Dr. Houston Wilson for their invaluable feedback on my thesis chapters along with their advice and guidance in various academic endeavors. I would also like to thank my graduate advisor, Dr. Jessica Purcell for her guidance in ensuring I met my degree requirements on time.

I would like to thank both past and present members of the Mauck Lab and Hoddle Lab, who made me feel welcome and supported my research. I am deeply thankful to Dr. Ivan Milosavljević for performing the statistical analysis and authoring the results section of my first chapter. I am profoundly thankful to Dr. Marco Gebiola for his expert guidance and training in molecular methods for my third chapter, a crucial skill set that promises to be of immense value in my future career endeavors. His ability to help me navigate through challenges and his consistent encouragement, even in the face of mistakes, have been invaluable sources of support and learning. I am immensely grateful to Ruth Amrich for not only being my companion on the monthly field trips to San Diego but also for her invaluable assistance in acquiring the necessary equipment for my experiments. Her expertise and willingness to go above and beyond have been fundamental to the progress of my research journey. I greatly appreciate Mike Lewis for his significant contribution in photographing my research species, which greatly enhanced the credibility of my thesis.

Special thanks to orchard owners, Judy Mackenzie, Van and Laila, Michael Natters and Rick De La O who provided access to study sites in San Diego County and cooperated with our sampling schedule and activities.

Dedication

This thesis is dedicated to my mother, whose faith in my dreams from an early age and continuous support during my academic pursuits have been invaluable.

Table of Contents

List of Figures

List of Tables

Introduction

Avocado, *Perseae americana* Miller (Lauraceae)

Biology and Cultivation

Avocado (*Persea americana* Miller [Lauraceae]) is an evergreen subtropical fruit tree that thrives in subtropical climates characterized by moderate year-round temperatures, regular rainfall (or consistent irrigation), and well-drained soil (Bhore et al., 2021).

Persea americana fruit is distinguished by a high content of healthy fats and an extensive array of nutrients that include significant amounts of vitamins K, C, and B6, as well as minerals such as potassium and folate (Dreher and Davenport, 2013; Fulgoni et al., 2013). Abundant in monounsaturated fatty acids, especially oleic acid, avocados enhance cardiovascular health, are fiber-rich, and potentially aid in weight management and improving metabolic health, contributing to the overall health of those who consume them (Naveh et al., 2002).

P. americana cultivars are classified into three main races, namely West Indian (tropical) Guatemalan (semi-tropical), and Mexican (sub-tropical), areas where this plant is native, which are based on their unique characteristics and environmental adaptability (Bhore et al., 2021). Biology affects cultivation practices; for example, their shallow root systems influence irrigation strategies, and native pollinators which, in turn, affects their adaptiveness to different climate and geographic areas (Crowley, 2007; Madhavi et al., 1995; Schaffer et al., 2012).

P. americana pollination is interesting in that it involves cross-pollination between A-type and B-type flowers which are open during different times of the day. *P. americana* trees are not self-pollinating, and they require cross-pollination between different trees to set fruit. Type A and Type B flowers have different timings for pollen production and receptivity, which facilitates

cross-pollination. *P. americana* trees with Type A flowers open as female in the morning when they are receptive to pollen. These flowers then close around midday and reopen later in the afternoon as male flowers that produce pollen. This sequential timing allows Type A trees to receive pollen from Type B trees when their flowers are open as male and releasing pollen. *P. americana* trees with Type B flowers operate in the opposite manner. They start the day as male, shedding pollen in the morning, and then switch to female in the afternoon when they are receptive to pollen from Type A trees. Bees and other pollinators (e.g., flies and thrips) can transfer pollen from the male-phase flowers of one type to the receptive female-phase flowers of the other type, which promotes successful cross fertilization and fruit set. Planting a mix of Type A (e.g., Hass) and Type B (e.g., Fuerte) *P. americana* trees in close proximity improves the chances of effective pollination and higher fruit production (Stout, 1923; Ish-Am et al., 1999).

U.S. Avocado Production

In the United States, California dominates avocado production, accounting for 90% of the country's total, generating approximately 280 million pounds from 48,000 acres, with an annual value of $487 million (CAC, 2023). The Hass variety of avocados accounts for approximately 94% of California's avocado production due to its consumer-preferred characteristics and longer shelf life, followed by other varieties, such as Lamb Hass, Gem and Fuerte, constituting 3%, 2% 1% of production, respectively (CAC 2023). Florida is the second largest producer, contributing about 9% to the national output, whereas Hawai'i makes up less than 1% of U.S. production (USDA/ERS, 2022).

Arthropod Pests of Avocado in California

Between 1982 and 2004, California saw the establishment of four non-native invasive avocado pests, the red-banded whitefly, *Tetraleurodes perseae* Nakahara (Hemiptera:

Aleyrodidae) (1982), persea mite, *Oligonychus perseae* Tuttle, Baker and Abbatiello (Acari: Tetranychidae) (1990); avocado thrips, *Scirtothrips perseae* Nakahara (Thysanoptera: Thripidae) (1996) and avocado lace bug, *Pseudacysta perseae* Heidemann (Hemiptera: Tingidae) (2004), all of which are native to Mexico. These non-native species were appearing at an interval of roughly every seven years (Hoddle, 2004), suggesting that California may be overdue for the introduction of another invasive pest. These four invasive pest species predominantly feed on avocado leaves and other closely related Lauraceae plants, and are unable to survive and develop on mature avocado fruit. Hence, the probable route of entry into California from Mexico or Central America was through the illegal transportation of avocado plant materials, including branches with leaves and budwood intended for grafting, which served as concealment and reproductive sites for these pests (Hoddle, 2004).

Global Tingidae Species on Avocado

Three species within the genus *Pleseobyrsa*, have been documented with *P. americana* as their host plant: *Pleseobyrsa chiriquensis* Champion, found in Costa Rica, Panama, Colombia, and Venezuela; *Pleseobyrsa boliviana* Drake and Poor, reported in Guatemala; and *Pleseobyrsa persea* Montemayor, identified in Costa Rica (Knudson, 2018). This identification increases the count of Tingidae species in Central and South America known to feed on avocados to four species.

Avocado lace bug, *Pseudacysta perseae* (Heidemann) (Hemiptera: Tingidae)

Phylogenetic Classification of the Family Tingidae

The avocado lace bug, *Pseudacysta perseae*, belongs to the family Tingidae. Tingidae belong to the suborder, Heteroptera; the infraorder, Cimicomorpha and the superfamily Miroidea.

Heteroptera is regarded as one of the most highly diversified clades of hemimetabolous insects constituting >42,000 species (Weirauch et al., 2019). The infraorder, Cimicomorpha constitutes approximately 50 percent of the heteropteran diversity (Schuh & Slater, 1995). Miroidea includes three phytophagous families, Thaumastocoridae (palm bugs) and Miridae (plant bugs) and Tingidae (lace bugs)

Tingidae, the family to which lace bugs belong, get their common name from the lace-like appearance of their wings and in some species, the "lacey-looking" outgrowths of their pronotum as well (Drake and Ruhoff, 1965). Researchers have described tingids from fossils dating back to the Mesozoic (Wappler et al., 2015). Tingidae is a cosmopolitan family accounting for approximately 300 genera with 2,500 species (Guidoti and Guilbert, 2015). Their piercing-sucking mouthparts are adapted for phytophagous feeding, hence some species are employed in agricultural settings to control unwanted weeds (e.g., *Teleonemia scrupulosa* used to control a highly invasive weed, *Lantana camara*) while some are meticulously studied due to their feeding habits that rupture plant cells and cause significant necrotic regions on the leaves which may eventually lead to the defoliation of the tree (e.g., *Corythucha ciliata* targets sycamore trees) (Guidoti and Guilbert, 2015; Simelane and Phenye, 2005; Kezik and Eroğlu, 2014). Many species of tingid have been accidentally introduced in non-native regions and cause economic injury to a numerous of agriculturally important plants including but not limited to avocado, banana, coffee, tea, sugarcane, almond, eggplant, apple, pear, camphor, coconut, cacao, cotton, cassava, black pepper, cherry; numerous species of ornamental shrubs, herbs and spices (Guidoti and Guilbert, 2015; Drake and Ruhoff, 1960). Tingids owe their evolutionary success to their ability to be either monophagous by specializing on a single host plant; or in seldom cases they are oligophagous, feeding on a relatively small group of closely related host plants (Drake and Ruhoff, 1960).

Phylogenetic trees can be extremely helpful in discerning the life history and behavior of pest species. The most controversial phylogenetic relationship of Tingidae within Cimicomorpha throughout evolutionary history has been its relationship with Thaumastocoridae. This has been attributed to multiple factors across various phylogenetic studies since the 1900s including the taxon sample size; the inability to score the morphological characters for all taxa in a dataset; and different methodological and statistical analyses that yield conflicting results or low to moderate support values leading to conjecture about relatedness. The most recent and comprehensive paper by Weirauch et al., 2019 has offered ample support for Tingidae belonging to the monophyletic clade Miroidea. Weirauch et al. (2019) conducted a combined morphological and molecular analyses of 60 families of heteropteran taxa. Within the clade Miroidea, their analysis included three taxa of Thaumastocoridae, three Tingidae and eighteen Miridae. Their analysis showed strong bootstrap support value, 90%, for the placement of Thaumastocoridae within Miroidea; and a sister group relationship to Tingidae + Miridae (Weirauch et al., 2019). The sister-group relationship of Tingidae and Miridae had moderate bootstrap support at 73% (Weirauch et al., 2019). Hence, we can conclude that Miridae (i.e., plant bugs) and Thaumastocoridae (i.e., palm bugs) are the closest living relatives of Tingidae.

Phylogenetic Classification of the Genus, *Pseudacysta*: Sub-Family and Tribal Relationships

Tingidae was first classified by Drake and Davis, 1960 into three subfamilies Vianaidinae, Cantacaderinae, and Tinginae. Vianaidinae consists of approximately ten species and can be easily distinguished from other tingids by the highly modified states of their pronotum, paranota and hemelytron (Guidoti and Montemayor, 2016). Cantacaderinae comprise of 70 species in 15 genera and are characterized by a well-developed exposed clavus, a region of

the hemelytron ("Tingini Report", 2016; Froeschner, 1996). Cantacaderinae was divided into two tribes, namely Cantacaderini and Phatnomini (Guidoti and Guilbert, 2015). Tinginae accounts for most of the lace bug diversity with 2415 species in 25 genera. Tinginae are characterized by a less robust clavus, concealed by the pronotum ("Tingini Report", 2016; Froeschner, 1996). The subfamily, Tinginae is further divided into three tribes: Ypsotingini, Litadeini, and Tingini (Drake and Ruhoff, 1965).

The avocado lace bug, *Pseudacysta perseae*, was originally described by Heidemann in 1908 as *Acysta perseae*. In 1926, Blatchley suggested that *Acysta perseae* was significantly different from the genus *Acysta*, which lead to the description of the genus *Pseudacysta* specifically for this species. *Pseudacysta* is a monospecific genus, containing only this single species. The genus *Pseudacysta* is taxonomically positioned within the subfamily Tinginae and the tribe Tingini ("Tingini Report", 2016). In the tribe Tingini, *Pseudacysta perseae* is distinguished by its diagnostic feature, a reduced sub-pentagonal paranotum (Mead and Peña, 1991). Their paranota are only present as “small ear-like flaps on the humeri” rather than a more developed paranotum of other Tingini (Hurd, 1945).

Distribution and Invasion History

Pseudacysta perseae was originally described from specimens collected in Florida between 1897 and 1907 (Heidemann, 1908). In the early 20th century *P. perseae* was also found in Georgia, Louisiana, and Texas in U.S.A and the east coast of Mexico (Hurd, 1945; Mead and Peña, 1991). For nearly a century, the distribution of this pest was known only from southeastern U.S. and eastern Mexico (Peña, et al., 2007). During the 1990s, there was a notable increase in the occurrence of outbreaks of *P. perseae* in Florida and *P. perseae* has since been discovered in Bermuda in the Atlantic Ocean and on several Caribbean islands (Barbados, British Virgin

Islands, Cuba, Dominican Republic, Jamaica, Puerto Rico, St. Croix, St. Lucia, St. Kitts and Nevis) (Peña, et al., 2007). In the early 2000s, *P. perseae* was documented in northern South America (Venezuela, French Guyana), Central America (Guatemala) and California, U.S. (Peña, et al., 2007; Rugman-Jones et al., 2012).

Pseudacysta persea is an invasive pest in California that was first detected infesting backyard avocados in southern San Diego County in 2004 (Rugman-Jones et al., 2012). Molecular work indicated that this pest likely originated from Las Vivosas, Nayarit, Mexico (west Mexico) (Rugman-Jones et al., 2012). This pest remained at low levels until 2017, when outbreaks were reported in commercial Hass orchards in northern San Diego (2017), Riverside (2017), Los Angeles (2018), Irvine (2022) and Santa Barbara (2023) (Hoddle, 2022). Since 2017, growing concern among growers, pest control advisors, and homeowners has emerged due to the feeding damage to commercially significant Hass avocado trees and the pest's newfound ability to disperse over considerably long distances. Collectively, these observations suggested something fundamental about *P. perseae* in California had changed, either a lag phase had ended, or perhaps, a second invasion by a more "aggressive" genotype had occurred in California.

In 2014, *P. perseae* was discovered in the Euro-Mediterranean region in Portugal (EPPO, 2015). In 2019, it was found causing extensive damage on islands of O'ahu, Hawaii, Kaui and Maui, in Hawai'i, U.S. (Hoddle, 2022), and most recently, in 2023*, P. perseae* was recorded in avocado orchards in Gabon, Africa (Poligui et al., 2023).

Host Plants

The literature highlights avocado trees, *Persea americana* (Lauraceae) as the primary host for *Pseudacysta perseae***.** Although*, P. perseae* can infest multiple species within the

Lauraceae family, such as camphor tree, *Cinnamomum camphora*; red bay, *Persea borbonia*; and swamp red bay, *Persea palustris* (Hoddle et al., 2005; Mead and Peña, 1991).

Biology

Adult *P. perseae* are approximately 2mm long with blackish-brown bodies, exhibiting a flattened appearance, with ridges on their thorax and intricate patterns on their iridescent light amber wings (Hoddle et al., 2005; Moznette, 1922; Sparks et al., 1994). They undergo a hemimetabolous life cycle, lasting 21 to 42 days from egg to adult stage, contingent on temperature, and undergo four instars to reach adulthood (Antun, 1991; Morales et al., 2000). Nymphs have oval-shaped reddish-brown to black bodies that feature several spines around the edges and at various points on their head, thorax, and abdomen (Hoddle et al., 2005; Sparks et al., 1994). *P. perseae* adults and nymphs have specialized mouthparts that allow them to extract sap from the undersides of avocado leaves. Their piercing-sucking mouthparts penetrate the cuticle and upper epidermis to target the palisade parenchyma, thereby causing chlorosis and stippling on the foliage (Braman et al., 2013).

Pseudacysta perseae exhibits sexual dimorphism, allowing for differentiation between males and females through the terminal segment of their abdomen; males possess an oblong terminal segment with small pygophores on each side, while females exhibit a rounded terminal segment. Female *P. perseae* lay exhibit a specialized oviposition behavior, laying their eggs on the undersides of avocado leaves. Using their ovipositor, they strategically deposit eggs in protected areas, adjacent to leaf veins, to enhance the eggs' survival chances (Guidoti et al., 2015). *P. perseae* often smear fecal matter around the surface of their deposited eggs, a behavior seen in other species, serving multiple functions. Primarily, it acts as a sealant, safeguarding the eggs from desiccation and moisture (Livingstone and Yacoob, 1987). While this smearing does

not deter parasitoids and can be easily washed away, fresh fecal matter does not attract fungi. However, dense fungal growth is frequently observed around the oviposition site post-hatching (Livingstone and Yacoob, 1987).

Damage and Economic Loss

Pseudacysta perseae has been the focus of increasing scrutiny due to its economic impact on avocado orchards. Since the early 2000s, *P. perseae* has emerged as a significant economic problem in Florida and the Dominican Republic, where they occasionally cause severe infestations leading to tree defoliation (Hoddle et al., 2005). More recently, since the 2019 invasion into O'ahu, Hawai'i, it has had devastating impacts on avocado orchards across four Hawai'ian islands (Lyte, 2021). Large infestations of *P. perseae* can have direct detrimental effects on avocado leaves, and indirectly by affecting yield and quality of fruit (Hoddle et al., 2007; Byrne et al., 2010). In a study examining the impact of lace bug damage on avocado leaves, it was found that photosynthetic activity decreased by approximately 50% in leaves that experienced 40% or more damage, compared to undamaged leaves (Peña et al., 1998). Research has also demonstrated that the impact of lace bug infestations on avocado yield can vary depending on the cultivar, with differences in susceptibility to infestations leading to corresponding variations in fruit yield (Peña et al., 1998).

Chemical Control

Among six evaluated insecticides, carbaryl, imidacloprid, and fenpropathrin have shown the highest effectiveness against *P. perseae* nymphs (Humeres et al., 2009a). Imidacloprid and carbaryl maintained efficacy for up to 112 days post-treatment, and fenpropathrin's effectiveness dropped after 77 days (Humeres et al., 2009a). However, use of some carbamates, such as carbaryl, and pyrethroids, such as fenpropathrin, are restricted due to their high toxicity to natural

enemies and negative environmental impacts (Dreistadt, 2014). Systemic insecticides recommended for use against lace bugs include dinotefuran, imidacloprid, and the organophosphate acephate, can provide season-long control with proper application. Studies on imidacloprid and dinotefuran uptake in avocado trees demonstrated that older leaves retain more insecticide, i.e. leaf tissue present on trees during insecticide treatments accumulates higher concentrations of chemicals than newly developing foliage, highlighting the critical importance of treatment timing to maximize impact on target pests (Byrne et al., 2009).

Conventional chemical control methods that are highly persistent are not recommended to treat low populations of *P. perseae* (Bender et al., 2007). For increasing populations expected to cause significant damage, it is advised to use insecticidal soaps, narrow-range oils, neem oil (extracted from neem seeds), azadirachtin (a.i. from neem oil), and pyrethrins, applying them thoroughly to the underside of leaves (Bender et al., 2007; Dreistadt, 2014). These methods are not only compatible with integrated pest management (IPM) principles but also have minimal toxicity to humans and low impact on natural predators (Bender et al., 2007).

Contact insecticides like pyrethrin mixtures were most effective against *P. perseae* nymphs, followed by potash soap and petroleum oil, with highly refined narrow range petroleum oil being highly effective on contact but fail as residual treatments (Humeres et al., 2009). In a predator bioassay, petroleum oil also resulted in the highest mortality of green lacewing larvae, *Chrysoperla rufilabris* (Burmeister) (Neuroptera: Chrysopidae), an important natural enemy of *P. perseae* (Humeres et al., 2009). Pyrethrin sprays and certain narrow-range oils are organically acceptable methods of control (Morse et al., 2017). Other contact insecticides, such as spinosad and abamectin, have been deemed ineffective, potentially due to *P. perseae's* feeding behavior or the mode of action of these insecticides (Humeres et al., 2009).

Biological Control

Laboratory studies demonstrated the efficacy of various natural enemies for controlling *P. perseae*, with second instar *C. rufilabris* identified as the most effective predator, by inflicting significant mortality across all *P. perseae* life stages (60-96%) (Humeres et al., 2009). Adult predatory thrips, *Franklinothrips orizabensis* (Johansen) (Thysanoptera: Aeolothripidae), showed a moderate success rate, killing 60% of early *P. perseae* instars but proving less effective against older nymphs and adults (Humeres et al., 2009). The predaceous mite, *Neoseiulus californicus* was the least effective, showing minimal control on *P. perseae* eggs, with limited predator activity observed near egg masses and no evidence of egg predation (Humeres et al., 2009). There are no field surveys to demonstrate how effective these natural enemies are at controlling *P. perseae* populations.

The primary biological control agents associated with *P. perseae* in Florida are two egg parasitoid species in the families Trichogrammatidae and Mymaridae which cause an estimated mortality of 16- 90% in the field (Hoddle et al., 2005; Peña et al., 2012). Other natural enemy species associated with *P. perseae* field populations include lady beetles, jumping spiders, and mirids, such as assassin bugs and pirate bugs (Dreistadt, 2014). Entomopathogenic fungal spray treatments with *Beauveria bassiana*, *Lecanicillium lecanii* and *Metarhizium anisopliae* has been reported to significantly reduce populations of *P. perseae* in Florida, Cuba, and Mexico (Peña et al., 1998; Cambero-Ayón et al., 2019; Romero and Ravelo, 2020).

Objectives of the Present Study

With respect to California and the relatively recent irruption and spread of *P. perseae* in 2017, knowledge gaps were identified regarding the effects of temperature on the development and reproductive biology of *P. perseae*, population dynamics of these more damaging populations

and resulting leaf damage from feeding, natural enemy associations in commercial Hass avocado orchards, use preferences across different avocado cultivars, and the distribution of haplotypes present in California in both native and invaded regions. Work presented in this thesis investigated these critical areas with the aim of better equipping the California avocado industry with updated information on the biology, phenology, damage, and natural enemy associated so that more effective management strategies for this pest can be developed within an IPM framework.

In Chapter One, temperature-driven degree-day models were developed to provide insights into how temperature affects the development and survival rates of different *P. perseae* life stages. This work analyzed the effects of six fluctuating temperature profiles (with daily averages of 15°C, 20°C, 25°C, 30°C, 32°C, and 35°C) on the life history traits (i.e., development times and longevity) of *P. perseae*. The aim of this work was to enhance understanding of the role of temperature on the development and reproductive biology, and phenology of *P. perseae*. These data are crucial for developing degree-day models for *P. perseae* and for understanding how high temperature events, such as heat waves and Santa Ana winds may affect pest populations in the field. Degree-day models developed in Chapter 1 provide a tool for predicting temperature-based population growth trajectories which can aid in the optimal timing of management strategies, such as insecticide applications or natural enemy releases, to control damaging populations of *P. perseae* in commercial Hass avocado orchards in California.

Chapter Two investigated *P. perseae* phenology by examining monthly variations in population density and leaf infestation rates of *P. perseae* across four commercial Hass avocado orchards in northern San Diego County (two orchards were in cooler coastal zones and two were in warmer interior regions) over a period of two years on five different avocado cultivars (i.e., Hass, Lamb Hass, Fuerte, Bacon, and Gem). This information will assist in predicting the timing

of population peaks and the likelihood of leaf damage, which will aid in the optimal scheduling of control measures. As part of monthly sampling efforts, densities of generalist predators were monitored to provide insights into the species identities of natural enemies, and the potential level of biological control provided by these biological control agents. Furthermore, leaf area damage from *P. perseae* and the perseae mite, *Oligonychus perseae* (Acari: Tetranychidae), feeding, along with tip burn resulting from too much chloride salt in irrigation water, were estimated using image analysis software to gain insight into the overall necrotic damage on leaves and to quantify the increase in leaf damage by the addition of *P. perseae* to the leaf feeding pest guild. This study took advantage of monthly leaf collections to examine an unusual egg-laying behavior, "egg-dumping," in *P. perseae*, where females oviposit into pre-existing clumps of eggs laid on leaves by conspecifics. “egg-dumping” is a trait observed in sub-social tingids (Tallamy, 1985; Tallamy and Horton, 1990).

In Chapter Three, molecular analyses were carried out to genetically characterize *P. perseae* populations from original infestation zones that established in southern San Diego County (i.e., National City and Chula Vista) sometime around 2004, newly infested groves (*circa* 2017) in northern San Diego, Los Angeles County, and Hawai'i (2019), with additional samples from the presumptive native regions in Florida and México, including Veracruz, Quintana Roo, Colima, and Baja California. These efforts aimed to discern whether new introductions of *P. perseae* had occurred in California sometime around 2017 or if the original population from 2004 exhibited a lag phase (i.e., a delayed expansion) and whether California's more “aggressive” *P. perseae* population had spread to Hawai’i sometime around 2019. Additionally, molecular analyses were conducted on the endosymbiont *Wolbachia*, which influences reproductive compatibility, and this work complemented controlled mating trials between different California *P. perseae* populations. These cross-mating trials were undertaken to determine if reproductive

barriers existed between *P. perseae* populations from the original 2004 invasion areas in southern San Diego County (these still existed and are still restricted to urban avocados and were identified by mitochondrial haplotype) and the new more "aggressive" populations of *P. perseae* infesting commercial avocado orchards in northern San Diego Country (these populations have a distinct mitochondrial haplotype that separates them from the 2004 populations). Mating incompatibility, if it exists, may explain, in part, observed variations in pest severity in different avocado growing areas of California.

References

"Tingini Report". 2016. Integrated Taxonomic Information System. www.itis.gov, CC0. Available at: https://doi.org/10.5066/F7KH0KBK (accessed 13 February 2022)

Antun, A. J. 1991. Presence of the avocado lace bug, *Pseudacysta perseae* (Heidemann) (Hemiptera: Tingidae) in Dominican Republic. *Primera Jornado de Proteccion Vegetal*, University of Santo Domingo, Santo Domingo, Dominican Republic, (Abstract, p. 4).

Bender, G. S., J. G. Morse, M. S. Hoddle, S. H. Dreistadt. 2007. Avocado Lace Bug, Integrated Pest Management for Home Gardeners and Landscape Professionals. *Pest Notes,* University of California Statewide IPM Program, UC ANR Publication 74134.

Bhore, S. J., D. S. Ochoa, A. Al Houssari, A. L. Zelaya, R. Yang, Z. Chen, and E. Eltantawy. 2021. The Avocado (*Persea americana* Mill.): A Review and Sustainability Perspectives. *Preprints* 2021120523.

Braman S. K., S. Nair, E. Carr. 2013. Influence of Temperature, CO_2 Concentration, and Species on Survival and Development of Lace Bugs (Hemiptera: Tingidae). *Journal of Entomological Science* 48(3): 251-254.

Byrne, F. J., E. C. Humeres, A. A. Urena, M. S. Hoddle, and J. G. Morse. 2010. Field evaluation of systemic imidacloprid for the management of avocado thrips and avocado lace bug in California avocado groves. *Pest Management Science* 66: 1129-1136.

Byrne, F. J., J. Morse and R. Krieger. 2009. Evaluation of systemic chemicals for the management of avocado pests. *Pest and Diseases.* Production Research Report, California Avocado Commission, UC Riverside, USA.

CAC. 2023. California Avocado Commission Annual Report 2022. Available online: https://www.californiaavocadogrowers.com/sites/default/files/2022-CAC-Annual-Report-Final.pdf

Cambero-Ayón, C. B., M. Rodríguez-Palomera, A. Robles-Bermúdez, J. M. Coronado-Blanco, C. Rios-Velasco, O. J. Cambero-Campos. 2019. Distribución y enemigos naturales de la chinche de encaje del aguacate *Pseudacysta perseae* (Hemiptera: Tingidae) en Nayarit, México. *Revista Colombiana de Entomología* 45(1): e7811.

Crowley, D. 2007. Managing Soils for Avocado Production and Root Health. *Calif. Avocado Soc. Yearbook* 90: 107-130.

Drake, C. J., and F. A. Ruhoff. 1960. Lace-bug genera of the world (Hemiptera: Tingidae). *Proceedings of the United States National Museum* 112(3431): 1-105.

Drake, C. J., and N. T. Davis. 1960. The morphology, phylogeny, and higher classification of the family Tingidae, including the description of a new genus and species of the subfamily Vianaidinae (Hemiptera: Heteroptera). *Entomologica Americana* 39, 1– 100.

Drake, C. J. and F. A. Ruhoff. 1965. "Lacebugs of the World: A Catalog (Hemiptera: Tingidae)." *Bulletin of the United States National Museum* 243: 1- 634.

Dreher, M. L., and A. J. Davenport. 2013. Hass avocado composition and potential health effects. *Critical Reviews in Food Science and Nutrition* 53: 738- 50.

Dreistadt S. H. 2014. Lace Bugs, Integrated Pest Management for Home Gardeners and Landscape Professionals. *Pest Notes,* University of California Statewide IPM Program, UC ANR Publication 7428.

EPPO, European Plant Protection Organization. 2015. First report of *Pseudacysta perseae* in Madeira (PT): addition to the EPPO Alert List EPPO Reporting Service no. 01 - 2015. No. article: 2015/010. Available online: https://gd.eppo.int/reporting/ (accessed in July 2023).

Froeschner, R. C. 1996. Lace bug genera of the world, I: introduction, subfamily Cantacaderinae (Heteroptera: Tingidae). *Smithsonian Contributions to Zoology* 574:1–43.

Fulgoni, V. L., M. Dreher, and A. J. Davenport. 2013. Avocado consumption is associated with better diet quality and nutrient intake, and lower metabolic syndrome risk in US adults: results from the National Health and Nutrition Examination Survey (NHANES) 2001-2008. *Nutrition Journal* 12: 1.

Guidoti M., Montemayor S. I. 2016. A new macropterous species of a rarely collected subfamily (Heteroptera, Tingidae, Vianaidinae). *Zootaxa* 4150: 185–192.

Guidoti, M., S. I. Montemayor, É. Guilbert. 2015. Lace Bugs (Tingidae). In: Panizzi A., Grazia J. (eds) *True Bugs (Heteroptera) of the Neotropics*. Entomology in Focus, Vol 2. Springer, Dordrecht.

Guilbert, E. 2001. Phylogeny and evolution of exaggerated traits among the Tingidae (Cimicomorpha, Heteroptera). *Zoologica Scripta*, 30: 313– 324.

Guilbert, E. 2004. Do larvae evolve the same way as adults in Tingidae (Insecta: Heteroptera). *Cladistics* 20: 139– 150.

Guilbert, E., J. Damgaard and C. A. D'haese. 2014. Phylogeny of the lacebugs (Insecta: Heteroptera: Tingidae) using morphological and molecular data. *Systemic Entomology* 39: 431-441.

Heidemann, O. 1908. Two new species of North American Tingidae. Proceedings of the *Entomological Society of Washington* 10: 103-108.

Hoddle, M. S. 2004. Invasions of leaf feeding arthropods: why are so many new pests attacking California grown avocados? *California Avocado Society Yearbook* 87: 65–81.

Hoddle, M. S. 2022. Avocado Lace Bug is Continuing to Spread in California. *From the Grove* 12(2): 22-25.

Hoddle, M. S., J. Morse, R. Stouthamer, E. Humeres, G. Jeong, W. Roltsch, G. S. Bender, P. Phillips, D. Kellum, R. Dowell, G. W. Witney. 2005. Avocado lace bug in California. *Calif Avocado Society Yearbook* 88: 67–79.

Hoddle, M., J. Morse, R. Stouthamer. 2007. Biology and management of avocado lace bug in California. *Proceedings of the California Avocado Research Symposium*, pp. 1-11. California Avocado Commission.

Humeres, E. C., J. G. Morse, R. Stouthamer, W. Roltsch, M. S. Hoddle. 2009. Evaluation of natural enemies and insecticides for control of *Pseudacysta perseae* (Hemiptera: Tingidae) on avocados in southern California. *Florida Entomologist* 92(1): 35-42.

Hurd, M. P. 1945. *Generic classification of North American Tingoidea (Hemiptera-Heteroptera)*. Iowa State University.

Ish-Am, G., F. Barrientos-Priego, A. Castañeda-Vildozola, and S. Gazit. 1999. Avocado (*Persea americana* Mill.) pollinators in its region of origin. *Revista Chapingo Serie Horticultura* 5: 137-143.

Kezik, U., and M. Eroğlu. 2014. The Damage of Turkey's new invasive species*, Corythucha ciliata* (Say, 1832) (Hemiptera: Tingidae) in the Eastern Black Sea Region. *Proceedings of Turkey II. Forest Entomology and Pathology Symposium*, pp. 7-9.

Knudson, A. 2018. *The Tingidae (Hemiptera: Heteroptera) of Southern Central America (with an emphasis on Costa Rica)* (Doctoral dissertation, North Dakota State University).

Lis, B. 1999. Phylogeny and classification of Cantacaderini (Hemiptera: Tingoidea). *Annales Zoologici* 49(3): 157–196.

Livingstone, D., and M. H. S. Yacoob. 1987. Biosystematics of Tingidae on the basis of the biology and micromorphology of their eggs. *Proceedings: Animal Sciences* 96: 587-611.

Lyte, B. 2021. *Hawaii's avocado farmers are bracing for a new threat*, *Honolulu Civil Beat*. Available online: https://www.civilbeat.org/2021/12/hawaiis-avocado-farmers-are-bracing-for-a-new-threat/ (accessed on 23 January 2024).

Madhavi, D. L., S. S. Deshpande, D. K. Salunkhe. 1995. *Handbook of Fruit Science and Technology*. CRC Press, Boca Raton.

Mead, F., J. E. Peña. 1991. Avocado lace bug, *Pseudacysta perseae* (Hemiptera: Tingidae). Florida Department Agriculture and Consumer Services, Division of Plant Industry. *Entomology Circular* 346: 4.

Morales, R. L., R. H. Grillo, & R. V. Hernández. 2000. Biology of *Pseudacysta perseae* (Heid.) (Heteroptera: Tingidae) at constant temperature. *Centro Agrícola* 27(3): 39-41.

Morse, J. G., A. Eskalen, B. A. Faber. 2017. Pest Management Guidelines: Avocado, UC Statewide Integrated Pest Management Program. UC ANR Publication 3436.

Moznette, G. F. 1922. *The avocado: Its insect enemies and how to combat them*. No. 1261. US Department of Agriculture.

Naveh, E., M. J. Werman, E. Sabo, I. Neeman. 2002. Defatted avocado pulp reduces body weight and total hepatic fat but increases plasma cholesterol in male rats fed diets with cholesterol. *Journal of Nutrition* 132: 2015-8.

Peña, J. E., Duncan, R.E., Roltsch, W.J., Carrillo, D., 2012. Mortality factors of the avocado lace bug, *Pseudacysta perseae* (Heteroptera: Tingidae), in Florida. *Florida Entomologist* 95(1): 179-182.

Peña, J. E., S. Sundhari, A. Hunsberger, R. Duncan, and B. Schaffer. 1998. Monitoring damage, natural enemies, and control of avocado lace bug, *Pseudacysta perseae* (Hemiptera: Tingidae). *Proceedings of the Florida State Horticultural Society* 111: 330–334.

Peña, J., R. Duncan, W. Roltsch, R. Gagné, and F. Agudelo. 2007. Natural enemies of the avocado lace bug, *Pseudacysta perseae* (Heteroptera: Tingidae) in Florida, USA. *Actas VI Congreso Mundial del Aguacate*, pp. 12-16.

Poligui R. N., L. E. Apinda, H. Nzandi, B. C. Odjele. 2023. Presence of *Pseudacysta perseae* (Heidemann) (Hemiptera: Tingidae) and it relate predatory mirid *Stethoconus praefectus* on *Persea americana* at Franceville, Gabon. *Acta Entomology and Zoology* 4(1): 37-43.

Romero, L. M., and V. H. Ravelo. 2020. The avocado lace bug: *Pseudacysta perseae* (Heid.) (Hemiptera: Tingidae). Bioecology and biological control in Cuba. *Centro Agrícola* 47: 59-62.

Rugman-Jones, P. F., M. S. Hoddle, P. A. Phillips, G. S. Jeong, R. Stouthamer. 2012. Strong genetic structure among populations of the invasive avocado pest *Pseudacysta perseae* (Heidemann) (Hemiptera: Tingidae) reveals the source of introduced populations. *Biological Invasions* 14(6): 1079-1100.

Schaffer, B., Wolstenholme, B. N., Whiley, A. W. 2012. *The Avocado: Botany, Production and Uses*; Eds., 2nd ed. CABI: Cambridge, MA.

Schuh, R.T., and J. A. Slater. 1995. *True Bugs of the World* (Hemiptera: Heteroptera): Classification and Natural History. Cornell University Press, Ithaca, NY.

Simelane, D. O., and M. S. Phenye. 2005. Suppression of growth and reproductive capacity of the weed Lantana camara (Verbenaceae) by *Ophiomyia camarae* (Diptera: Agromyzidae) and *Teleonemia scrupulosa* (Heteroptera: Tingidae). *Biocontrol Science and Technology* 15(2), 153-163.

Sparks, B., S. K. Braman, and Balsdon, J. 1994. *Control of lace bugs on ornamental plants*. Cooperative Extension Service, University of Georgia, College of Agricultural & Environmental Sciences.

Stout, A. B. 1923. A study in cross-pollination of avocado in southern California. *California Avocado Association Annual Report* 8: 29-45.

Tallamy, D. W. 1985. "Egg dumping" in lace bugs (*Gargaphia solani*, Hemiptera: Tingidae). *Behavioral Ecology and Sociobiology* 17: 357-362.

Tallamy, D. W. & L. A. Horton, 1990. Costs and benefits of the egg-dumping alternative in *Gargaphia* lace bugs (Hemiptera: Tingidae). *Animal Behaviour* 39: 352–359.

USDA/ERS. 2022. Avocados: Production, season-average grower price, and value, by state, 1980/81 to date. United States Department of Agriculture, Economic Research Service, Washington, D.C.

Wappler, T., E. Guilbert, C. C. Labandeira, T. Hörnschemeyer, S. Wedmann. 2015. Morphological and Behavioral Convergence in Extinct and Extant Bugs: The Systematics and Biology of a New Unusual Fossil Lace Bug from the Eocene. *PLOS ONE* 10 (8): e0133330.

Weirauch, C., R.T. Schuh, G. Cassis, and W. C. Wheeler. 2019. Revisiting habitat and lifestyle transitions in Heteroptera (Insecta: Hemiptera): insights from a combined morphological and molecular phylogeny. *Cladistics* 35: 67-105.

Chapter 1. The Effects of Fluctuating Temperatures on Life History Parameters of *Pseudacysta perseae* (Hemiptera: Tingidae)

INTRODUCTION

Avocado lace bug (ALB), *Pseudacysta perseae* (Heidemann) (Hemiptera: Tingidae), has a host range that is restricted to plant species in the family Lauraceae (Hoddle, 2004). This tingid has predominantly been observed feeding on avocados (*Persea americana* Miller). The presumed native range of *P. perseae* is thought to include parts of the southeastern United States (e.g., Florida, Georgia and Texas), the Caribbean, Mexico, and Central and South America (Mead and Peña, 1991). *Pseudacysta perseae* was first found in California in 2004, infesting residential avocado trees in southern San Diego County, and was considered a minor pest problem as it failed to spread into commercial avocado production areas. In 2017, *P. perseae* outbreaks were reported for the first time in commercial Hass avocado orchards in northern San Diego and Riverside Counties in California. This pest subsequently spread to Los Angeles (2019), Orange (2022), and Santa Barbara (2023) Counties (Hoddle et al., 2007; Hoddle, 2022a). In 2014, *P. perseae* was found in Portugal on the island of Madeira, threatening the avocado industry in the Euro-Mediterranean region, but may have failed to establish (EPPO, 2015). In 2019, *P. perseae* was found attacking avocado groves on the Hawaiian Islands of O'ahu, Maui, Hawai'i and Kaui (Hoddle, 2022b). In 2023, *P. perseae* was reported in Franceville town in Gabon, Africa, (Poligui et al., 2023).

In the United States, California is the leading producer of avocados with 90% of the production, followed by Florida and Hawai'i (USDA/ERS, 2022). In California, avocados are grown on 19,420 hectares, with the Hass cultivar accounting for 94.17% of the crop and was valued at $458 million (US) in 2022 (CAC, 2023). Female *P. perseae* lay eggs on the underside

of leaves and eggs are often covered in protective black “tar-like” secretion (Hoddle et al., 2005). Adult and nymphal *P. perseae* feed primarily on the undersides of mature leaves. Consequently, economic damage results from feeding damage by adults and nymphs which often manifests as large necrotic islands in the central regions of leaves. Feeding damage may be amplified by pathogenic fungi, *Colletotrichum* spp., that infest leaves through feeding wounds (Mead and Peña, 1991). Consequently, *P. perseae* poses a significant threat to avocado cultivation due to its ability to cause significant levels of damage to foliage which results in reduced photosynthetic capacity and premature abscission of heavily damaged leaves which exposes immature fruit to the sun, causing sunburn. Collectively, these damages accumulate and adversely affect fruit yield. Economic losses are further increased when insecticide applications for reducing damaging populations densities are needed (Peña et al., 1998; Hoddle et al., 2005; Humeres et al., 2009).

Abiotic environmental factors, particularly temperature, influence the development, behavior, reproduction, mortality, phenology, and population dynamics of insects (Pedigo, 1989; Hallman and Denlinger, 1998; Neven, 2000; Nelson et al., 2013). Insects are poikilothermic and important life history functions, like metabolic rates, are affected by ambient temperature (Neven, 2000). Insects can tolerate a wide range of temperature conditions, although their performance, development rate, and reproductive success differs across varying daily temperature profiles (Hallman and Denlinger, 1998). Insight into the influence of temperature on life history parameters for *P. perseae* may enable avocado growers to make informed decisions to manage this invasive pest. For example, the timing of insecticide applications or deployment of biological control agents can be optimized so that vulnerable stages are targeted when they are most abundant. These control decisions can be made with an understanding of how prevailing temperatures are driving development rates and population dynamics. Furthermore, the identification of the upper and lower threshold temperatures for *P. perseae* facilitates ecological

niche modeling that can be used to predict and model the potential expansion of this pest into new geographical areas.

Limited information on the effects of temperature on *P. perseae* development and reproductive biology is available. In the Dominican Republic, *P. perseae* development from egg to adult required 22 days at an average outdoor temperature of 26 ± 2 ºC on the Hass avocado cultivar (Antum, 1991). The developmental times of immature *P. perseae* have been quantified across five (20, 22, 25, 28, and 30ºC) constant temperature conditions (Morales et al., 2000). Under these static temperature conditions, the life cycle of *P. perseae* from egg to adult spans 42 days at 20°C, 34 days at 22°C, 28 days at 25°C, 24 days at 28°C and 21 days at 30°C (Morales et al., 2000). The minimum temperature above which development occurs was identified as 10°C while the upper developmental threshold temperature remains to be established (Morales et al., 2000).

Prevailing ambient outdoor temperatures are not constant and *P. perseae* encounter temperature cycles that fluctuate between daily highs and nighttime lows over any given 24-hour period. Consequently, fluctuating temperature variations may affect development times and survivorship rates when compared to similarly collected data obtained under constant temperature regimes. To date, no studies have investigated the effects of fluctuating temperature cycles which are characteristic of avocado production regions on the life history traits of *P. perseae* (e.g., development time). To address this shortcoming, this study investigated the effects of six fluctuating temperature profiles (i.e., the fluctuating temperature regimens average 15°C, 20ºC, 25ºC, 30ºC, 32 °C and 35°C over a 24-hour period) on selected life history parameters of *P. perseae*. These temperatures are representative of climatic conditions across infested areas in southern California. The intent of this work was to improve understanding of the effects of temperature on *P. perseae* phenology and reproductive biology and provide the necessary

baseline information for the development of degree-day models. When taken together, this information on the effects of temperature on *P. perseae* development and thermal tolerances can support the development of sustainable management strategies for this pest in avocado orchards.

MATERIALS AND METHODS

Source of Experimental *Pseudacysta perseae*

Pseudacysta perseae adults used for experiments were collected from avocado orchards in northern San Diego County. Adult males and females were confined in Munger cells (Munger 1942) on Hass avocado leaves upon which they fed and oviposited. Leaves were collected from unsprayed trees on the UC Riverside campus and were thoroughly washed and dried before use. Munger cells were maintained in a climate-controlled cabinet at a fluctuating temperature that averaged 30°C, 60 ± 5% relative humidity, and a 14:10 h light: dark photoperiod. The progeny of field-collected adult *P. perseae* maintained under these controlled laboratory conditions were used in experiments detailed below.

Experimental Rearing Set-Up and Temperature Cabinet Programing

Pseudacysta perseae were reared on Hass avocado leaves and maintained in an observation arena that was constructed using a modified Munger cell set-up (Figure 1.1). To create the observation arena, earthquake putty (QuakeHold!™ museum putty, Ready America™, San Marcos, CA, USA) was used to secure a Hass avocado leaf to a central Munger cell plate (7.5 cm wide x 10.5 cm long) made of plexiglass, with a central 3 cm diameter hole and two 6 mm diameter aeration holes drilled into the wall of the arena. The central hole allowed access to the avocado leaf on which *P. perseae* were placed. This central portion of the Munger cell with *P. perseae* was sealed with a thin clear plexiglass cover (7.5 x 10.5 cm) to prevent insect escape.

Munger cells attached to avocado leaves with *P. perseae* nymphs were placed on water-saturated foam pads contained within a stainless-steel pan (25 cm x 22 cm x 4 cm) to retain water. Assays with egg-bearing leaves were left uncovered to prevent condensation and excessive fungus growth. As leaves deteriorated, *P. perseae* nymphs and adults were transferred to new Munger cells with fresh Hass avocado leaves using a 0.5 mm camel-hair paintbrush.

Temperature-driven development studies were conducted at six fluctuating temperature profiles that averaged 15°C, 20 °C, 25 °C, 30 °C, 32 °C and 35 °C over a 24-hour period. To achieve the target average temperatures of 15°C, 20°C, 25°C and 30°C, the oscillating temperature cycle used to program climate-controlled cabinets (Darwin Chambers, St. Louis, MO, USA) was modeled using an average of five years (1st January 2017- 31st December 2021) of hourly daily temperature data from the California Irrigation Management Information System (CIMIS) weather station, Escondido SPV #153 in San Diego County, California, USA. For average temperatures of 32°C and 35°C, daily temperature data were obtained from the CIMIS weather station, Borrego Springs #207 in the Imperial/Coachella Valley region in San Diego County for the same five-year period. These temperature data were used to program the climate-controlled cabinets with incremental hourly temperature changes over a 24-hour period to produce each target mean temperature (Table 1.1; CIMIS 2021). Humidity in cabinets was maintained at 60 ± 5% RH which was the average relative humidity recorded in San Diego County (CIMIS 2021). Photoperiod was set at 14:10 h (L:D) with light intensity of 100 μE m−2 s−1 for every experimental temperature profile. To ensure the desired experimental temperature profiles and relative humidity were achieved, HOBO Pro V2 Temperature/RH loggers (Onset Computer, Pocasset, Massachusetts, USA) were programmed to record temperature and humidity at 30-minute intervals inside the climate-controlled cabinets throughout the duration of the

experiment. These data were used to confirm temperature cabinets were performing the programmed temperature cycles.

Quantification of Number of Nymphal Instars and Photo-Documentation of *P. perseae* Life Stages

The number of nymphal instars was quantified at 30°C. The transition from 1st instar to 2nd instar, 2nd instar to 3rd instar and 3rd instar to 4th instar was monitored for 20 specimens under a microscope every 12-14 hours. A clear plastic tray (12 cm x 18 cm x 1.2 cm) with 14 mm circular wells, 18 mm in diameter (Falcon™) was utilized for these studies. Circular Hass avocado leaf disks, 16 mm diameter, excised from whole leaves with a 16 mm cork borer were placed with the lower leaf side facing up on the floor of each well. Each well was inoculated with one first instar nymph and leaf disks were replaced every three days. Observation of an ecdysed exoskeleton indicated when a specimen had advanced to the next instar.

Live specimens of *P. perseae* eggs, instar nymphs, and both male and female adults, were digitally photographed in the laboratory at 2X magnification using a digital camera (Canon 90d DSLR; Macro Twin Lite MT-24EX with the Canon MP-E 65mm lens). Digital photographs were edited using Adobe Photoshop and annotated on Adobe Illustrator (Adobe Systems Inc., San Jose, CA) to visually document life stages and sexual dimorphism of adult *P. perseae* (Figure 1.2 a-c). The most extensive description of *P. perseae* life stages are provided by Heidemann (Heidemann, 1908) and this digital image work was done to improve upon these written descriptions.

Temperature-Driven Development Experiments

For each experimental temperature (Table 1.1), a total of ~30 field collected adult male and female *P. perseae* adults (~1-2 weeks of age) (i.e., G_0) were set up in Munger cells and left to

mate and oviposit on Hass avocado leaves. Each day adults were transferred to new leaves and freshly oviposited eggs (i.e., G_1) were maintained on labeled leaves, kept on water saturated foam pads held in stainless steel pans, and observed daily for nymph eclosion under a microscope at 10X-40X magnification. Leaves were discarded once no further nymphs emerged for a continuous period of 5 days. Emerged *P. perseae* nymphs (i.e., G_1) were placed individually into Munger cells with Hass avocado leaves and development was monitored daily until adulthood. The duration of nymphal development was recorded for each instar, which was confirmed by the presence of discarded exoskeletons. Nymphs that died prematurely due to unnatural causes (e.g., trapped in a water droplet, stuck on quake putty) were excluded from data analyses.

Adults were sexed under a dissecting microscope, and mating pairs consisting of one male and one female were established to measure the lifetime fecundity, fertility and longevity of adults. For each experimental temperature, 10- 15 mating pairs were set up and monitored for egg laying, hatching and mortality until death. In the event of adult mortality, a new male or female was introduced as a replacement. This arrangement ensured that both males and females had the chance to mate with alternative individuals throughout their entire natural lifespan. Adult longevity was assessed every 24-hours; individuals that perished from unnatural causes (e.g., drowning in water droplets, adhering to museum putty, or escaping and drowning in the pan) were excluded from the longevity estimates.

To ensure adequate sample sizes for development studies conducted at 15 and 35ºC, *P. perseae* eggs (i.e., G_1) laid at 32ºC, or first instar nymphs (< 12 hr of age) that emerged at 32ºC were transferred to the 15 and 35ºC temperature cabinets. This departure from the preceding experimental protocol described above was necessary to obtain nymphs for development studies as oviposition either did not occur (15ºC) or laid eggs failed to emerge (35ºC) at these lower and upper temperature extremes.

Daily and Lifetime Fertility and Fecundity Estimates

Female fecundity was recorded daily at a fluctuating average temperature of 32°C until female death from natural causes occurred. This temperature was selected for daily and lifetime fecundity studies as it was the optimal temperature for development of *P. perseae* (see Results below). Adults utilized for this fecundity experiment were reared to adulthood at 32°C. Twenty-three mating pairs (< 24-hour of age) that emerged at 32°C were set-up in 23 Munger cells with Hass avocado leaves as the feeding and oviposition substrate. The daily number of eggs laid by each female was recorded from the first day of adulthood until the day of death. A digital photograph of the observation arena enclosing the avocado leaf was captured using a microscope-mounted camera at 2.5X magnification. Labeled (i.e., mating pair identifier and date) digital images were used for mapping of eggs and determining developmental fate (i.e., hatching status). In the event of male mortality, a new male was introduced as a replacement, to ensure that females had the opportunity to continuously mate with males throughout their entire lifespan. Hass avocado leaves in Munger cells with eggs were removed, labeled, and replaced with fresh leaves every 6-8 days. Labeled leaves removed from Munger cells were cross-referenced to their corresponding digital maps and eggs were examined daily under a microscope at 10-40X magnification for nymph emergence. Nymph emergence from individual eggs laid on specific days was determined from digital photos with mapped eggs. Daily observations of Hass leaves with eggs continued for 15 days from the date of the last egg that hatched. Average daily egg oviposition rates, egg hatch rates (i.e., fertility), lifetime fecundity (i.e., total number of eggs laid), and longevity in days for each experimental female was determined.

Statistical Analyses of Preimaginal Developmental, Adult Longevity Times, and Female Fertility Data Across Fluctuating Temperature Regimens

SAS (SAS Statistical Analysis Software version 9.4, 2013) was used for all statistical analyses reported here. Generalized linear mixed models (GLMMs) and the PROC GLIMMIX procedure were used to evaluate the correlation between temperature and developmental duration times in G_1 *P. perseae* offspring. All models included fixed effects such as the fluctuating temperature profile (15 to 35°C), sex, and their interaction. Separate models were created for each developmental stage, encompassing *P. perseae* eggs, first, second, third, and fourth instar nymphs, along with combined male and female egg-to-adult development and adult longevity. Only data from individuals that reached adulthood and sexed as males or females were included in analyses for examined variables. Individuals that did not reach adulthood were omitted from analyses. A nested structure was included in all models to address potential statistical dependencies, this approach incorporated G_1 *P. perseae* within G_0 parent identity and temperature profile (Hoddle et al., 2023). Poisson distributions were used across all models, as determined by the variances of the response variables.

For the 35°C data, a substantial proportion (0.97) of eggs laid at this temperature failed to hatch, and nymphs that emerged typically died shortly after eclosing. Consequently, a subgroup of first instars, which comprised a total of 37 nymphs, that emerged from eggs laid at 32°C were moved to 35°C (see Materials and Methods above for details) for data collection on developmental times at 35°C for each stage, overall developmental times, and adult longevity. To justify this approach, egg hatching times for individuals that hatched at 35°C but subsequently died (hereafter referred to as 35-to-35°C hatching times) were initially compared with both egg hatching times for individuals that hatched at 32°C and were reared to adulthood at 32°C

(hereafter referred to as 32-to-32°C hatching times) and egg hatching times for individuals that hatched at 32°C and were transferred to 35°C (hereafter referred to as 32-to-35°C hatching times). Utilizing GLMMs and the PROC GLIMMIX procedure in SAS (SAS version 9.4, 2013), the analysis incorporated a fluctuating temperature profile (32-to-32°C, 32-to-35°C, and 35-to-35°C) as a fixed variable, with egg hatching times in days as the dependent variable. A nested structure was incorporated into the model to address potential statistical dependencies, involving G_1 *P. perseae* eggs within G_0 parent identity and temperature profile (Hoddle et al., 2023). Hatching times were modeled with a Poisson distribution as dictated by the variance of the response variable. No significant differences in egg hatching times were observed among 32-to-32°C, 32-to-35°C, and 35-to-35°C conditions (see results below). Consequently, for the comprehensive models covering temperatures from 15 to 35°C, calculations for 32°C utilized 32-to-32°C egg hatching times, and 35°C utilized 32-to-35°C egg hatching times.

Similarly, GLMMs and the PROC GLIMMIX procedure in SAS (SAS version 9.4, 2013) were used to evaluate the effect of varying temperatures on both the G_2 eggs laid by G_1 female *P. perseae* and the resulting percentage of hatched eggs. Considering the fluctuating temperature profile (excluding 35°C, where no eggs were laid and no hatch occurred) as a fixed effect in all models, G_2 egg counts followed a negative binomial distribution, while the resulting percentage of hatched eggs was modeled using a binomial distribution. Additionally, the model for egg counts incorporated G_1 female longevity and the interaction of egg counts with temperature as covariates to account for potential influences on the outcomes. Conversely, the model for the resulting percentage of hatched eggs omitted these covariates and focused solely on the fixed effect of temperature. A nested structure was integrated into all models to address potential statistical dependencies, incorporating G_1 *P. perseae* females within G_0 parent identity and temperature profile (Hoddle et al., 2023).

In all GLMMs utilized, temperature was categorized instead of treated as a continuous variable due to its highly nonlinear relationship with each analyzed variable (Streiner, 2002; Pasta, 2009; McCalla et al., 2019; Milosavljević et al., 2019). Significant main effects were verified through pairwise comparisons using the least-squared means option (utilizing SAS GLIMMIX procedure and LSMEANS statement [SAS version 9.4, 2013]), adjusting for multiple comparisons using the Tukey-Kramer method at a significance level below 0.05. Importantly, no significant differences in egg-to-adult developmental times were observed between G_1 females and G_1 males (refer to Tables 1.2 & 1.3 in the results section), and their values were combined by generation by combining G_1 male and G_1 female data for subsequent model fitting.

Fitting of Models to Temperature-Driven *Pseudacysta perseae* Development Data

One linear model (Ordinary Linear [Campbell et al., 1974]) and seven nonlinear regression functions (Beta [Yin et al., 2003; Auzanneau et al., 2011; Shi et al., 2015], Brière-2 [Brière et al., 1999], Lactin-2 [Logan et al., 1976; Lactin et al., 1995], Lobry-Rosso-Flandrois [Lobry et al., 1991; Rosso et al., 1993], Performance-2 [Shi et al., 2011; Wang et al., 2013], Ratkowsky [Ratkowsky et al., 1983], and Weibull [Angilletta, 2006]) were utilized to investigate the correlation between fluctuating temperature profiles and *P. perseae* developmental times (refer to McCalla et al., 2019, Milosavljević et al., 2019, and Table 1.5 for model equations). All models were fitted to data spanning 15 to 35 °C, representing egg-to-adult developmental rates (1/d), which are the reciprocals of mean egg-to-adult developmental times ($days^{-1}$) for G_1 *P. perseae* (i.e., combined male and female development data). Among the seven nonlinear models examined, the Beta and Weibull models failed to converge and fit to G_1 *P. perseae* development rates, which resulted in the exclusion of these two models from further analyses.

Linear regression (Campbell et al., 1974) was conducted using the PROC REG procedure in SAS to determine the degree-days necessary for egg-to-adult development of G_1 *P. perseae* (i.e., *K*; combined male and female data) under fluctuating temperatures and the theoretical lower developmental threshold (i.e., T_{min}). Parameter *K* was calculated as the reciprocal of the line slope, and T_{min} was obtained by solving for $y = 0$ for the fitted regression equation (Campbell et al., 1974). Linear model goodness-of-fit was assessed using *R*-squared adjusted (R^2_{adj}), where an $R^2_{adj} > 0.9$ indicated a satisfactory fit to the data (see Table 1.5; [Campbell et al., 1974]). Cook's *D* metric was utilized to identify and exclude influential outliers from the analysis. Outliers were categorized as observations with $D > 4$/number of observations as being overly influential (Bollen and Jackman, 1990).

The PROC NLIN procedure in SAS (SAS version 9.4, 2013) was applied to G_1 *P. perseae* egg-to-adult developmental rates to parameterize nonlinear models (Shi & Ge, 2010). All five tested nonlinear models featured four parameters, which resulted in identical degrees of freedom (*df*) (Ratkowsky & Reddy, 2017; Mirhosseini et al., 2017). Consequently, the assessment of goodness-of-fit for the nonlinear models relied on the residual sum of squares (*RSS*), expressed as:

$$RSS = \sum_{i=1}^{n} (y_i - \hat{y}_i)^2$$

where, *n* denotes number of observations, and y_i and $\hat{y}_i$ represent observed and expected developmental rates at *i*-th temperature, respectively. Nonlinear models with the smallest *RSS* values were indicative of a superior fit to datasets (Shi et al., 2015; Ratkowsky & Reddy, 2017; McCalla et al., 2019; Milosavljević et al., 2019; Milosavljević et al., 2020). R^2_{adj} was not employed to evaluate the goodness of fit for nonlinear models as it inaccurately characterizes the validity of a nonlinear fit to data (Spiess and Neumeyer, 2010).

All temperature-based development models were fitted by considering the developmental rate as the response variable which satisfied homogeneity assumptions (Ratkowksy, 2004). No additional transformations were required for the Brière-2, Lactin-2, LRF, and Performance-2 expressions, and each model was subjected to least squares estimation in its original form (Ratkowksy 2004). In the case of the square-root model (i.e., the Ratkowsky model), both sides of the equation were squared, ensuring that the left-hand side represented the developmental rate and not the square root of the rate (Shi and Ge 2010). All model outputs were visualized in SigmaPlot (SigmaPlot. Version 12.3, 2013).

RESULTS

Effects of Temperature on G_1 *Pseudacysta perseae* Developmental Times

No significant differences were found in egg hatching times among 32-to-32°C, 32-to-35°C, and 35-to-35°C rearing conditions ($F = 0.98$; $df_{2,47}$; $P = 0.39$). Consequently, for the models fitted to developmental times for G_1 *P. perseae* eggs, nymphal instars, and combined egg-to-adult development (this section), and adult longevity (see section below) at temperatures ranging from 15 to 35°C, calculations for 32°C used 32-to-32°C egg hatching times, and 35°C used 32-to-35°C egg hatching times, as outlined in the statistical analysis section above.

Consequently, mean developmental times for G_1 *P. perseae* eggs, nymphal instars, and egg-to-adult development varied with temperature (temperature effects: $P < .0001$ for all response variables; Tables 1.2 and 1.3), and no significant differences based on sex were detected (sex effects: $P > 0.67$ for all response variables; Table 1.2). Additionally, the interaction between sex and temperature had no significant effect (sex × temperature interaction effects: $P > 0.84$ for all response variables; Table 1.2) on the duration of G_1 *P. perseae* eggs, nymphal instars, and combined egg-to-adult development time.

Effects of Temperature on G_1 *P. perseae* Longevity Times and Female Fecundity and Fertility Rates

G_1 *P. perseae* males and females exhibited different longevity times with exposure to fluctuating temperature regimens (temperature effect; Tables 1.2 and 1.3), and the effect of sex was not significant (sex effect; Table 1.2). The interaction between sex and temperature was not significant (sex × temperature effect; Table 1.2). Longevity for *P. perseae* individuals was shortest at 35°C and longest at 15°C, followed by 20°C (Table 1.3). Mean G_2 egg counts for G_1 *P. perseae* females varied significantly with temperature ($F = 3.62$; $df_{4,61}$; $P = 0.01$), reaching the highest numbers at 25, 30, and 32 °C (Table 1.4). Additionally, G_2 egg counts increased with G_1 female longevity (female longevity effect: estimate: 0.075; $df_{1,53}$; $t = 8.41$; $P < .0001$), and these effects remained consistent across different temperature profiles (interaction between sex and female longevity effect: $F = 11.44$; $df_{4,58}$; $P < .0001$). Similar to G_2 egg counts, the resulting percentage of hatched G_2 eggs varied across different temperature conditions ($F_{4,59}= 4.41$; $P = 0.0035$), with the highest values observed over the temperature range 20-32 °C (Table 1.4).

Fitting Models to Temperature-Driven Development Data

The Ordinary Linear model demonstrated a strong fit to data for G_1 *P. perseae*, with an R^2adj value exceeding 0.91 (Table 1.5). For G_1 *P. perseae*, the linear regression equation predicted a T_{min} (i.e., lower development threshold) of 9.29°C and a thermal requirement for development completion (i.e., K) of 476.19 degree-days above this minimum threshold (Table 1.5; Figure 1.3a). All five nonlinear models that converged exhibited good fits, with *RSS* values below 0.0001 for G_1 *P. perseae* (Table 1.5). Estimations of T_{opt} (i.e., estimated optimal temperature for development) were consistent among models for G_1 *P. perseae*, ranging from 31.04 to 31.57°C (Table 1.5; Figure 1.3 b-f). However, there was notable divergence in model

predictions for T_{min} (i.e., minimum temperature for development), with estimates ranging from 1.72 to 9.78°C for G_1 *P. perseae* (Table 1.5; Figure 1.3 b-f). A somewhat smaller variance in model predictions was observed for T_{max} (i.e., upper temperature limit for development), with a predicted range spanning 34.05 to 39.38°C for G_1 *P. perseae* (Table 1.5; Figure 1.3 b-f).

Daily fertility, measured as the number of eggs that hatched at the optimal developmental temperature, 32°C (Figure 1.4) indicated that *P. perseae* eggs begin to hatch reliably from the sixth day following the commencement of oviposition which is around the seventh day of female adulthood. Peak fertility at 32ºC was observed between days 12 and 19, followed by a decline, before rebounding and exhibiting a secondary peak between days 30 to 33 (Figure 1.4).

DISCUSSION

The relationship between temperature and life cycle characteristics such as reproductive capacity, development, and mortality rates strongly influences the impacts of pest species in terms of economic and ecological damage and speed and patterns of spread (Rebaudo and Rabhi, 2018). To better understand the effects of temperature on the potential pestiferousness of *P. perseae*, fluctuating temperature cycles that ranged from 15°C to 35°C over a 24-hour period aimed to encapsulate the breadth of thermal environments that *P. perseae* might encounter in avocado orchards in California. The findings of this study provide important insights into the developmental biology and thermal tolerance of *P. perseae* which are essential for understanding how an important abiotic factor, like temperature, drives the population dynamics of *P. perseae* across different avocado growing climates in California (e.g., cool coastal and hotter interior growing areas) and elsewhere (e.g. the Caribbean). Improved understanding of abiotic factors, like temperature, that underlie population growth can assist with the development of regionalized Integrated Pest Management (IPM) strategies for this pest. These programs can be custom-

designed to specific growing areas to target specific life stages or to assess when population build-up and associated economic damage is likely to be highest.

This study confirmed that *P. perseae* has only four nymphal instars (i.e. 4 molts were observed) and not five as stated in other studies (Heidemann 1908; Morales 2002; Peña at al., 2012; Guidoti et al., 2015). Owing to the ambiguous nature of experimental conditions that previously investigated and described *P. perseae* instar development (Morales 2002) it was unclear how transitions between stadia occurred. In this study, the transition between instars was closely monitored for molted exoskeletons which confirmed ecdysis had occurred and transition to the next instar had happened. Consequently, the confirmation of four instars in *P. perseae* deviates from the typically reported pattern of five instars found among other members of the Tingidae (Heidemann 1908; Nair and Braman, 2012; Guidoti et al., 2015). A review of decreased or variable number of instars in Heteroptera lists two other tingid species that have been documented and confirmed as having four nymphal stages, *Stephanitis rhododendri* (Horváth 1905), and *Tanybyrsa cumberi* (Drake, 1959) that feed on *Rhododendron spp.* (Ericaceae) and *Astelia banksia* (Liliaceae), respectively (Johnson, 1936; May, 1977; Štys and Davidová, 1989).

Heidemann (1908) speculated that the last instar of *P. perseae* was the fifth instar, mirroring the number of instars observed in other tingid species described at that time. This assumption by Heidemann (1908) likely influenced Morales (2002) who also reported that *P. perseae* had five instars. Morales (2002) detailed a dichotomous key for identifying five instars of *P. perseae*, utilizing head diameter, body length and coloration. A close examination of the descriptions in Morales (2002) on how first and second instars were separated indicates that what was considered two separate stages is in fact just one, the first instar, which exhibits two color morphs, a very pale brown color upon hatching (first instar according to Morales [2002]) which then transitions to a darker dull red color (second instar according to Morales [2002]), which is

likely due to post-emergence melanization. In comparison to Morales (2002) who used color change from light to dark in the first instar nymph to indicate transition to the second instar, this study tracked exoskeleton shedding instead and determined that observed color changes in first instar *P. perseae* does not correspond with ecdysis to the second instar. This finding challenges the five-instar dogma by demonstrating that *P. perseae* has only four nymphal instars.

Additionally, this study identified a new sexual dimorphism trait that distinguishes male and female *P. perseae*. Contrary to Blatchley's description (Blatchley 1926) of adult *P. perseae* antennae as having a 'blackish apical half of the fourth antennal segment' (Mead and Peña, 2016) findings reported here indicate that females can be distinguished by having a light brown apical half on the fourth antennal segment, while males display a dark almost black colored segment. This finding greatly simplifies sex determination when field sampling.

Fluctuating temperature regimes that averaged 15, 20, 25, 30, 32, or 35 °C, over a 24-hour period significantly influenced the developmental times, fecundity, and adult longevity of *P. perseae*. Mean egg hatching times and mean developmental times of *P. perseae* nymphs varied significantly with temperature. However, temperature did not significantly influence the difference in developmental times for male and female *P. perseae*. The total developmental time of *P. perseae* males and females decreased significantly as temperature increased from 15 to 32 °C. The non-linear developmental rate models provided estimates for the temperature ranges of T_{min},1.72 to 9.78°C; T_{opt}, 31.04 to 31.57°C and T_{max}, 34.05 to 39.38°C. The T_{min} prediction from the ordinary linear regression was 9.29ºC aligning closely with estimates from two non-linear models, Lactin-2 (9.77 ºC) and Performance-2 (9.87 ºC). However, notable deviations in T_{min} estimates were observed with values of 1.72, 2.94, and 4.94 ºC, returned by the non-linear Ratkowsky, Lobry-Rosso-Flandrois (LRF) and Brière-2 models, respectively. Linear regression

analysis estimated a thermal requirement for development completion (i.e., *K*) of 476.19 degree-days above T_{min} (i.e., 9.29 ºC) were required for *P. perseae* to complete egg-to-adult development.

The variation in adult longevity times and female fertility (i.e., egg hatching) rates with temperature further indicates how thermal conditions influence the life history traits of *P. perseae*. Notably, longevity decreases significantly as temperature increases over the range of 15 to 35°C. Additionally, fecundity (i.e., total number of eggs laid) increases from 25°C to 32°C, suggesting a trade-off between lifespan and reproductive success. This finding indicates that while higher temperatures may decrease average longevity, warmer temperatures can positively influence reproductive rates, which may potentially result in more severe infestations when ambient environmental conditions fall within this optimal 25°C to 32°C temperature range. This finding has important implications for pest management, as monitoring, and possibly control strategies, may need to be intensified under these prevailing temperature conditions to mitigate the proliferation of *P. perseae* populations which could cause economic damage.

The high mortality rates observed among eggs, nymphs and adults of *P. perseae* at the upper threshold temperature that averaged 35°C over a 24-hour period, underscores the negative impact of upper-level temperature extremes on the survivorship rates and fitness of this pest. Our finding of negative effects of high temperatures on *P. perseae* suggests there could be significant and deleterious impacts on *P. perseae* populations. High temperatures such as those used in this study are a consequence of potential climate warming scenarios, seasonal temperature peaks, or intensive heat waves of short duration such as Santa Ana winds in California. Additionally, as climate change increases average temperature levels in southern California (Pathak et al., 2018), the effects of heat on *P. perseae* (and avocado production in general) may become more pronounced and extreme heat events could naturally limit the geographic spread and population growth of *P. perseae*.

The identification of a dual-peak fertility pattern in *P. perseae* at the optimal developmental temperature of 32°C highlights the necessity for continuous monitoring and developing biologically-based timed interventions to curb population surges. The occurrence of a second fertility peak approximately one-month post-adulthood suggests that *P. perseae* females can maintain substantial reproductive momentum as they age. This could cause populations to rebound unexpectedly after the first population surge, which necessitates the need for regular population monitoring at times when temperatures favor *P. perseae* development and reproduction. However, as females enter their second month, fertility significantly decreases and, in many instances, ceases entirely.

In comparing the developmental parameters of *P. perseae* across previously conducted temperature-development studies (Morales 2000 and Humeres unpublished data 2008 [see Supp. Table 1.1]), this study, conducted under fluctuating temperature regimes that are representative of climatic conditions across infested areas in southern California, enables important comparisons to the findings of Morales (2000) and Humeres (2008, unpublished data), who conducted development studies under constant temperature conditions (Supp. Table 1.1). The T_{min} value observed in both this study (9.29ºC) and Morales (2000) (9.29ºC) is slightly lower than that reported by Humeres (2008) (11.32ºC), which may be attributable to the narrower temperature ranges (i.e., 28-33 °C) used in those experiments. The higher *K* value of this study (i.e., 476.19 vs 434.78 [Morales 2000] and 217.33 [Humeres 2008 unpublished]) in this study suggests that under average fluctuating temperature conditions that are representative of avocado production areas in California, *P. perseae* may require increased cumulative temperature exposure above T_{min} to complete development. However, there is one important caveat that needs consideration; this being the *P. perseae* haplotype used for temperature-driven development studies. Haplotype G was used in this study and by Morales (2000). In comparison studies by Humeres (unpublished

2008) were conducted with Haplotype A. Genetic differences as identified by haplotype designation may introduce a confounding genetic variable that could influence measured development parameters across a range of temperatures.

Conclusions

The clarification of the number of nymphal instars (i.e. four not five), coupled with the identification of antennal sexual dimorphism (fourth antennal segment in males is darker than females), enriches our understanding of important basic aspects of the taxonomy and biology of *P. perseae*. These findings also have practical pest management applications in terms of pest development stages that need to be monitored and easier identification of males and females when sampling in the field. Identification of T_{min}, T_{opt}, and T_{max} for *P. perseae* development can assist pest managers with control decisions based on the anticipated effects of temperature on pest emergence, developmental rates, and population build up. This understanding may permit the development of management practices that can use temperature data to time control applications so that impacts are optimized with the most vulnerable stages of the pest's lifecycle or when population growth is expected to be most rapid and subsequently damaging. Leveraging these insights on aspects of *P. perseae* biology may help growers to better protect avocados from this invasive pest and to minimize economic losses, thereby promoting sustainable and profitable avocado production. The potential for *P. perseae* to spread further into new geographical areas can now be more accurately assessed with ecological niche modeling through the inclusion of upper and lower thermal thresholds (i.e., T_{min} and T_{max}) and degree-days accumulation (i.e., K) which collectively have significant impacts on rates of survival, reproduction, and generation times.

REFERENCES

Angilletta, M. J. Jr. 2006. Estimating and comparing thermal performance curves. *J. Therm. Biol.* 31: 541–545.

Antun, A. J. 1991. Presence of the avocado lace bug, *Pseudacysta perseae* (Heidemann) (Hemiptera: Tingidae) in Dominican Republic. *Primera Jornado de Proteccion Vegetal*, University of Santo Domingo, Santo Domingo, Dominican Republic, (Abstract, p. 4).

Auzanneau, J., C. Huyghe, A. J. Escobar-Gutiérrez, B. Julier, F. Gastal, P. Barre. 2011. Association study between the gibberellic acid insensitive gene and leaf length in a Lolium perenne L. synthetic variety. *BMC Plant Biol.* 11: 183.

Bollen, K. A., R. W. Jackman. 1990. Regression diagnostics: an expository treatment of outliers and influential cases. *Mod. Methods Data Anal.* 13: 257–291.

Brière, J. F, P. Pracros, A. Y. Le Roux, J. S Pierre. 1999. A novel rate model of temperature-dependent development for arthropods. *Environ. Entomol.* 28: 22–29.

CAC. 2023. California Avocado Commission Annual Report 2022. Available online: https://www.californiaavocadogrowers.com/sites/default/files/2022-CAC-Annual-Report-Final.pdf

Campbell, A., B. D. Frazer, N. Gilbert, A. P. Gutierrez, M. Mackauer. 1974. Temperature requirements of some aphids and their parasites. *J. Appl. Ecol.* 11: 431–438.

CIMIS – California Irrigation Management Information System. 2021. California Department of Water Resources' California Irrigation Management Information System. State of California, Sacramento, California, USA. http://www. cimis.water.ca.gov (Accessed in November 2021).

EPPO, European Plant Protection Organization. 2015. First report of *Pseudacysta perseae* in Madeira (PT): addition to the EPPO Alert List EPPO Reporting Service no. 01 - 2015. No. article: 2015/010. Available online: https://gd.eppo.int/reporting/ (Accessed in July 2023).

Guidoti, M., S.I. Montemayor, É. Guilbert. 2015. Lace Bugs (Tingidae). In: Panizzi, A., J. Grazia, (eds) *True Bugs (Heteroptera) of the Neotropics*. Entomology in Focus, Vol 2. Springer, Dordrecht.

Hallman, G. J., and D. L. Denlinger. 1998. Introduction: temperature sensitivity and integrated pest management, pp. 1–5. In G. J. Hallman and D. L. Denlinger (eds.), Temperature sensitivity in insects and application in integrated pest management. Westview Press, Boulder, CO.

Heidemann, O. 1908. Two new species of North American Tingidae. Proceedings of the *Entomological Society of Washington* 10: 103-108.

Hoddle, M. S. 2004. Invasions of leaf feeding arthropods: why are so many new pests attacking California grown avocados? *Calif Avocado Society Yearbook* 87: 65–81.

Hoddle, M. S. 2022a. *Avocado lace bug*. Applied Biological Control research. Department of Entomology, University of California. Available online: http://cisr.ucr.edu/avocado_lace_bug.html (Accessed in June 2023).

Hoddle, M. S. 2022b. Avocado Lace Bug is Continuing to Spread in California. *From the Grove* 12(2): 22-25.

Hoddle, M. S., I. Milosavljević, and R. Amrich. 2023. Effects of Temperature on the Developmental and Reproductive Biology of North American Bean Thrips, Caliothrips fasciatus (Pergande)(Thysanoptera: Thripidae: Panchaetothripinae). *Insects* 14(7): 641.

Hoddle, M. S., J. Morse, R. Stouthamer, E. Humeres, G. Jeong, W. Roltsch, G. S. Bender, P. Phillips, D. Kellum, R. Dowell, G. W. Witney. 2005. Avocado lace bug in California. *Calif Avocado Society Yearbook* 88: 67–79.

Hoddle, M., J. Morse, R. Stouthamer. 2007. Biology and management of avocado lace bug in California. *Proceedings of the California Avocado Research Symposium*, pp. 1-11. California Avocado Commission.

Humeres, E. C., J. G. Morse, R. Stouthamer, W. Roltsch, M. S. Hoddle. 2009. "Evaluation of Natural Enemies and Insecticides for Control of *Pseudacysta perseae* (Hemiptera: Tingidae) on Avocados in Southern California," *Florida Entomologist* 92(1): 35-42.

Lactin, D. J., N. J. Holliday, D. L Johnson, R. Craigen. 1995. Improved rate model of temperature-dependent development by arthropods. *Environ. Entomol.* 24: 68–75.

Lobry, J. R., L. Rosso, J. P. Flandrois. 1991. A FORTRAN subroutine for the determination of parameter confidence limits in non-linear models. *Binary* 3: 86–93.

Logan, J. A, D. J. Wolkind, S. C. Hoyt, L. K. Tanigoshi. 1976. An analytic model for description of temperature dependent rate phenomena in arthropods. *Environ. Entomol.* 5: 1133–1140.

May, B. M. 1977. The immature stages and biology of the lacebug, *Tanybyrsa cumberi* Drake (Heteroptera: Tingidae). *Journal of the Royal Society of New Zealand* 7(3): 303-312.

McCalla, K. A., M. Keçeci, I. Milosavljević, D. A. Ratkowsky, M. S. Hoddle. 2019. The influence of temperature variation on life history parameters and thermal performance curves of *Tamarixia radiata* (Hymenoptera: Eulophidae), a parasitoid of the Asian citrus psyllid (Hemiptera: Liviidae). *J. Econ. Entomol.* 112: 1560-1567.

Mead, F. W. & J. E. Peña. 1991. Avocado lace bug, *Pseudacysta perseae* (Hemiptera: Tingidae). Florida Department Agriculture and Consumer Services, Division of Plant Industry. *Entomology Circular* 346: 4.

Mead, F. W. & J. E. Peña. 2016. Avocado lace bug, *Pseudacysta perseae* (Heidemann) (Insecta: Hemiptera: Tingidae). IFAS Extension, University of Florida.

Milosavljević, I., K. A. McCalla, D. A. Ratkowsky, M. S. Hoddle. 2019. Effects of constant and fluctuating temperatures on development rates and longevity of *Diaphorencyrtus aligarhensis* (Hymenoptera: Eulophidae). *J. Econ. Entomol.* 112: 1062-1072.

Milosavljević, I., K. A. McCalla, D. J. W. Morgan, M. S. Hoddle. 2020. The effects of constant and fluctuating temperatures on development of *Diaphorina citri* (Hemiptera: Liviidae), the Asian citrus psyllid. *J. Econ. Entomol.* 113: 633-645.

Mirhosseini, M., A. Y. Fathipour, G. V. Reddy. 2017. Arthropod development's response to temperature: a review and new software for modeling. *Ann. Entomol. Soc. Am.* 110: 507–520.

Morales, R. L., R. H. Grillo, & R. V. Hernández. 2000. Biology of *Pseudacysta perseae* (Heid.) (Heteroptera: Tingidae) at constant temperature. *Centro Agrícola* 27(3): 39-41.

Morales Romero, L., H. Grillo Ravelo & V. Hernández Rodríguez. 2002. Description of the developmental stages and nymphal instars of *Pseudacysta perseae* (Heid.) (Heteroptera: Tingidae). *Centro Agrícola* 29(3): 30-36.

Munger, F. A. 1942. A method for rearing citrus thrips in the laboratory. *J. Economic Entomology* 35: 373-375.

Nair, S., & S. K. Braman. 2012. A scientific review on the ecology and management of the azalea lace bug *Stephanitis pyrioides* (Scott) (Tingidae: Hemiptera). *Journal of Entomological Science*, *47*(3): 247-263.

Nelson, W. A., O. N. Bjørnstad, and T. Yamanaka. 2013. Recurrent insect outbreaks caused by temperature-driven changes in system stability. *Science* 341: 796–799.

Neven, L. G. 2000. Physiological responses of insects to heat. *Postharvest Biology and Technology*, 21(1): 103–111.

Pasta, D. 2009. Learning when to be discrete: continuous vs. categorical predictors. *SAS Glob. Forum. Pap.* 248: 1–10.

Štys, P, & J. V. Davidová. 1989. Unusual numbers of instars in Heteroptera: a review. *Acta Entomol. Bohemosioy*. 86: 1-32.

Pathak, T. B., M. L. Maskey, J. A. Dahlberg, F. Kearns, K. M. Bali and D. Zaccaria. 2018. Climate change trends and impacts on California agriculture: a detailed review. *Agronomy*, 8(3): 25.

Pedigo, L. P. 1989. Entomology and Pest Management. Macmillan Publishing Company.

Peña, J. E. 2003. Pests of avocado in Florida. *Proceedings of V world avocado congress*, pp 487–494.

Peña, J. E., Duncan, R.E., Roltsch, W.J., Carrillo, D., 2012. Mortality factors of the avocado lace bug, *Pseudacysta perseae* (Heteroptera: Tingidae), in Florida. *Florida Entomologist* 95(1): 179-182.

Poligui, R. N., L. E. Apinda, H. Nzandi, B. C. Odjele. 2023. Presence of *Pseudacysta perseae* (Heidemann) (Hemiptera: Tingidae) and it relate predatory mirid *Stethoconus praefectus* on *Persea americana* at Franceville, Gabon. *Acta Entomol Zool* 4(1): 37-43.

Ratkowsky, D. A., G. V. Reddy. 2017. Empirical model with excellent statistical properties for describing temperature-dependent developmental rates of insects and mites. *Ann. Entomol. Soc. Am.* 110: 302–309.

Ratkowsky, D. A., R. C. McKellar, X. Lu. (Eds.). 2004. Model fitting and uncertainty. Modeling microbial responses in food; CRC Press, Boca Raton, Florida U.S., pp 151–196.

Ratkowsky, D. A., R. K. Lowry, T. A. McMeekin, A. N. Stokes, R. Chandler. 1983. Model for bacterial culture growth rate throughout the entire biokinetic temperature range. *J. Bacteriol.* 154: 1222–1226.

Rebaudo, F., & V. B. Rabhi. 2018. Modeling temperature-dependent development rate and phenology in insects: review of major developments, challenges, and future directions. *Entomologia Experimentalis et Applicata* 166(8): 607-617.

Rosso, L., J. R. Lobry, J. P. Flandrois. 1993. An unexpected correlation between cardinal temperatures of microbial growth highlighted by a new model. *J. Theor. Biol.* 162: 447–463.

Rugman-Jones, P. F., M. S. Hoddle, P. A. Phillips, G. S. Jeong, R. Stouthamer. 2012. Strong genetic structure among populations of the invasive avocado pest *Pseudacysta perseae* (Heidemann) (Hemiptera: Tingidae) reveals the source of introduced populations. *Biological Invasions* 14(6): 1079-1100.

SAS. 2013. Statistical Analysis Software. Users' Guide Statistics Version 9.4. SAS Institute Inc., Cary.

Shi, P., F. Ge, Y. Sun, C. Chen. 2011. A simple model for describing the effect of temperature on insect developmental rate. J. *Asia Pac. Entomol.* 14: 15–20.

Shi, P., F. Ge. 2010. A comparison of different thermal performance functions describing temperature-dependent development rates. *J. Therm. Biol.* 35: 225–231.

Shi, P., J. G. V Reddy, L. Chen, F. Ge. 2015. Comparison of thermal performance equations in describing temperature-dependent developmental rates of insects: (I) empirical models. *Ann. Entomol. Soc. Am.* 109: 211–215.

Spiess, A. N., N. Neumeyer. 2010. An evaluation of R2 as an inadequate measure for nonlinear models in pharmacological and biochemical research: a Monte Carlo approach. *BMC Pharmacol.* 10: 6.

Streiner, D. L. 2002. Breaking up is hard to do: the heartbreak of dichotomizing continuous data. *Can. J. Psychiatry* 47: 262–266.

USDA/ERS. 2022. Avocados: Production, season-average grower price, and value, by state, 1980/81 to date. United States Department of Agriculture, Economic Research Service, Washington, D.C.

Wang, L., P. Shi, C. Chen, F. Xue. 2013. Effect of temperature on the development of Laodelphax striatellus (Homoptera: Delphacidae). *J. Econ. Entomol.* 106: 107–114.

Yin, X., J. Goudriaan, E. A. Lantinga, J. Vos, H. J. Spiertz. 2003. A flexible sigmoid function of determinate growth. *Ann. Bot.* 91: 361–371.

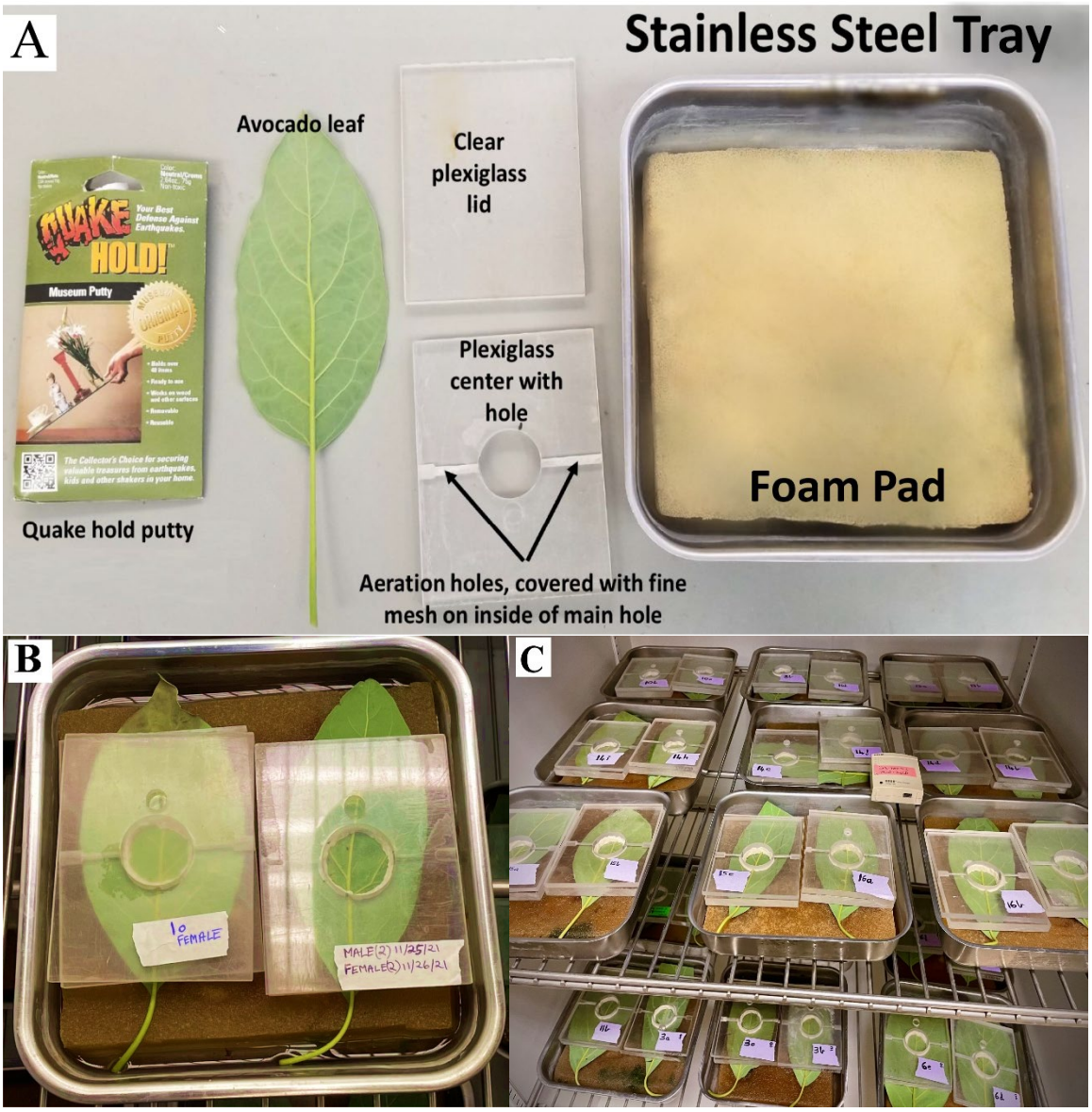

Figure 1.1 (a) Components needed to set up a Munger cell for rearing *Pseudacysta perseae* on Hass avocado leaves in climate-controlled cabinets. (b) Constructed Munger cell used in experiments. (c) Munger cells inside climate-controlled cabinet with HOBO Temperature/RH logger.

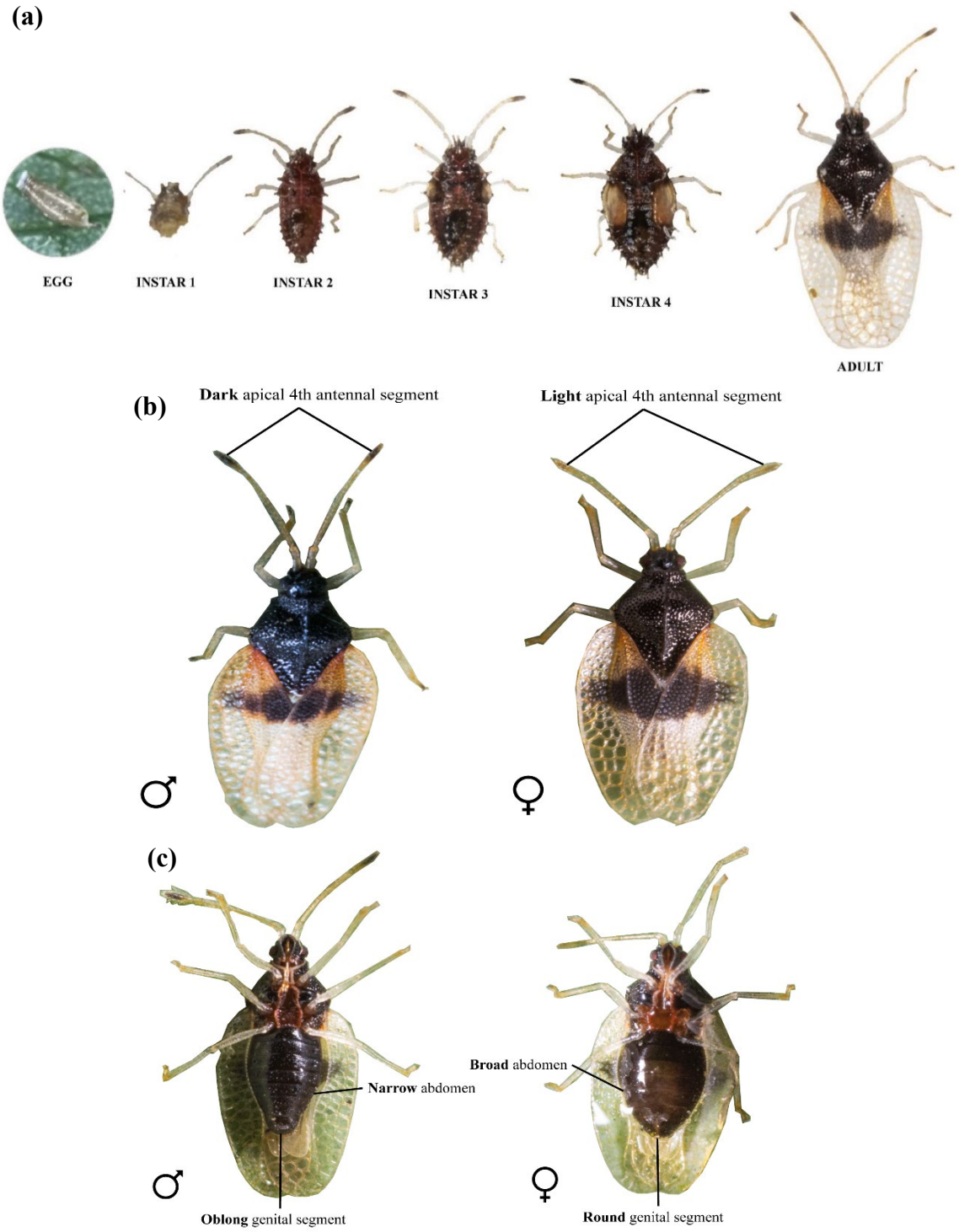

Figure 1.2 (a) Life stages (egg to adult) of *Pseudacysta perseae*. (b) The color of the apical 4th antennal segment can be used to separate male and female *P. perseae.* (c) The ventral view of abdomen and genital segment of male (♂) and female (♀) *P. perseae*.

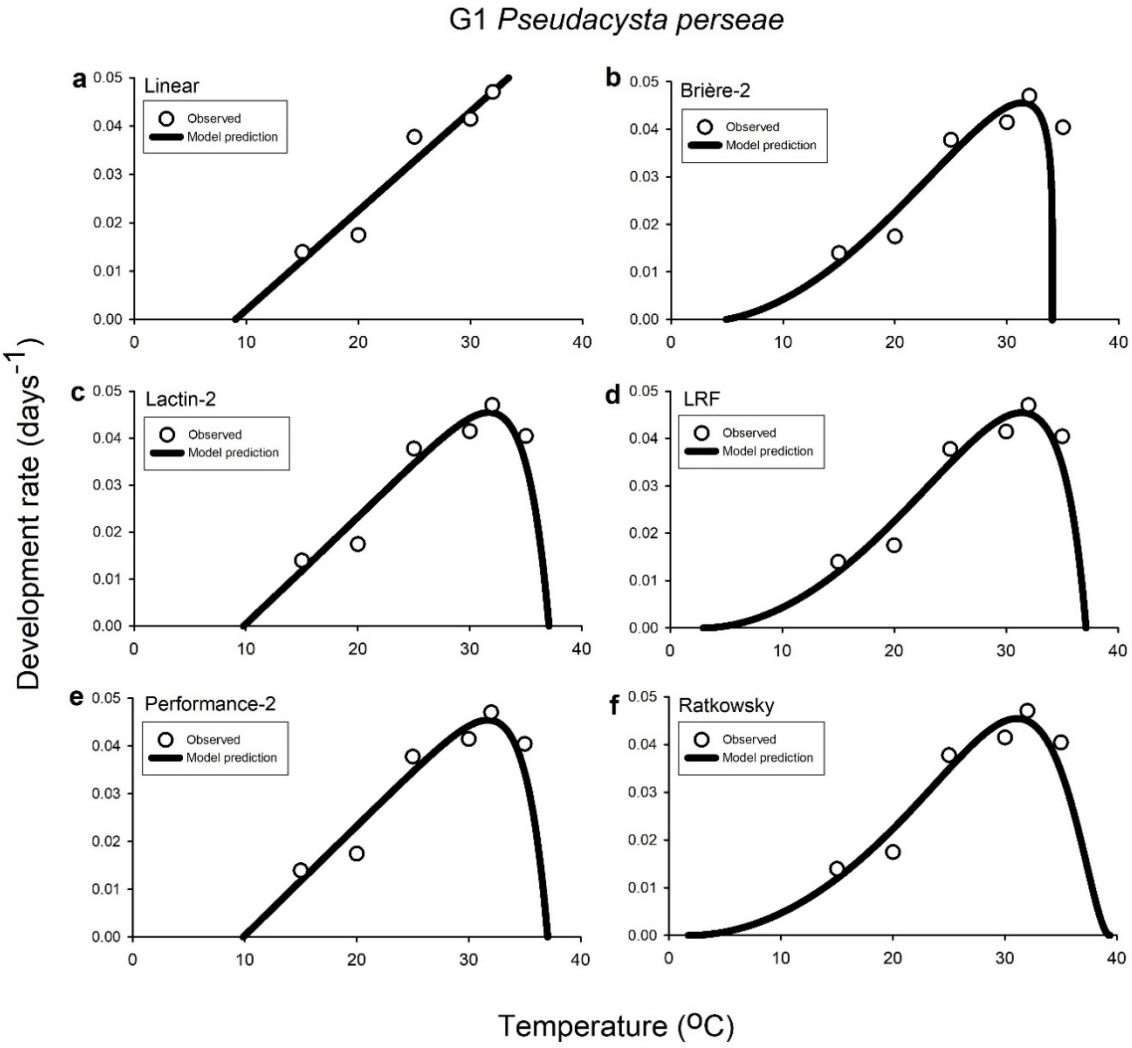

Figure 1.3 Projected rates of total development for G_1 (a-f) *Pseudacysta perseae* (males and females combined) were assessed across six fluctuating temperature profiles (15, 20, 25, 30, 32, or 35 °C) using linear (a), Brière-2 (b), Lactin-2 (c), LRF (d), Performance-2 (e), and Ratkowsky (f) models. In all charts, the ordinate represents the developmental rate (1/D, in days^{-1}), while the abscissa indicates the mean fluctuating temperature (°C). *Symbols* denote observed data in all charts. For the linear regression model (a), the final data point (i.e., 35°C) for *P. perseae* development times was excluded due to significant deviations from a straight line as determined by Cook's *D* metric.

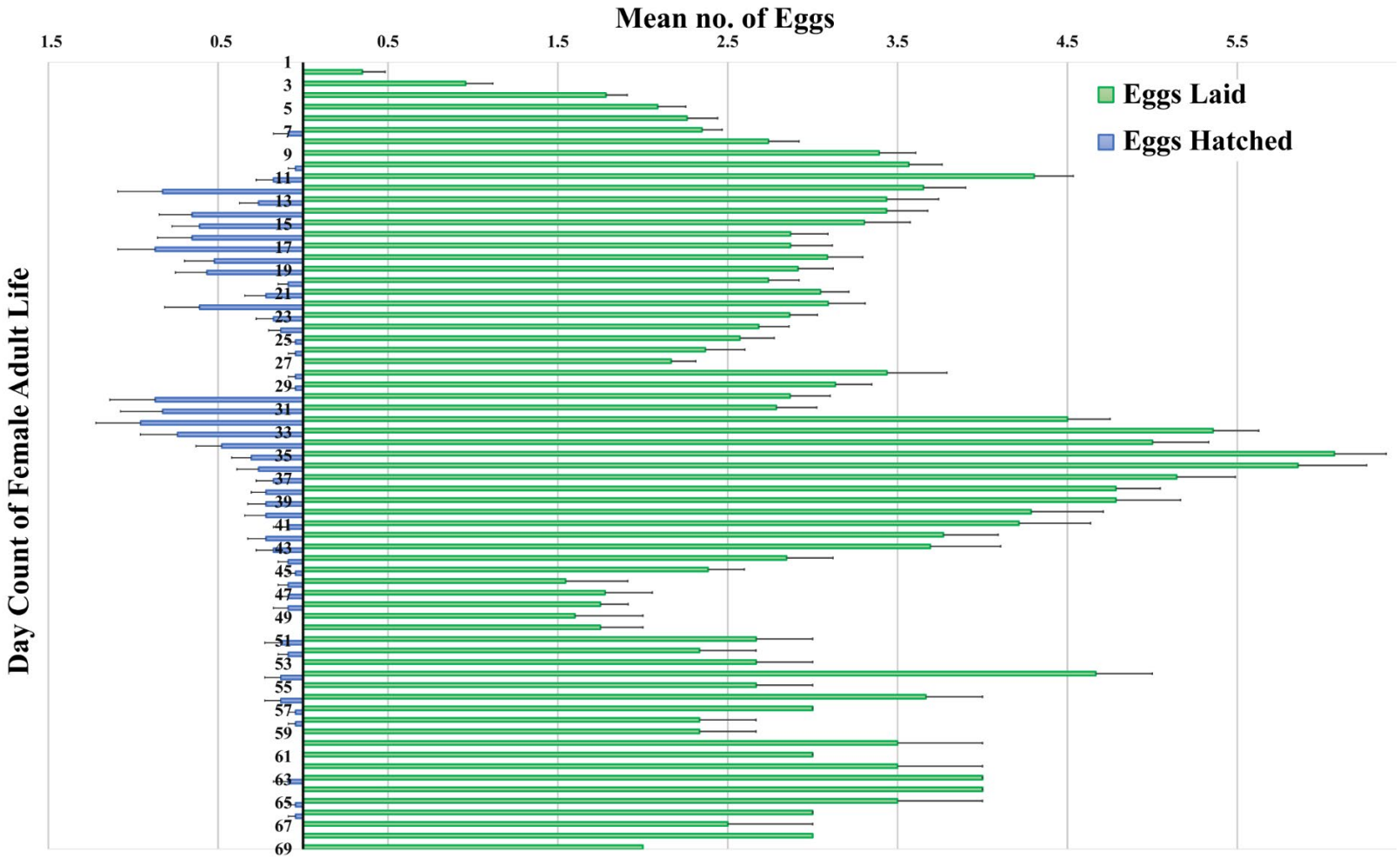

Figure 1.4 Daily fecundity (i.e., eggs laid) and fertility (i.e., eggs hatched) of *Pseudacysta perseae* females at 32°C (n= 23). Y axis: Day count of female adult life, refers to each successive day the female specimens were observed throughout their adult lifespan.

Table 1.1 Stepwise hourly temperature ramping in temperature cabinets used for fluctuating temperature regimens.

Hour	Mean Temperature (°C)						Photoperiod
	15	20	25	30	32	35	
0100	11.4	15.3	19.5	25.2	23.9	28.4	
0200	11.1	15	19.2	24.0	23.2	27.7	
0300	10.7	14.8	18.8	24.0	22.3	26.8	dark
0400	10.3	14.5	18.4	23.3	21.5	26.0	
0500	10.0	14.2	18.0	22.7	21.5	26.2	
0600	9.8	14.3	17.8	23.0	22.7	26.6	
0700	10.2	15.4	19.2	24.9	27.7	30.0	
0800	12.0	17.6	21.5	27.2	32.1	33.2	
0900	14.5	20.4	24.6	31.1	34.6	35.2	
1000	17.2	23.1	28.0	33.2	36.1	36.8	
1100	19.4	25.6	30.6	35.6	37.3	38.1	
1200	21.1	27.1	32.8	36.4	38.3	39.1	light
1300	21.7	27.8	33.9	37.4	39.2	40.2	
1400	21.8	27.7	33.6	38.0	39.9	41.0	
1500	21.3	27.1	32.6	37.2	40.3	41.6	
1600	20.5	26.1	31.5	34.6	40.4	42.0	
1700	19.1	24.7	30.0	33.7	39.9	41.9	
1800	17.2	22.4	28.2	32.0	39.2	41.2	
1900	15.5	20.1	26.0	31.0	37.0	39.2	
2000	14.3	18.6	23.8	30.0	34.8	37.3	
2100	13.7	17.4	22.9	29.3	32.4	35.6	
2200	13.1	16.6	22.0	27.0	30.6	34.1	dark
2300	12.6	16.2	21.3	26.0	28.3	32.1	
2400	11.9	15.8	20.4	25.0	26.1	30.2	
Total Steps	24	24	24	24	24	24	

Table 1.2 Results from generalized linear mixed models analyzing the effects of sex, temperature (characterized by fluctuating temperature regimens averaging 15, 20, 25, 30, 32, or 35 °C, over a 24-hour period), and their interactions on the developmental times of first-generation (G_1) *Pseudacysta perseae* eggs (A), first, second, third, and fourth instar nymphs (B-E), combined egg-to-adult transition (F), and adult longevity (G) when subjected to fluctuating temperature regimes.

(A) Eggs (Development)	Num df	Den df	*F*	*P*
Sex (S)	1	146	0.06	0.8082
Temperature (T)	5	146	63.80	<.0001*
S × T	5	146	0.11	0.9897
(B) 1st Instar (Development)	Num df	Den df	*F*	*P*
Sex (S)	1	146	0.18	0.6700
Temperature (T)	5	146	82.48	<.0001*
S × T	5	146	0.05	0.9983
(C) 2nd Instar (Development)	Num df	Den df	*F*	*P*
Sex (S)	1	146	0.01	0.9850
Temperature (T)	5	146	66.77	<.0001*
S × T	5	146	0.18	0.9700
(D) 3rd Instar (Development)	Num df	Den df	*F*	*P*
Sex (S)	1	146	0.03	0.8723
Temperature (T)	5	146	74.62	<.0001*
S × T	5	146	0.11	0.9899
(E) 4th Instar (Development)	Num df	Den df	*F*	*P*
Sex (S)	1	146	0.02	0.8765
Temperature (T)	5	146	52.88	<.0001*
S × T	5	146	0.14	0.9826
(F) Egg-to-Adult (Development)	Num df	Den df	*F*	*P*
Sex (S)	1	146	0.04	0.8388
Temperature (T)	5	146	324.32	<.0001*
S × T	5	146	0.09	0.9932
(F) Adults (Longevity)	Num df	Den df	*F*	*P*
Sex (S)	1	143	0.01	0.9796
Temperature (T)	5	143	89.67	<.0001*
S × T	5	143	0.41	0.8420

*Indicates significance at a level below 0.05

Table 1.3 Mean developmental times (mean days ± SE) for first-generation (G1) *Pseudacysta perseae* eggs, along with first, second, third, and fourth instar nymphs, combined egg-to-adult transition, and adult longevity, observed under six fluctuating temperature regimes that averaged 15, 20, 25, 30, 32, or 35 °C, over a 24 h period.

Temp. (°C)	Average duration times (mean days ± SE)													
	Eggs		1st instar		2nd instar		3rd instar		4th instar		Eggs-to-Adults		Adults	
	Female	Male	Female	Male	Female	Male	Female	Male	Female	Male	Female	Male	Female	Male
15	24.08 ± 0.56^{a} [13]	24.73 ± 0.44^{a} [15]	12.38 ± 0.38^{a} [13]	12.73 ± 0.38^{a} [15]	10.61 ± 0.31^{a} [13]	11.07 ± 0.37^{a} [15]	11.31 ± 0.28^{a} [13]	11.41 ± 0.29^{a} [15]	12.61 ± 0.46^{a} [13]	12.21 ± 0.38^{a} [15]	71.07 ± 0.97^{a} [13]	72.13 ± 0.72^{a} [15]	69.61 ± 4.71^{a} [13]	64.87 ± 2.96^{a} [15]
20	20.08 ± 0.33^{b} [13]	19.27 ± 0.33^{b} [11]	11.38 ± 0.38^{a} [13]	12.09 ± 0.37^{a} [11]	10.92 ± 0.33^{a} [13]	11.27 ± 0.49^{a} [11]	12.15 ± 0.46^{a} [13]	12.09 ± 0.46^{a} [11]	10.08 ± 0.33^{a} [13]	10.01 ± 0.49^{a} [11]	64.61 ± 0.62^{b} [13]	64.73 ± 0.88^{b} [11]	39.54 ± 2.03^{b} [13]	42.54 ± 3.14^{b} [11]
25	11.06 ± 0.17^{c} [16]	10.81 ± 0.21^{c} [16]	2.94 ± 0.17^{b} [16]	3.31 ± 0.15^{b} [16]	3.63 ± 0.18^{b} [16]	3.69 ± 0.18^{b} [16]	3.69 ± 0.27^{b} [16]	3.56 ± 0.16^{b} [16]	5.19 ± 0.19^{b} [16]	5.06 ± 0.14^{b} [16]	26.51 ± 0.24^{c} [16]	26.44 ± 0.22^{c} [16]	26.56 ± 1.44^{c} [16]	29.51 ± 1.26^{c} [16]
30	11.38 ± 0.22^{c} [16]	11.53 ± 0.24^{c} [15]	3.51 ± 0.16^{b} [16]	3.61 ± 0.19^{b} [15]	2.75 ± 0.14^{b} [16]	3.13 ± 0.21^{b} [15]	2.94 ± 0.14^{b} [16]	3.07 ± 0.21^{b} [15]	3.56 ± 0.18^{b} [16]	4.02 ± 0.29^{b} [15]	24.13 ± 0.41^{c} [16]	25.33 ± 0.47^{c} [15]	27.38 ± 2.81^{c} [13]	28.41 ± 3.21^{c} [15]
32	9.93 ± 0.27^{c}[15]	10.29 ± 0.22^{c} [17]	2.27 ± 0.12^{b} [15]	2.29 ± 0.14^{b} [17]	2.81 ± 0.11^{b} [15]	2.47 ± 0.17^{b} [17]	2.53 ± 0.13^{b} [15]	2.76 ± 0.18^{b} [17]	3.73 ± 0.12^{b} [15]	3.41 ± 0.21^{b} [17]	21.27 ± 0.27^{d} [15]	21.23 ± 0.35^{d} [17]	22.87 ± 2.52^{c} [15]	23.35 ±1.14^{c} [17]
35	10.01 ± 0.36^{c} [6]	10.61 ± 0.61^{c} [5]	3.51 ± 0.43^{b} [6]	3.41 ± 0.51^{b} [5]	3.33 ± 0.21^{b} [6]	3.01 ± 0.32^{b} [5]	3.83 ± 0.31^{b} [6]	3.21 ± 0.21^{b} [5]	4.33 ± 0.21^{b} [6]	4.21 ± 0.21^{b} [5]	25.01 ± 0.58^{c} [6]	24.41 ± 0.81^{c} [5]	5.51 ± 1.99^{d} [6]	4.61 ± 1.47^{d} [5]
P	<.0001		<.0001		<.0001		<.0001		<.0001		<.0001		<.0001	

Means sharing the same column and marked with the same letter were not significantly different at α = 0.05 (LSMEANS), number within square brackets indicates the count of individuals.

Table 1.4 Mean fecundity rates (i.e., egg hatch), represented by the numbers of second-generation (G_2) *Pseudacysta perseae* eggs laid (± SE) and mean fertility rates (± SE) as estimated by the percentage of G_2 *Pseudacysta perseae* nymphs that hatched, were examined for first-generation (G_1) female *Pseudacysta perseae* reared under six fluctuating temperature profiles (i.e., 15, 20, 25, 30, 32, or 35 °C).

Temperature (°C)	**Mean fecundity and fertility rates per G_1 female**	
	Mean no. G_2 eggs laid (± SE)	**Mean % G_2 eggs hatched (± SE)**
15	15.69 ± 2.78^{c} [13] (204)	4.45 ± 1.93^{b} [13] {11}
20	27.15 ± 1.61^{b} [13] (353)	22.65 ± 2.98^{a} [13] {75}
25	53.87 ± 3.84^{a} [16] (862)	28.26 ± 1.39^{a} [16] {239}
30	53.12 ± 10.27^{a} [16] (850)	21.59 ± 2.86^{a} [15] {202}
32	46.86 ± 8.39^{a} [15] (656)	24.53 ± 2.87^{a} [14] {155}
35	No eggs were laid [6] (0)	No hatching occurred [0] (0)
P	<.0001	0.0035

Means within the same column, denoted by the same letter, exhibited no significant differences at $\alpha = 0.05$ (LSMEANS). The number in [square brackets] denotes the quantity of evaluated G_1 female *P. perseae* at each temperature profile, while the number in (round brackets) indicates the total count of G_2 *P. perseae* eggs laid at each temperature profile; and the number in {curly brackets} represents the total number of resulting G_2 *P. perseae* eggs hatched at each temperature profile. No eggs were laid, and no hatching occurred at 35 °C; hence, the 35 °C temperature profile was excluded from both analyses.

Table 1.5 Mathematical models, parameter estimates, and goodness-of-fit metrics for six performance functions describing the relationship between temperature and development rates (D_r) of first-generation (G_1) *Pseudacysta perseae* (male and female data were combined) reared under six fluctuating temperature profiles, averaging 15, 20, 25, 30, 32, or 35 °C, over a 24-hour period.

Model	Model Equation†	Parameter	Parameter Estimate	Reference
Ordinary Linear‡	$D_r = a + bT$	a	-0.0195	Campbell et al. (1974)
		b	0.0021	
		K *(degree-days)*‡	476.19	
		T_{min}‡	9.29	
		R^2_{adj}	0.9109	
Lactin-2 (Logan-Lactin)	$D_r = \lambda + e^{\rho T} - e^{(\rho T_u - (T_u - T)/\delta T)}$	λ	-1.0217	Logan et al. (1976) Lactin et al. (1995)
		ρ	0.0022	
		δ	2.1158	
		T_{min}*	9.77	
		T_u (T_{max}*)	37.05	
		T_{opt}*	31.57	
		RSS	0.000019	
Brière-2	$D_r = aT(T - T_{min})(T_{max} - T)^{1/b}$	a	0.000046	Brière et al. (1999)
		b	5.346	
		T_{min}	4.94	
		T_{max}	34.05	
		T_{opt}*	31.39	
		RSS	0.000032	
Lobry-Rosso-Flandrois (LRF)	$D_r = \mu_{opt} \frac{(T - T_{max})(T - T_{min})^2}{(T_{opt} - T_{min})[(T_{opt} - T_{min})(T - T_{opt}) - (T_{opt} - T_{max})(T_{opt} + T_{min} - 2T)]}$	μ_{opt}	0.0455	Lobry et al. (1991) Rosso et al. (1993)
		T_{min}	2.94	
		T_{max}	37.14	
		T_{opt}	31.51	
		RSS	0.000016	
Performance-2	$D_r = b(T - T_{min})(1 - e^{c(T - T_{max})})$	T_{min}	9.87	Shi et al. (2011) Wang et al. (2013)
		T_{max}	36.09	
		T_{opt}*	31.04	
		b	0.0023	
		c	0.4435	
		RSS	0.000019	
Ratkowsky	$\sqrt{D_r} = b(T - T_{min})(1 - e^{c(T - T_{max})})$; $D_r = [b(T - T_{min})(1 - e^{c(T - T_{max})})]^2$	b	0.0082	Ratkowsky et al. (1983)
		c	0.2596	
		T_{min}	1.72	
		T_{max}	39.38	
		T_{opt}*	31.11	
		RSS	0.000015	

†In every model, T represents the temperature in degrees Celsius, and D_r signifies the developmental rate at temperature T; in the Ratkowsky, Lactin-2, and Performance-2 models, e signifies the base of the natural logarithms; other symbols represent specific model parameters, and a comprehensive description of models and parameters can be found in the respective references.

‡Linear regression was used to calculate the theoretical minimum developmental threshold ($T_{min} = -a/b$, with a representing the developmental rate at $T = 0$ °C and b as the slope), along with the thermal constant or degree-days required for development completion ($K = 1/b$); temperatures at which developmental rate of *P. perseae* nymphs deviated from rectilinearity were omitted from analyses (i.e., developmental rate at 35 °C)

*In all nonlinear models, with the exception of the LRF model, the optimal development point (T_{opt}) was derived from the peak of the development curve (where D_r = max); in the Lactin-2 model, the theoretical minimum and maximum developmental thresholds (T_{min} and T_{max}) were determined at the points where the curve intersected the temperature axis (where $D_r = 0$).

Supplementary Table 1.1 Estimated parameters and R^2_{adj} values for the linear model describing the relationship between development rate (D_r) and temperature for immature stages of *P. perseae* (combined male and female data) under constant temperature conditions from Humeres ([2008, unpublished data]; *P. perseae* reared at 28, 30, and 33 °C) and Morales ([2000]; *P. perseae* reared at 20, 22, 25, 28, and 30 °C), as well as fluctuating temperature conditions from the current study ([2023] *P. perseae* reared at 15, 20, 25, 30, 32, and 35 °C).

			Parameter Estimate			
Model	Model Equation	Parameter	Fluctuating 2023	Constant Humeres (2008, unpublished data)	Constant Morales (2000)	Reference
Ordinary Linear	$D_r = a + bT$	a	-0.0195	-0.0521	-0.0216	Campbell et al. (1974)
		b	0.0021	0.0046	0.0023	
		K	476.19	217.33	434.78	
		T_{min}	9.29	11.32	9.39	
		R^2_{adj}	0.9109	0.9911	0.9957	

See corresponding reference for full description of model parameters

In all datasets, temperatures where the development rate of *Pseudacysta perseae* nymphs deviated from linearity were excluded from analyses, such as the development rate at 35 °C in this study. Additionally, all temperature-dependent data from Humeres (2008, unpublished data) and Morales (2000) studies were aligned with the linear portions of their respective dataset.

Chapter 2. Phenology, Behavioral Ecology and Natural Enemies of *Pseudacysta perseae* in commercial Hass avocado orchards in California, U.S.A.

INTRODUCTION

Effective pest management relies on a comprehensive understanding of the life cycle of the pest species of concern in conjunction with its phenology (Pedigo and Rice, 2006). Phenological studies provide valuable insights into temporal periods of pest population increases and declines, which allows growers to implement targeted control measures as population densities increase towards levels that can cause economic damage (Pedigo and Rice, 2006). Since insect development is strongly influenced by temperature, assessing the degree-day (DD) requirements for successive life stages (e.g., eggs, nymphs), along with their developmental thresholds (i.e., T_{min}, T_{opt}, and T_{max}), can be used to develop predictive phenology models that provide insight into the timing, progression, and duration of life stages (Chapter 1; Nietschke et al., 2007). The identification of the presence of vulnerable life stages such as egg-laying periods, through use of DD models, enables growers to strategically intervene when the pest is likely to be most impacted by a selected control method (e.g., insecticide applications or augmentative releases of natural enemies). Growers may also target critical pestiferous life stages to suppress insect numbers prior to when they cause economic injury by disrupting the pest's life cycle and curbing population growth. Integrating phenology models into comprehensive decision support systems (e.g., forecasting models) can assist with the development of control programs that operate over wide geographical scales with varying climatic conditions. Additionally, phenological models can also contribute to risk assessment by predicting the potential establishment, spread, and damage risks for pest species based on local climatic conditions (Jarvis and Baker, 2001; Jones et al., 2009). Therefore, phenology data collected from replicated field

surveys over time can be used to develop sustainable pest management strategies that minimize reliance on broad-spectrum pesticides because of increased precision of treatment timings targeting specific life stages (e.g., eggs). This field data-driven approach ultimately supports the foundations of integrated pest management (IPM) programs targeting agricultural pests (Pedigo, 1999).

Pseudacysta perseae (Heidemann) (Hemiptera: Tingidae), commonly known as the avocado lace bug (ALB), is an oligophagous insect specializing on species in the family Lauraceae (Hoddle, 2004). *Pseudacysta perseae* has predominantly been observed feeding on avocados (*Persea americana* Miller), along with ornamental plants such as redbay (*Persea borbonia* [L.]) and camphor (*Camphora officinarum* Nees) (Hoddle et al., 2005). *Pseudacysta perseae* is purportedly native to parts of the Caribbean, Mexico, and the southeastern United States (Mead and Peña, 1991). In 2004, *P. perseae* (haplotype A [Rugman-Jones et al., 2012]) was discovered infesting backyard avocado trees in southern San Diego County (Hoddle et al. 2007). In 2017, *P. perseae* suddenly expanded its range and was discovered for the first time in commercial avocado orchards in northern San Diego Co. (2017), Riverside Co. (2017), Los Angeles Co. (2019), Orange Co. (2022), and Santa Barbara Co. (2023) (Hoddle, 2022). In 2019, *P. perseae* was detected for the first time from four islands in Hawai'i (Hoddle, 2022). This more "aggressive" *P. perseae* population was subsequently identified as haplotype G (see Chapter 3).

California is the top avocado-producing state in the United States, contributing to 90% of the nation's total production, with over 48,000 acres in production and an annual crop valued at $487 million (US) (USDA/ERS, 2022). The Hass cultivar of avocados represents 94% of the total production in California with a value of $458 million (US), followed by Lamb Hass (~3%), Gem (~2%) and other cultivars (e.g., Fuerte) (~1%) (CAC 2023). Consequently, *P. perseae* feeding activity presents a significant threat to avocado producers, as nymphs and adults feed in large

colonies clustered on the undersides of mature avocado leaves (Hoddle, 2004; Humeres et al., 2009b; Peña et al., 2012). *Pseudacysta perseae* infestations can cause significant damage to foliage, leading to premature leaf drops and reduced fruit yields (Hoddle et al., 2005). This pest regularly reaches economically damaging levels in Florida, Dominican Republic, and most recently, Hawai'i (Peña, 2003; Hoddle et al., 2005; Lyte, 2021). Additionally, extensive feeding damage renders leaf tissue susceptible to opportunistic leaf anthracnose fungi, particularly *Colletotrichum* spp. (Hoddle et al., 2005). The proliferation of fungi in damaged leaf tissue results in large necrotic areas, often centrally located on leaves that can also lead to premature defoliation (Peña et al., 1998).

A previous two-year study (1995-1997) on *P. perseae* phenology conducted in Florida (likely haplotype G), found that *P. perseae* density and the associated leaf area damage began to increase in September, reaching a peak between February and March, followed by a rapid decline from April through September (Peña et al., 1998). This trend is believed to be influenced, in part, by flower bloom and leaf flush periods of infested avocado varieties (Peña et al., 1998). A three-year study (2005-2008) carried out in San Diego indicated that *P. perseae* populations (haplotype A [Rugman-Jones et al., 2012]) begin to increase in June, peak in October, and then steadily decline from November through May (Humeres et al., 2009a).

Significant leaf feeding damage caused by persea mite, *Oligonychus perseae* Tuttle, Baker and Abbatiello (Acari: Tetranychidae), an invasive spider mite native to Mexico, occurs annually in the majority of California avocado orchards (Hoddle, 1998; Hoddle and Morse, 2013). The addition of *P. perseae* has increased damage from an invasive guild of leaf feeding pests, and together with tip burn, which results from excessive chloride salts in irrigation water, has increased levels of necrotic damage to leaves. Despite the probable deleterious impacts from

P. perseae and *O. perseae* feeding damage and tip burn, there are no estimates on their concurrent contributions to overall leaf damage.

The behavior wherein females lay eggs and incrementally add to the cluster over time, is a deliberate reproductive strategy, termed as "egg dumping," a behavior observed in a sub-social tingid, *Garaphia solani* (Tallamy, 1985; Tallamy and Horton, 1990). The trade-off between maternal care time and fecundity suggests egg clustering is an adaptive strategy, enabling females to indirectly enhance their fitness by minimizing risk to offspring from predators (Tallamy and Horton, 1990; Loeb et al., 2000). There are currently no studies on the reproductive behavior of *P. perseae* that tend to lay their eggs in clusters.

In this study, we quantified *P. perseae* (haplotype G) and natural enemy densities, percent leaf infestation levels and estimations of leaf area damaged by *P. perseae* and *O. perseae* feeding, and tip burn, across four commercial Hass avocado orchards (two sites within a cool coastal influence zone and two interior sites with higher average temperatures) in northern San Diego County. Each metric was evaluated monthly over a two-year period. Additionally, patterns of egg laying by *P. perseae* females on avocado leaves were investigated as "egg-dumping" was suspected to occur. The results of this field work are presented here, offering insights into the reproductive strategies of the species and their implications for avocado cultivation.

MATERIALS AND METHODS

Study Sites

Field data on *Pseudacysta perseae* infestations across five avocado cultivars (Hass, Gem, Fuerte, Reed, and Zutano) were collected every four weeks from four commercial avocado orchards in San Diego County, California over a two-year period from November 2021 to

October 2023, inclusive, for a total of 26 sampling dates. Sites 1 and 2 were in Oceanside, San Diego County (within the cool coastal influence zone) at an elevation of 90m and 122m respectively. Sites 3 and 4 were in Bonsall, San Diego County (within the warmer interior zone) at an elevation of 205m and 315m respectively. Orchard sizes ranged from ~2 to ~4 hectares. Study sites 1 and 2 (CCOF certified organic) did not use any insecticides over the course of this study. Sites 3 and 4 received one aerial spray with active ingredient, Abamectin, (Agri-Mek® SC miticide/insecticide, 8% conc., 0.2 liters applied per hectare) for persea mite (*O. perseae*), avocado brown mite (*Oligonychus punicae* Hirst [Acari: Tetranychidae]), and a foliar fertilizer application in July 2022.

For each month of this study, data on average air temperature (°C) and average relative humidity (%) were sourced from nearby weather stations (data were downloaded from https://www.wunderground.com/). Station 48 in Carlsbad, located within 20 km of the two Oceanside study sites; and Station 43 in Bonsall, approximately 8 km from the two Bonsall study sites, facilitated comparisons between the cooler coastal Oceanside area and the warmer inland Bonsall area.

The Hass cultivar (all trees were approximately 2- 25 years of age and around 15- 20 m in height) accounted for >95% of planted trees at all four study sites. Four non-Hass cultivars were identified across the four orchards and marked with flagging tape; Fuerte (four at site 4 only), Gem (four at site 2 only), Reed (four at site 1 and two at site 4), and Zutano (one at site 1 and four at site 4).

Every month, ten Hass trees were randomly selected throughout orchards 1-4 for sampling for a total of 40 trees. Additionally, a total of three Reed (two at site 1 and one at site 4), three Zutano (one at site 1 and two at site 4), two Fuerte (at Site 4) and two Gem (at site 2) were

sampled. Trees selected for sampling were subjected to three different sampling methods; (1) random leaf selection for estimating percentage leaves infested with *P. perseae*, (2) targeted sampling of infested leaves to determine average infestation rates by *P. perseae* life stage, and (3) tap sampling for natural enemies.

Monitoring Infestation Rates and Densities of *Pseudacysta perseae* and *Oligonychus perseae*

Random sampling of leaves consisted of selecting two leaves in each cardinal quadrant (i.e., north, south, west, and east) of the tree for a total of eight leaves per randomly sampled tree in each orchard. Leaves were scored for the presence or absence of *P. perseae,* and these data were used to calculate the percentage of leaves infested with *P. perseae* for each sampling date at each orchard. Targeted sampling required the removal of two leaves infested with at least one *P. perseae* life stage (i.e., egg, nymph, or adult) from each cardinal quadrant. Targeted sampling was conducted to determine average *P. perseae* densities on infested leaves. For targeted sampling, infested leaves were identified by the presence of necrotic feeding spots caused by *P. perseae* colonies. Excised leaves with *P. perseae* were placed in cotton bags with labels that identified orchard, cultivar, tree number, and cardinal quadrant from which the leaves were collected. Cloth bags were stored in coolers and returned to the laboratory and stored in a refrigerator at ~4ºC. Leaves were examined under a stereoscopic microscope and all *P. perseae* life stages (i.e., eggs [hatched and unhatched], first through fourth instar nymphs, and adult males and females) were counted and recorded by sampling date, cultivar, site, tree number sampled, cardinal quadrant, and leaf number from each quadrant. To monitor *O. perseae* densities on leaves infested with *P. perseae*, the absolute number of all feeding life stages (i.e., proto and deuteronymphs and adults)

of *O. perseae* was recorded for each leaf sample. The presence or absence of *O. perseae* feeding damage on *P. perseae* sampled leaves was also recorded.

Egg Clusters

Numerous field observations of *P. perseae* females on sampled leaves alongside multiple egg clusters prompted an investigation into the size of these egg clusters and the impact of female density on them. To investigate "egg dumping" by *P. perseae*, the variation in egg cluster size was assessed by sampling a sub-set of the two-year sampling period between November 2022 and May 2023. The precise number of eggs in each egg cluster (n= 1,550 clusters counted) laid during the sampling period was recorded for each leaf sample.

Natural Enemy Sampling

Each month, each of the ten randomly selected trees were tap sampled for potential *P. perseae* natural enemies. Foliage was sampled in each cardinal quadrant of sampled trees by hitting branches with a wooden stick under which an elliptical shallow white plastic dish (35 cm long x 25 cm wide) was placed to catch dislodged arthropods that could be potential natural enemies of *P. perseae*. Potential natural enemy taxa including predatory thrips (Aeolothripidae), predatory insects (Coccinellidae and Chrysopidae) and mites (Anystidae) were aspirated into vials labelled by site and collection date. Aspirated natural enemies in labeled vials were preserved in 95% ethanol and maintained in a freezer at ~-3ºC until identified.

Measuring Leaf Damage caused by *Pseudacysta perseae* and *Oligonychus perseae* Feeding and Tip Burn

To assess levels of *P. perseae* feeding damage to leaves over time, and the relationship between observed damage levels and *P. perseae* population densities, avocado leaves with *P.*

perseae feeding damage were subjected to automated image analyses. Each month, the eight avocado leaves collected from each of the ten experimental avocado trees at each of the four study sites using the targeted sampling method were used to estimate the area of the leaf damaged by *P. perseae* feeding.

Of the maximum total number of 320 leaves collected each month from targeted sampling across the four sampling sites, a randomly selected sub-sample of up to 100 damaged Hass avocado leaves were digitally-scanned using a flatbed scanner (Epson Perfection V600 Photo, Seiko Epson Corp.) at 600 DPI. Each digitized leaf image was saved with its unique collection details (i.e., date of collection, avocado cultivar, site number, tree number, and quadrant-leaf number).

When the total number of damaged leaves exceeded 100, a proportional sub-sampling method was used to account for the variation in numbers of damaged leaves across the four study sites. Hence the number of leaves analyzed for each site was determined as the proportion of total leaves damaged across all sites and these estimated proportions were used to divide the total number of 100 leaves accordingly (i.e., if site 1 accounted for 33% of the total damaged leaves collected for a particular month, 33 randomly selected leaves were scanned for site 1). Random selection of leaves from each site for scanning was accomplished using the "RAND" function in Excel. For sampling events when the total number of damaged leaves was less than 100 all damaged leaves were scanned.

Image J software (see Pride et. al., 2020 for details on using Image J to measure leaf damage; software was downloaded from https://imagej.net/Fiji/Downloads) was used to analyze scanned leaf images. Image J was used to calculate the total area of the leaf and leaf area damaged by *P. perseae* and *O. perseae* feeding, and tip burn (Figure 2.1). The leaf area damaged

by *P. perseae* feeding was characterized by necrotic areas on the underside of the leaf accompanied by the presence of at least one *P. perseae* life stage. *O. perseae* feeding damage was characterized by circular necrotic spots along the midribs and lateral leaf veins, and leaf area damaged due to leaf tip burn, the accumulation of chloride salts from irrigation water, was characterized by "burned" necrotic leaf tips and margins.

Yellow Sticky Trap Monitoring

To monitor monthly flying activity by adult *P. perseae* three yellow sticky traps (18 cm x 24 cm, Great Lakes IPM GL/OL-0612-12) were attached to branches of three randomly selected avocado trees across each of the four study sites for a total of twelve sticky traps deployed each month. Each month, labeled traps in each orchard were removed and replaced with new traps. Upon collection, a clear acetate sheet was placed on each sticky trap and returned to the lab in a cooler. Sticky traps were stored at −4°C until they were examined under a stereoscopic microscope for the presence of adult *P. perseae*. The number of *P. perseae* males and females for each trap were recorded by trap deployment date for each study site.

Preparation of Data Summaries

All graphs (Figure 2.2- 2.16) were created in Microsoft Excel using pivot tables or the chart function. Each avocado variety (i.e., Hass [n=40 trees sampled], Fuerte [n=2], Gem [n=2], Reed [n=3], and Zutano [n=3]) was analyzed separately for *P. perseae* infestation rates and density due to the significant difference in sample sizes.

Egg cluster sizes were categorized into bins of 1, 2, 3, 4-6, 7-9, 10-12, 13-15, 16-20, 21-25, 26-35, up to 180-220 to analyze the distribution of variation in egg cluster sizes. Log to base

10 was utilized to visualize variation in egg cluster size accommodating for disparities in sample sizes among egg clusters.

The number of sampled leaves with and without *P. perseae* and *O. perseae* feeding damage was determined using the COUNTIFS function in Microsoft Excel.

RESULTS

Pseudacysta perseae Phenology and Cultivar Use

The two-year survey data from four commercial Hass avocado orchards on percent infestation and density of *P. perseae* feeding stages indicated that infestation levels are highest during fall and winter (i.e., September- February), and the highest population densities are observed from summer through Fall (i.e., June- October) (Figure 2.2). Analyses of the mean densities for each *P. perseae* feeding life stage showed that adult densities peaked in October, early (i.e., 1st and 2nd) instar nymphs peaked in winter (i.e., January- February), and late (i.e., 3rd and 4th) instar nymphs peaked in summer (i.e., June- July) (Figure 2.3). The mean density of *P. perseae* eggs showed a peak winter, particularly in February, when the highest numbers of unhatched eggs were observed. Egg density, both hatched and unhatched, increased in the fall, and peaked in winter (October- February), and subsequently decreased from spring into summer (March- August) (Figure 2.4).

Over the 26 sampling dates over November 2021 to October 2023, the mean densities of female adults were higher than those of males on 17 of these dates (Figure 2.5). Male densities showed a tendency to exceed those of females during the fall months (September- November).

Monthly sampling of four non-Hass avocado cultivars (i.e., Fuerte, Gem, Reed, and Zutano) showed that among the non-Hass cultivars, Reed had the highest levels of *P. perseae*

infestation and feeding stage densities, followed by Zutano with slightly lower infestation levels, and feeding stage densities. Gem experienced minimal to no infestations, and Fuerte had no measurable *P. perseae* infestations for the full two years of this study despite close proximity to infested Hass trees (Figure 2.6 and Figure 2.7).

Climate Conditions

In a weather-based comparative analysis between the cooler coastal Oceanside sites and the warmer inland Bonsall sites, Oceanside recorded higher mean monthly average densities of *P. perseae* on 20 of the 26 sampling dates (Figure 2.8 a-b). In the first year, Bonsall had higher average temperatures in spring and summer compared to Oceanside, while in the second year, temperatures at both locations were similar (Figure 2.8 a). Oceanside consistently showed higher humidity levels across both years of this study (Figure 2.8 b).

Egg Cluster Size

The variation in egg cluster sizes demonstrated a trend of higher frequency for smaller clusters, and fewer larger cluster sizes observed on sampled leaves (Figure 2.9). For very small cluster sizes (1-3 eggs), the highest frequency is observed in the smallest cluster size of 1 (i.e., 32,727 single egg depositions were observed) followed by a significant drop for egg clusters consisting of two (i.e., 5,940 clusters of two eggs), and three eggs (i.e., 2,450 clusters of three eggs). Small to medium cluster sizes (4-12 eggs) showed a gradual decline in frequency from clusters of size 4-6 (2,378) to clusters of size 10-12 (523), indicating that as egg clusters increased in size, they became less common. Medium to large cluster sizes (i.e., 13-45 eggs) showed relatively consistent frequencies, ranging from 190 to 285, without a sharp decline. A slight increase in frequency for egg clusters of size 36-45 (227) was observed. This may indicate a specific biological or environmental factor favoring this size range under certain conditions. The

frequency of large cluster sizes (i.e., 46-85), declined sharply. Very large clusters (i.e., 86-220 eggs) were rare with very low frequencies of occurrence on Hass avocado leaves (1- 9 clusters observed). Sampled leaves with egg clusters made up of two or more eggs (n=1,304) had a positive significant relationship (r^2 =0.048; P< 0.0001) between the number of females counted on leaves and the number of observed egg clusters (Figure 2.10).

Predator Abundance

The natural enemy sampling targeting generalist predator families indicated that there is an increase in predator population densities during late fall and winter (Figure 2.11), These periods coincide with the highest densities of *P. perseae* feeding life stages in the fall and the peak in *P. perseae* egg densities during the winter. Aeolothripidae populations peak in the winter months (i.e., November- January) and appear to be the sole generalist predator that is correlated with fluctuations in the density of *P. perseae* feeding stages. (Figure 2.11). Aeolothripidae populations increased significantly after *P. perseae* densities peaked in February 2022, June 2022, October 2022, February 2023, July 2023, and September 2023. Chrysopidae increases in abundance were observed between October to January (Fall- Winter). Coccinellidae densities peaked in October. Salticidae increased in abundance between August and October (Summer-Fall); and Anystidae peaked in late Fall (November- December) and spring (April- May) (Figure 2.11).

Leaf Area Damage Analyses

Leaf area analyses revealed that the highest percentage of damage caused by *P. perseae* feeding was observed in Fall, specifically from September to November (Figure 2.12). *P. perseae* leaf damage ranged from 1.3 to 16% each month. Generally, an increase in *P. perseae* population during any given month was observed to precede a corresponding rise in percent leaf damage in

the subsequent month. The cumulative mean leaf damage caused by *O. perseae* feeding and leaf tip burn along with *P. perseae* feeding damage surpassed 10% in most months, with peak cumulative damage recorded in October 2021 and April 2022 reaching 28% and 27%, respectively (Figure 2.13). A notable increase in leaf tip burn was observed during the winter and spring months (i.e., January- April).

The comparative analysis of mean percent leaf area damage and mean feeding stage densities of *O. perseae* and *P. perseae* showed that both species caused varied levels of feeding damage. *Pseudacysta perseae* caused a higher percentage leaf area damage than *O. perseae* on 21 out of the 26 sampling dates (Figure 2.14). The increase in *O. perseae* density in September 2022 was followed by an increase in mite feeding damage to leaves in October and November. Similarly, a sharp increase in *O. perseae* density in July 2023 was followed by an increase in leaf damage in September and October. The likelihood of both species causing damage to the same avocado leaf peaked in fall (September- November) and winter (December- February) with the proportion of leaves with damage from both species being around 0.43 and 0.46, respectively (Figure 2.15). In spring (March- May), there was a higher likelihood of neither species causing leaf damage, though when present, *O. perseae* caused more damage than *P. perseae*. Conversely, in summer (June- August), *P. perseae* was more damaging than *O. perseae*.

Sticky Trap Captures

Sticky trap capture data indicates that *P. perseae* adults engage in active flight or wind-assisted dispersal from summer through fall (i.e., July-November) (Figure 2.16). Sticky card sampling revealed that a higher number of male counts were typically detected on traps, except in fall (i.e., September and October) when captured females outnumbered males (Figure 2.16).

DISCUSSION

The analysis of two-years of field data collected from four commercial Hass avocado orchards in San Diego County provides a comprehensive view of the seasonal population dynamics of *P. perseae* and the first time these types of data have been collected for haplotype G in California. Observed infestation levels and temporal changes in densities of *P. perseae* life stages indicates that time of year has an important effect on the phenology of this pest in commercial Hass avocado orchards. Densities of *P. perseae* life stages showed a pattern of low densities from winter through spring (i.e., December- April), followed by an increase from summer through fall (i.e., June- October). The peak incidence of necrotic leaf damage caused by *P. perseae* feeding damage occurred in the fall, coinciding with population increases over summer through fall. Notably, despite this increase in *P. perseae* population density during the summer, the percentage of Hass avocado leaves infested in sampled orchards remained relatively low (ranging from 2- 8%). This observation is likely attributed to the period of leaf drop and subsequent leaf flush for Hass avocados in San Diego, which spans March to June (Dreistadt et al., 2008). During this period, as older leaves from the previous season are shed in the spring, *P. perseae* populations become concentrated on a smaller number of newly emerged leaves. As the summer progresses, the number of maturing leaves that are most preferred for feeding and egg laying increases, and *P. perseae* percent infestation levels rise correspondingly, with densities peaking in the fall.

The increase in percent leaf infestation during fall and winter months can be attributed to the life cycle of *P. perseae*. The density of adult *P. perseae* peaks in October. Adults mate and lay eggs during this time, leading to a surge in egg-laying activity by February. Subsequently, the population of early instars rises as eggs laid over winter and spring begin to hatch. The peak

densities of late instar nymphs were observed in the summer reflecting the developmental requirements of *P. perseae* when the warmer summer months accelerate growth (see Chapter 1 on the effects of temperature on *P. perseae* developmental rates). Consequently, this leads to a new generation of adults by October, ready to reproduce and lay eggs, thus continuing this observed phenological cycle. The predominance of females (i.e., 35-80%) in the majority of sampling periods contributed to population growth. Furthermore, the timing of these summer through fall infestations coincided with the availability of suitable mature leaves following the spring leaf flush for nymphs and adults to feed on, and for oviposition. Identifying these seasonal population dynamics, characterized by a predictable cyclical pattern of egg laying, nymph development, and adult maturation of *P. perseae* is key to determining crucial intervention periods for effective population management by targeting vulnerable life stages most susceptible to control.

Comparison of climatic data for the coastal Oceanside to the inland Bonsall sites showed consistently higher humidity and generally lower overall temperatures in Oceanside, coupled with greater pest densities when compared to Bonsall. This suggests that these climatic factors, especially humidity, may have an impact on *P. perseae* population growth. The cooler temperatures in Oceanside during the first sampling year, relative to Bonsall, suggests that *P. perseae* may favor cooler, more humid climates. Furthermore, the similarity in temperatures between the sites in the second year, with ongoing higher pest densities in Oceanside, suggests that humidity could be a more crucial factor than temperature influencing *P. perseae* population densities. This finding underscores the importance of incorporating prevailing temperature and humidity trends into pest management plans.

The monthly sampling of a small number of four non-Hass avocado cultivars: Fuerte (n=2), Gem (2), Reed (3), and Zutano (3) indicated that the Reed cultivar was the most susceptible to *P. perseae* infestation, exhibiting the highest levels of infestation and densities of

feeding stages. Following Reed, the Zutano cultivar showed the next highest infestation levels and pest densities. In contrast, the Gem cultivar displayed minimal to no infestation and maintained very low densities of *P. perseae*. Remarkably, the Fuerte variety showed complete resistance, with no observed *P. perseae* feeding stages throughout the two-year sampling period despite close proximity to infested Hass trees.

Studies to investigate egg dumping showed a preference of *P. perseae* for producing small egg clusters (i.e., 1-6 eggs in a cluster) laid on leaves. This was coupled with a noticeable decline in frequency as cluster size increased, possibly due to the increased time required to find and contribute eggs to existing clusters. Interestingly, the stability in frequency of medium to large cluster sizes, and the peculiar increase in clusters of 36-45 eggs, may suggest environmental (e.g., optimal humidity maintenance) or biological (e.g., increased protection from natural enemies) influences that favor certain egg cluster sizes. Furthermore, the positive correlation between increasing densities of ovipositing females on leaves and the number of eggs in clusters suggests that there may be a communal aspect to egg laying behavior, as it is likely that different females contribute eggs to clusters. This possibility hints at sub-social behavior in *P. perseae* and warrants further exploration to determine if there are fitness advantages (e.g., lower risk of predation or increased protection from humidity extremes as egg cluster size increases) for females that engage in communal egg clustering (Tallamy, 1985; Tallamy and Horton, 1990).

Laboratory studies have shown that larval and adult *Franklinothrips orizabensis* (Johansen) (Thysanoptera: Aeolothripidae) and larval *Chrysoperla rufilabris* (Burmeister) (Neuroptera: Chrysopidae) actively prey on *P. perseae* eggs and nymphs, though their impacts under field conditions are unknown (Humeres, 2009b). In this study, *F. orizabensis*, *Franklinothrips vespiformis* (Crawford), and *C. rufilabris* were collected during tap sampling, indicating the presence of these natural enemies in commercial Hass avocado orchards infested

with *P. perseae*. Previous studies have identified Coccinellidae as predators of tingids, and this study corroborated the presence of the genera *Chilocorus*, *Coccinella*, *Stethorus*, *Harmonia*, and *Psyllobora*, all previously recognized as predators of tingid species (Aysal and Kivan, 2014; Maral et al., 2020; Aysal and Kivan, 2023), with *P. perseae* infestations. Anystidae, which are widespread generalist predators, are known to attack hemipterans, including aphids and psyllids, and this suggests that these mites might prey on vulnerable *P. perseae* life stages (e.g., eggs and small nymphs). In this study, *Anystis baccarum* (Linnaeus) (Acari: Anystidae) was collected during tap sampling, indicating the regular presence of this natural enemy. In general, natural enemy densities appeared to increase over late fall and into winter, possibly showing a delayed density dependent response to *P. perseae* densities that increased during summer through fall. Apart from Aeolothripidae, there were no apparent relationships between predator densities and *P. perseae* densities, suggesting that these predators do not react to the availability of *P. perseae* as a food source. This observation suggests that the sampled natural enemy guilds likely do not exert substantial control over *P. perseae* populations, because their phenological cycles and densities do not align closely with *P. perseae* density fluctuations. Consequently, *P. perseae* may be benefiting from a lack of natural enemies which facilitates population growth in California avocado orchards.

The addition of *P. perseae* feeding damage to two existing damage sources (*O. perseae* and leaf tip burn), increased the overall leaf damage levels by 8%. Automated image analyses of damaged leaves indicated that Hass avocado leaves are most susceptible to *P. perseae* feeding damage in the fall (September- November). *O. perseae* feeding damage increases over fall through winter (September- October), and leaf tip damage accumulates during winter through spring (January- April). This clear delineation of seasonal leaf damage from three different sources provides insights for growers when considering the timing of management strategies to

maximize pest control impacts and water management to reduce pest densities and subsequent leaf damage from pest feeding and irrigation water with high salt content. However, the overall impacts of leaf damage from pest feeding and chloride-heavy water on avocado tree health and productivity and associated management strategies to ameliorate damage (i.e., insecticide applications) remains uncertain. This uncertainty highlights the need for additional research into how these factors (damage sources and management) affect overall fruit yields and quality (e.g., fruit size) and subsequent economic returns from performing necessary interventions (e.g., increased watering with higher quality water to mitigate chloride build up and tip burn severity).

Pseudacysta perseae and *O. perseae* occupy near identical niches, the undersides of mature avocado leaves. Over the two-year sampling period during which this study was conducted, distinct seasonal variations in the phenology of these two pests were observed. During winter and fall, there was a higher likelihood of both species co-occurring on the same leaf than either species being present alone, which suggests a potential for coexistence or possibly mutualistic relationships. Potential mutualisms from cohabitation of leaves may result from reduced risk from shared predators (e.g., predatory mites), beneficial alterations to the leaf environment that deter colonization by other pests that specialize on mature leaves (e.g., *Heliothrips haemorrhoidalis* [Bouchè] Thysanoptera: Thripidae]), or other interactions operating on or within the phylloplane that may create a more favorable environment for co-existence (e.g., reduction of secondary plant defense compounds to favor increased herbivory).

Sticky trap data showed consistent capture of more male *P. perseae* when compared to females, except during fall (September- October), suggesting that a gender-specific dispersal pattern may exist which could be dependent on time of year. The peak in *P. perseae* counts on sticky traps (i.e., July- November) corresponded with the peak in *P. perseae* density on the leaves (i.e., June- October) suggesting that dispersal may occur when population densities on infested

leaves are peaking, and leaf resources are deteriorating due to feeding damage. In comparison to the relatively high numbers of adult *P. perseae* collected on leaves in orchards, relatively few adults were captured on sticky traps. One potential explanation is that yellow is not an attractive color to flying *P. perseae* adults, which may potentially be attracted more strongly to different colors (e.g., blue, green, or white). This possibility warrants further investigation to identify sticky trap colors with increased attraction if sticky cards are to be used for monitoring *P. perseae* dispersal in orchards. Alternatively, it is possible that *P. perseae* adults seldom fly, and they are primarily dispersed by the wind (or human movement of infested plants) and exert minimal control over aerial movement and the flight path once airborne, and adults captured on yellow sticky cards are due to chance interceptions.

REFERENCES

Aysal, T., and M. Kivan. 2023. Natural enemies of Tingidae (Hemiptera) species in Tekirdağ province. *Journal of Tekirdag Agricultural Faculty* 20(2): 461–477.

Aysal, T., and M. Kivan. 2014. Occurrence of an invasive alien species *Harmonia axyridis* (Pallas) (Coleoptera: Coccinellidae) in Turkey. *Turkey Entomology Bulletin* 4.3: 141-146.

CAC. 2023. California Avocado Commission Annual Report 2022. Available online: https://www.californiaavocadogrowers.com/sites/default/files/2022-CAC-Annual-Report-Final.pdf (Accessed in January 2024)

Dreistadt, S. H., D. Rosen, and M. L. Flint. 2008. *Integrated Pest Management for Avocados*. Statewide Integrated Pest Management Program. University of California, Agriculture and Natural Resources, Publication 3503. Oakland, CA.

Hoddle, M. S. 1998. Biology and management of the persea mite. *California Avocado Society Yearbook* 82: 75-85.

Hoddle, M. S. 2004. Invasions of leaf feeding arthropods: why are so many new pests attacking California grown avocados? *California Avocado Society Yearbook* 87: 65–81.

Hoddle, M. S. 2022. Avocado lace bug is continuing to spread in California. *From the Grove* 12(2): 22-25.

Hoddle, M. S., and J. G. Morse. 2013. The persea mite invasion into California: History, biology, management and current status. *California Avocado Society Yearb*ook 95: 106-136.

Hoddle, M. S., J. Morse, R. Stouthamer, E. Humeres, G. Jeong, W. Roltsch, G. S. Bender, P. Phillips, D. Kellum, R. Dowell, G. W. Witney. 2005. Avocado lace bug in California. *California Avocado Society Yearbook* 88: 67–79.

Hoddle, M., J. Morse, R. Stouthamer. 2007. Biology and management of avocado lace bug in California. *Proceedings of the California Avocado Research Symposium*, pp. 1-11. California Avocado Commission.

Humeres, E. C., J. G. Morse, W. Roltsch, M. S. Hoddle. 2009a. Detection surveys and population monitoring for *Pseudacysta perseae* on avocados in Southern California. *Florida Entomologist* 92(2): 382-385.

Humeres, E. C., J. G. Morse, R. Stouthamer, W. Roltsch, M. S. Hoddle. 2009b. Evaluation of natural enemies and insecticides for control of *Pseudacysta perseae* (Hemiptera: Tingidae) on avocados in southern California. *Florida Entomologist* 92(1): 35-42.

Jarvis, C. H., and R. H. A. Baker. 2001. Risk assessment for nonindigenous pests: Mapping the outputs of phenology models to assess the likelihood of establishment. *Diversity and Distributions* 7: 223-235.

Jones, V. P., T. R. Unruh, D. R. Horton, N. J. Mills, J. F. Brunner, E. H. Beers, and P. W. Shearer. 2009. Tree fruit IPM programs in the western United States: the challenge of enhancing biological control through intensive management. *Pest Management Science.* 65: 1305–1310.

Loeb, M. L., L. M. Diener and D. W. Pfennig. 2000. Egg-dumping lace bugs preferentially oviposit with kin. *Animal Behavior* 59(2): 379-383.

Lyte, B. 2021. "Hawaii's avocado farmers are bracing for a new threat." Honolulu Civil Beat. Available online: https://www.civilbeat.org/2021/12/hawaiis-avocado-farmers-are-bracing-for-a-new-threat/.

Maral, H., M. R. Ulusoy and H. Bolu. 2020. Natural enemies of Tingidae (Hemiptera) species on trees in agricultural and non-agricultural areas in Diyarbakır, Mardin and Elazığ Provinces of Turkey. *Turkish Journal of Biological Control* 11(1): 7-2.

Mead, F. W. & J. E. Peña. 1991. Avocado lace bug, *Pseudacysta perseae* (Hemiptera: Tingidae). Florida Department Agriculture and Consumer Services, Division of Plant Industry. *Entomology Circular* 346: 4.

Nietschke, B. S., R. D. Magarey, D. M. Borchert, D. D. Calvin, and E. Jones. 2007. A developmental database to support insect phenology models. *Crop. Protection.* 26: 1444–1448.

Pedigo, L. P. 1999. *Entomology and pest management*, 3rd ed. Prentice Hall, Englewood Cliffs, NJ.

Pedigo, L. P., & M. E. Rice. 2006. *Entomology and pest management*, 5th ed. Pearson Prentice Hall, Upper Saddle River, N.J.

Peña, J. E. 2003. Pests of avocado in Florida. *Proceedings of V world avocado congress*, pp 487–494.

Peña, J. E., Duncan, R.E., Roltsch, W.J., Carrillo, D., 2012. Mortality factors of the avocado lace bug, *Pseudacysta perseae* (Heteroptera: Tingidae), in Florida. *Florida Entomologist* 95(1): 179-182.

Peña, J. E., S. Sundhari, A. Hunsberger, R. Duncan, and B. Schaffer. 1998. Monitoring damage, natural enemies, and control of avocado lace bug, *Pseudacysta perseae* (Hemiptera: Tingidae). *Proceedings of the Florida State Horticultural Society* 111: 330–334.

Pride, L., Vallad, G., Agehara, S. 2020. How to measure leaf disease damage using image analysis in ImageJ. UF IFAS Extension. Available online: https://edis.ifas.ufl.edu/publication/HS1382 (Accessed in November 2021).

Rugman-Jones, P. F., M. S. Hoddle, P. A. Phillips, G. S. Jeong, R. Stouthamer. 2012. Strong genetic structure among populations of the invasive avocado pest *Pseudacysta perseae*

(Heidemann) (Hemiptera: Tingidae) reveals the source of introduced populations. *Biological Invasions* 14(6): 1079-1100.

Tallamy, D. W. 1985. “Egg dumping” in lace bugs (*Gargaphia solani*, Hemiptera: Tingidae). *Behavioral Ecology and Sociobiology* 17: 357-362.

Tallamy, D. W. & L. A. Horton, 1990. Costs and benefits of the egg-dumping alternative in *Gargaphia* lace bugs (Hemiptera: Tingidae). *Animal Behaviour* 39: 352–359.

USDA/ERS. 2022. Avocados: Production, season-average grower price, and value, by state, 1980/81 to date. United States Department of Agriculture, Economic Research Service, Washington, D.C.

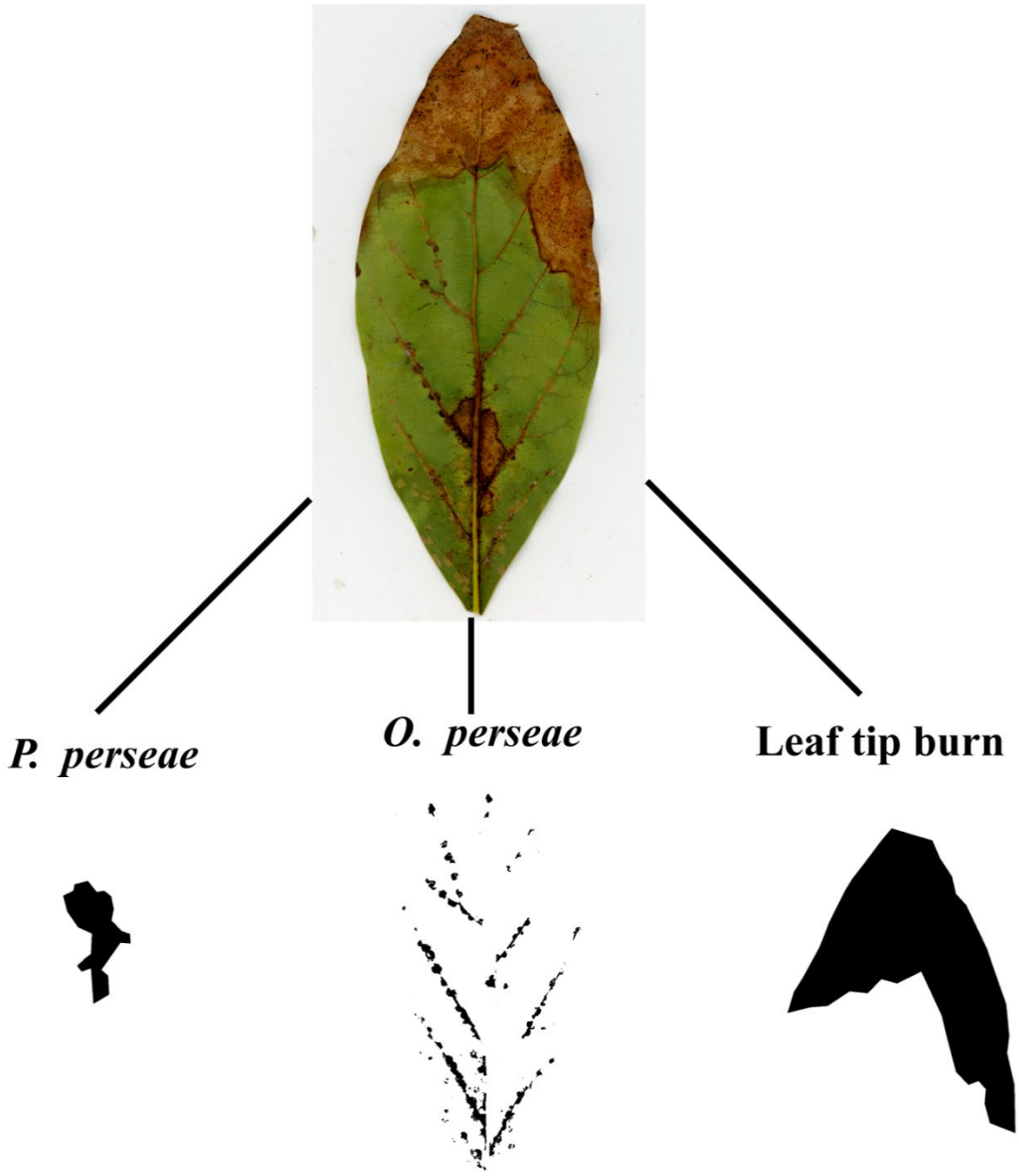

Figure 2.1 An example of an avocado leaf analyzed using Image J for image-based quantification of leaf area damage caused by *Pseudacysta perseae, Oligonychus perseae* feeding, and leaf tip burn.

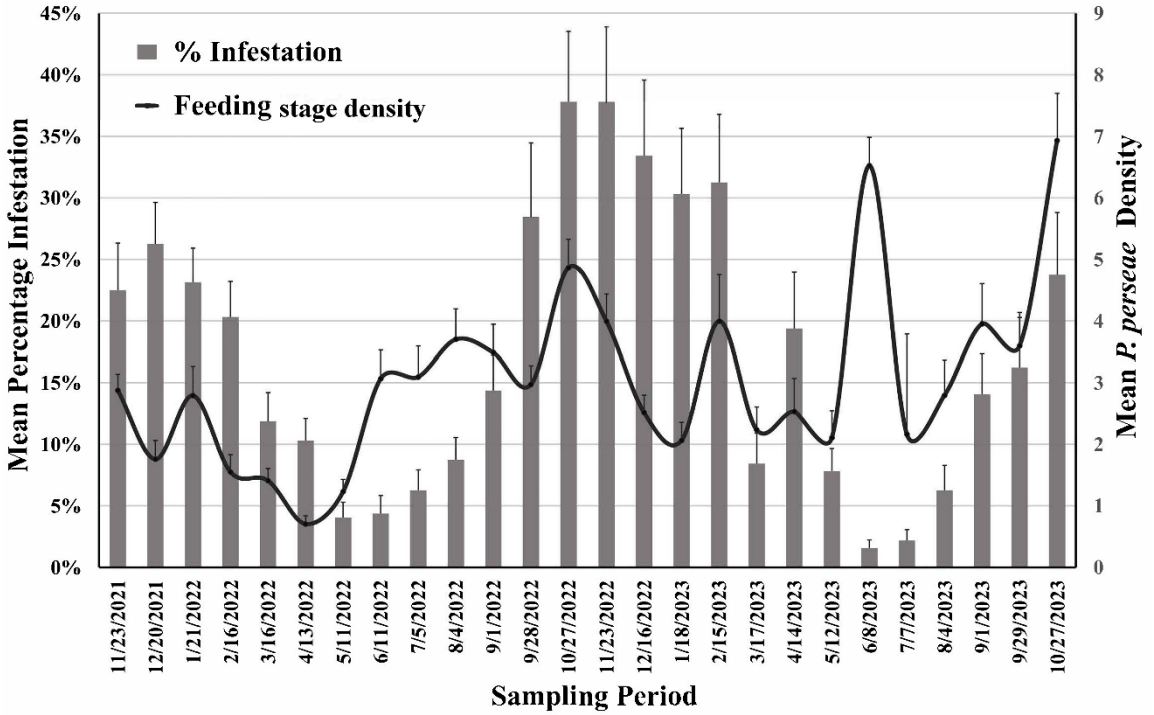

Figure 2.2 Relationship between mean monthly percent leaf infestation and mean monthly density of *Pseudacysta perseae* of all feeding life stages (i.e., first, second, third, and fourth instar nymphs, and adults) on Hass avocado leaves across four commercial Hass avocado orchards over a two-year sampling period (November 2021- October 2023).

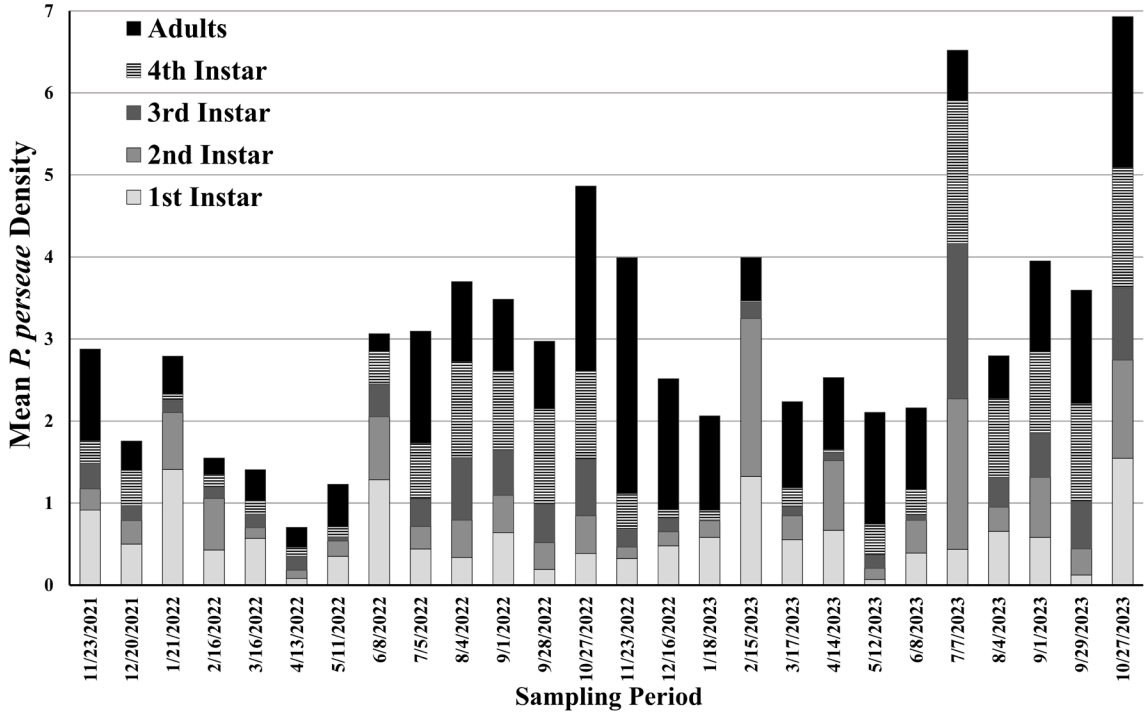

Figure 2.3 Mean monthly densities of *Pseudacysta perseae* feeding life stages (first, second, third, and fourth instar nymphs, and adults) across four commercial Hass avocado orchards over a two-year sampling period (November 2021- October 2023).

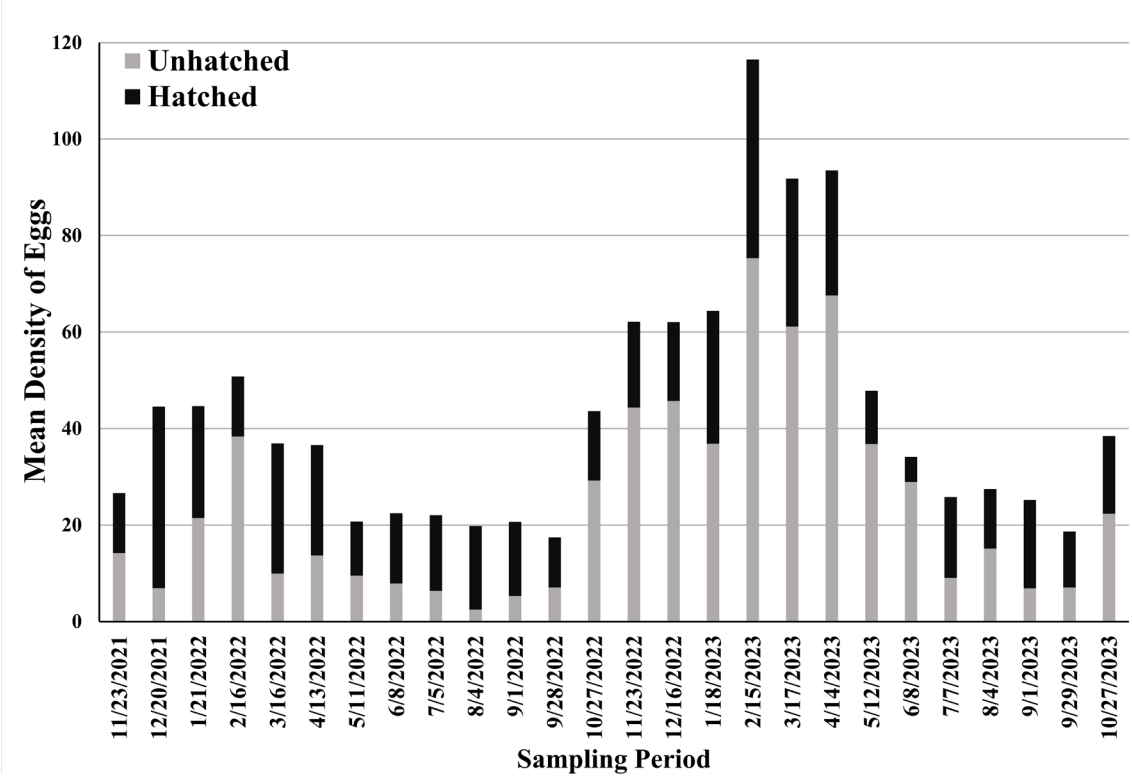

Figure 2.4 The mean monthly density of *Pseudacysta perseae* eggs (unhatched and hatched) across four commercial Hass avocado orchards over a two-year sampling period (November 2021- October 2023).

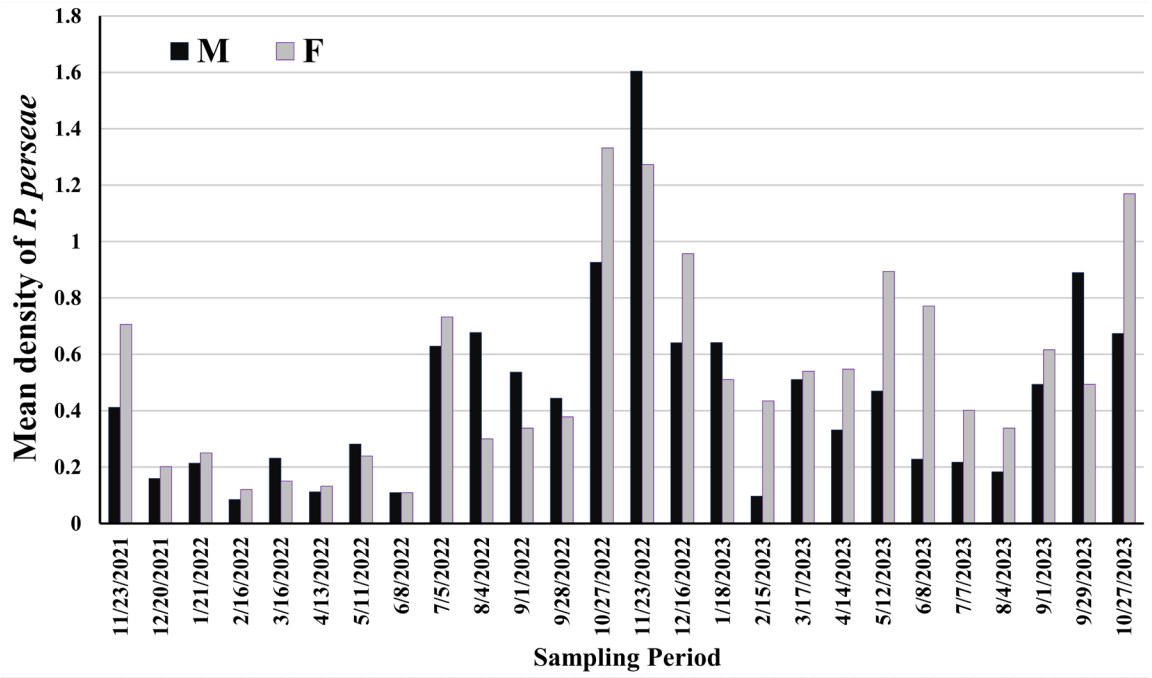

Figure 2.5 A summary of the mean monthly density of *Pseudacysta perseae* males (M) and females (F) across four commercial Hass avocado orchards over a two-year sampling period (November 2021- October 2023).

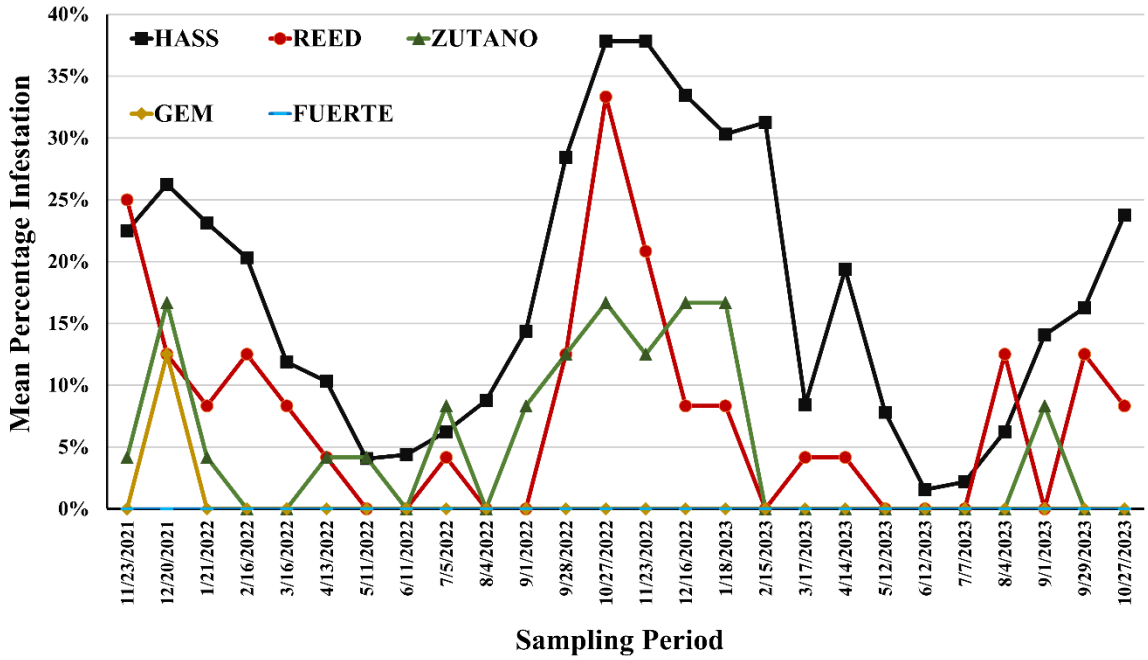

Figure 2.6 Mean percentage leaf infestation by *Pseudacysta perseae* on five avocado cultivars: Hass, Fuerte, Gem, Reed, and Zutano and across four avocado orchards over a two-year sampling period (November 2021- October 2023).

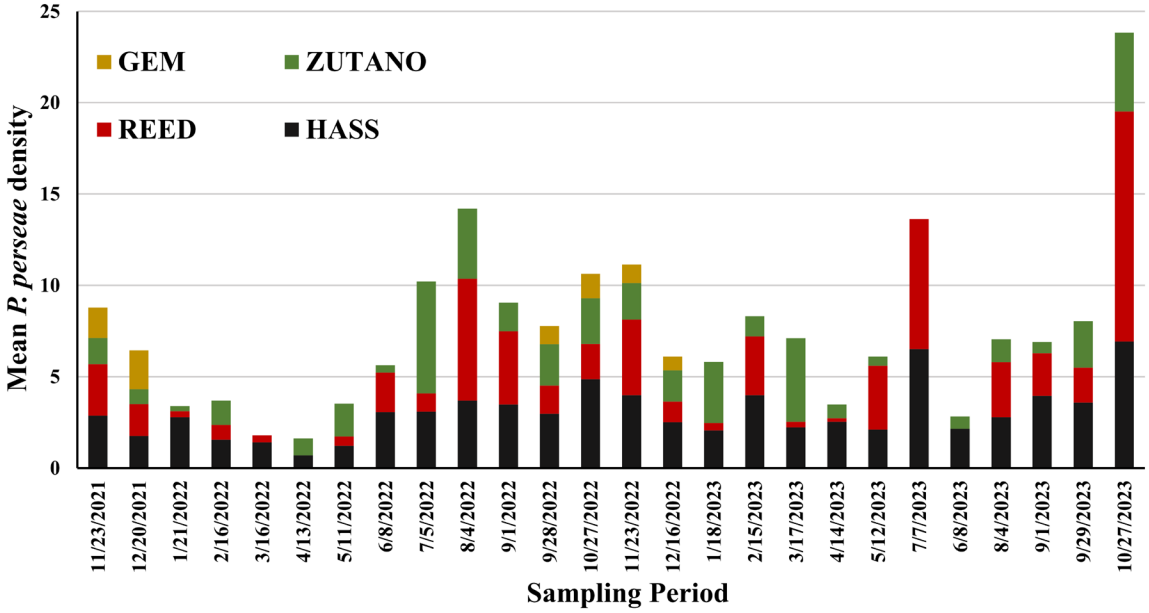

Figure 2.7 A summary of the mean monthly densities of *Pseudacysta perseae* feeding life stages for four cultivars: Hass, Gem, Reed, and Zutano across four avocado orchards over a two-year sampling period (November 2021- October 2023).

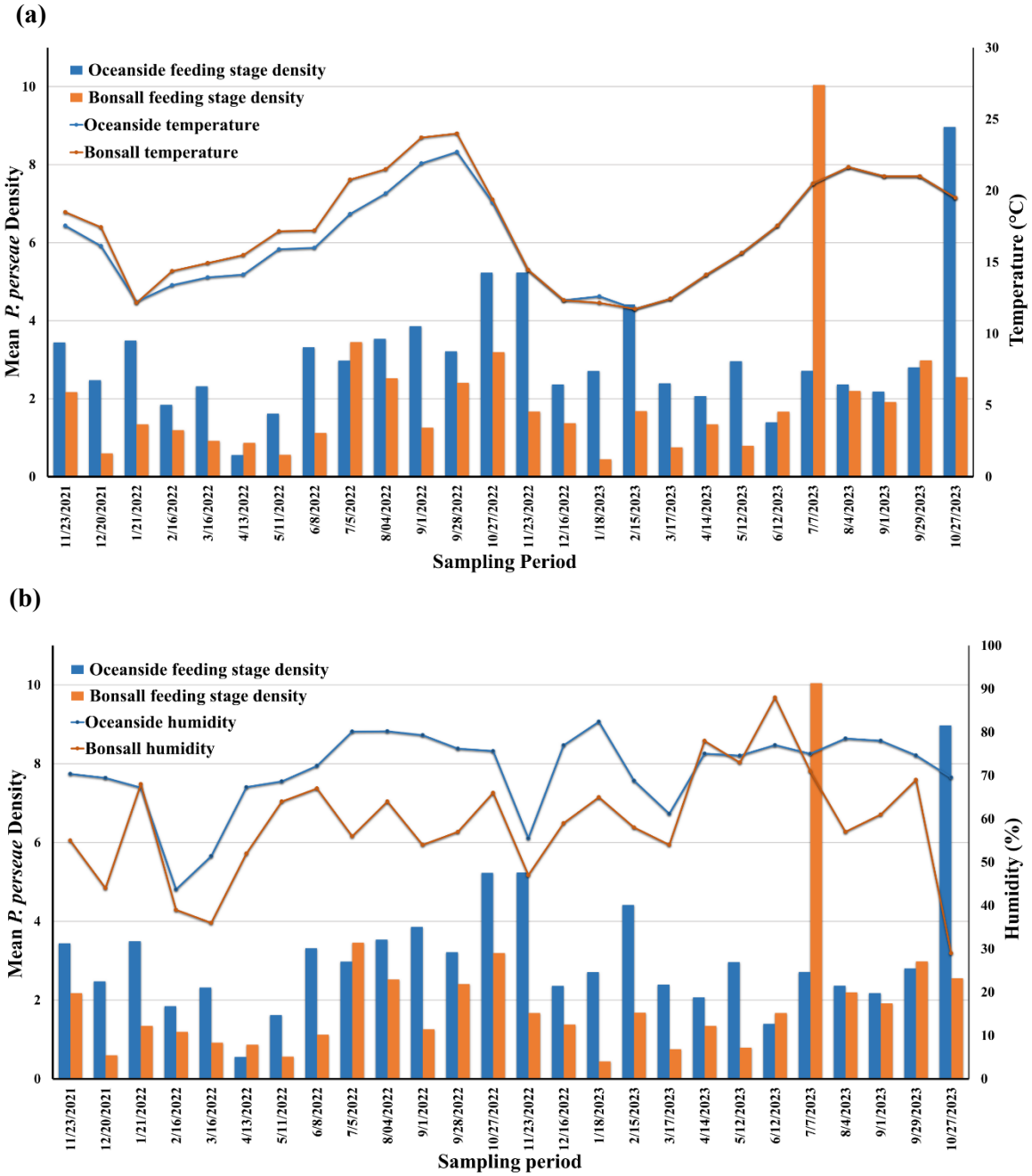

Figure 2.8 (a) Relationship between mean monthly densities of *Pseudacysta perseae* feeding life stages and average air temperature (in °C) (b) Relationship between mean monthly densities of *P. perseae* feeding life stages and average relative humidity (%) for four commercial Hass avocado orchards over a two-year sampling period (November 2021-October 2023).

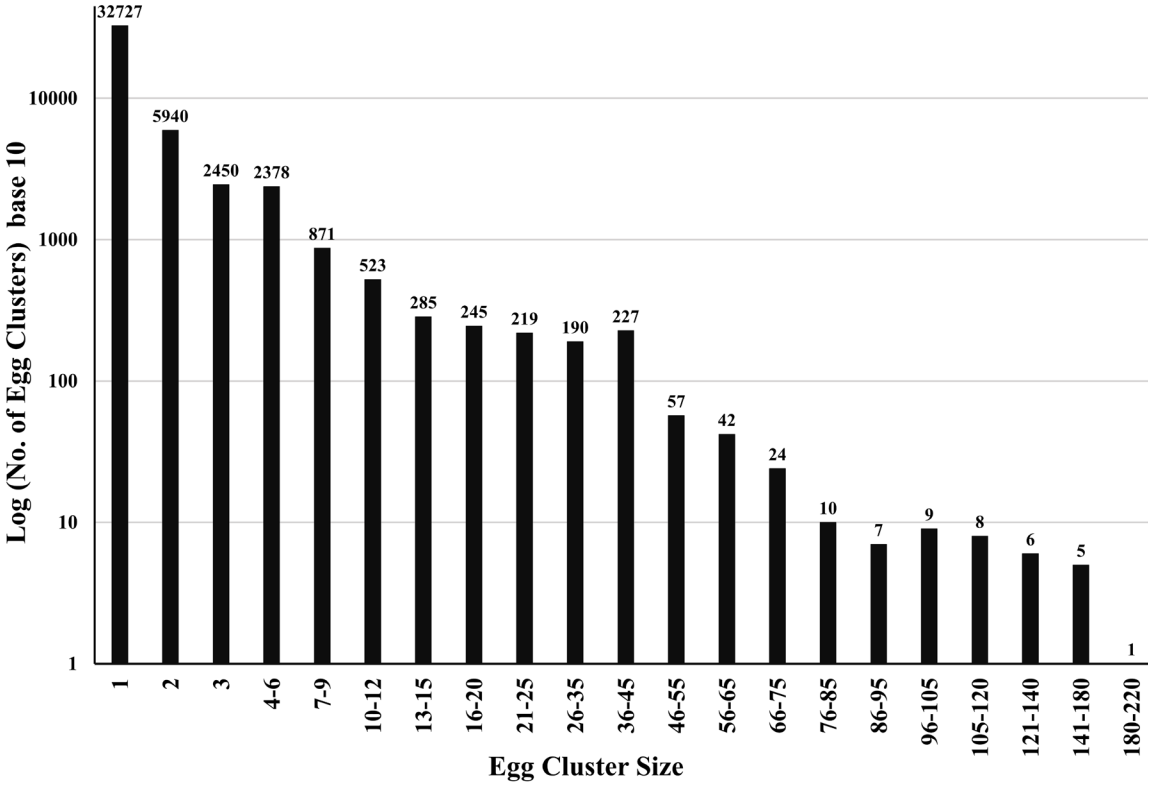

Figure 2.9 Variation in egg cluster size of *Pseudacysta perseae* observed on avocado leaves (n= 1550 egg masses) examined with number of clusters per bin size provided above each bar. Egg data were collected over a seven-month period, November 2022- May 2023.

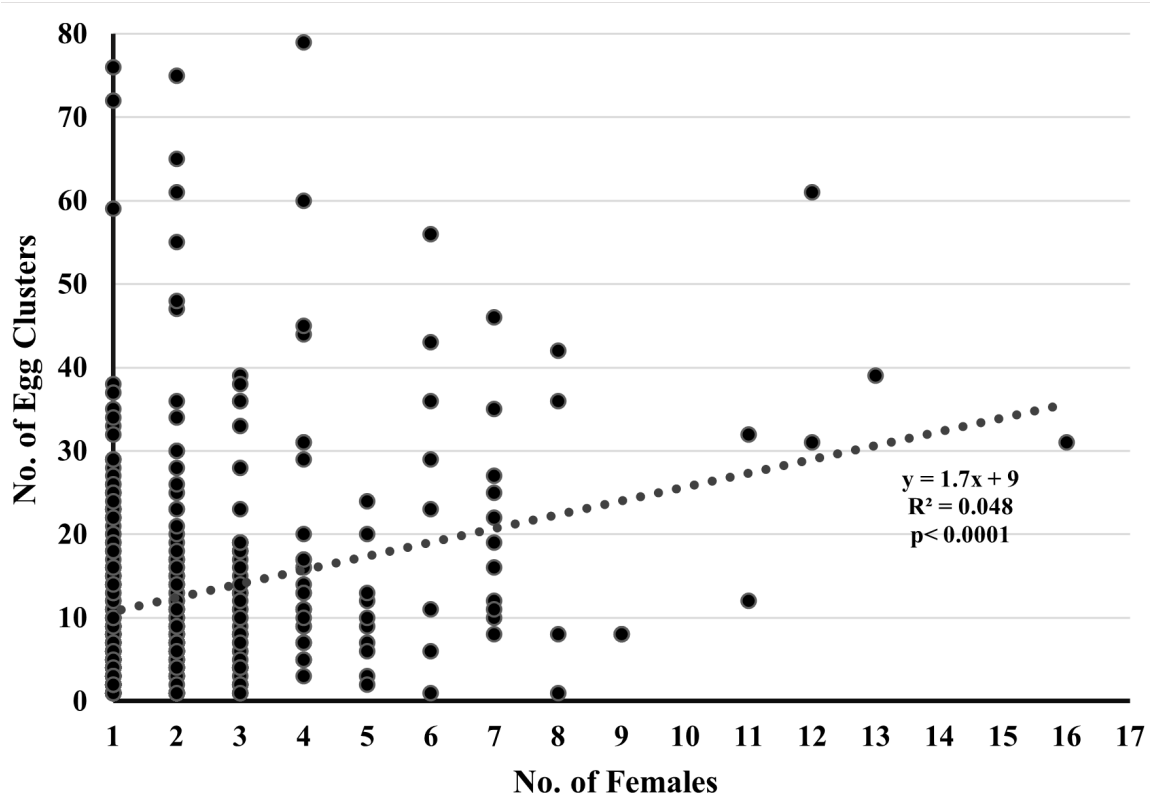

Figure 2.10 The effect of the number of females counted on sampled Hass avocado leaves on the number of egg clusters made up of two or more eggs on leaves (n=1,304) collected over a seven-month period (November 2022- May 2023).

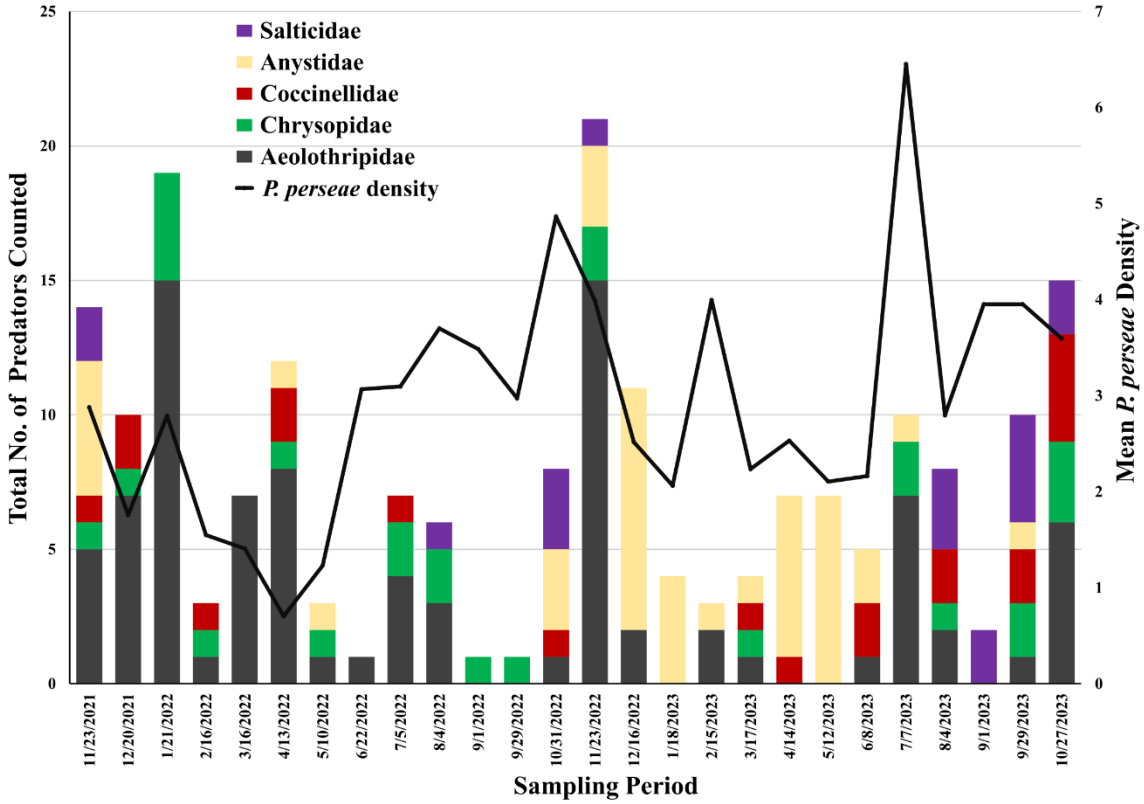

Figure 2.11 Total number of generalist predator taxa (Aeolothripidae, Chrysopidae, Coccinellidae, Anystidae, and Salticidae) found from tap sampling ten randomly selected Hass avocado trees across four commercial orchards infested with *Pseudacysta perseae* over a two-year sampling period (November 2021- October 2023).

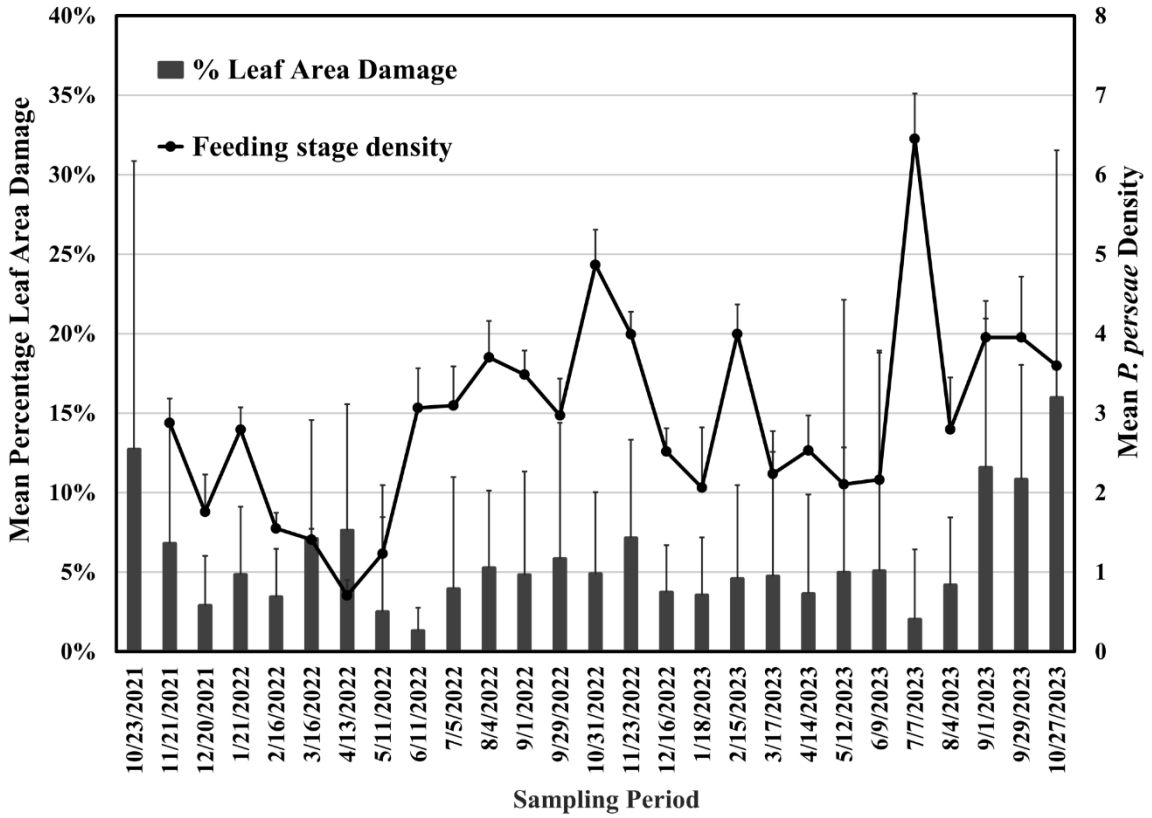

Figure 2.12 Relationship between percentage leaf area damaged by *Pseudacysta perseae* feeding and mean density of *P. perseae* feeding life stages on leaves sampled across four commercial Hass avocado orchards over a two-year sampling period (November 2021-October 2023).

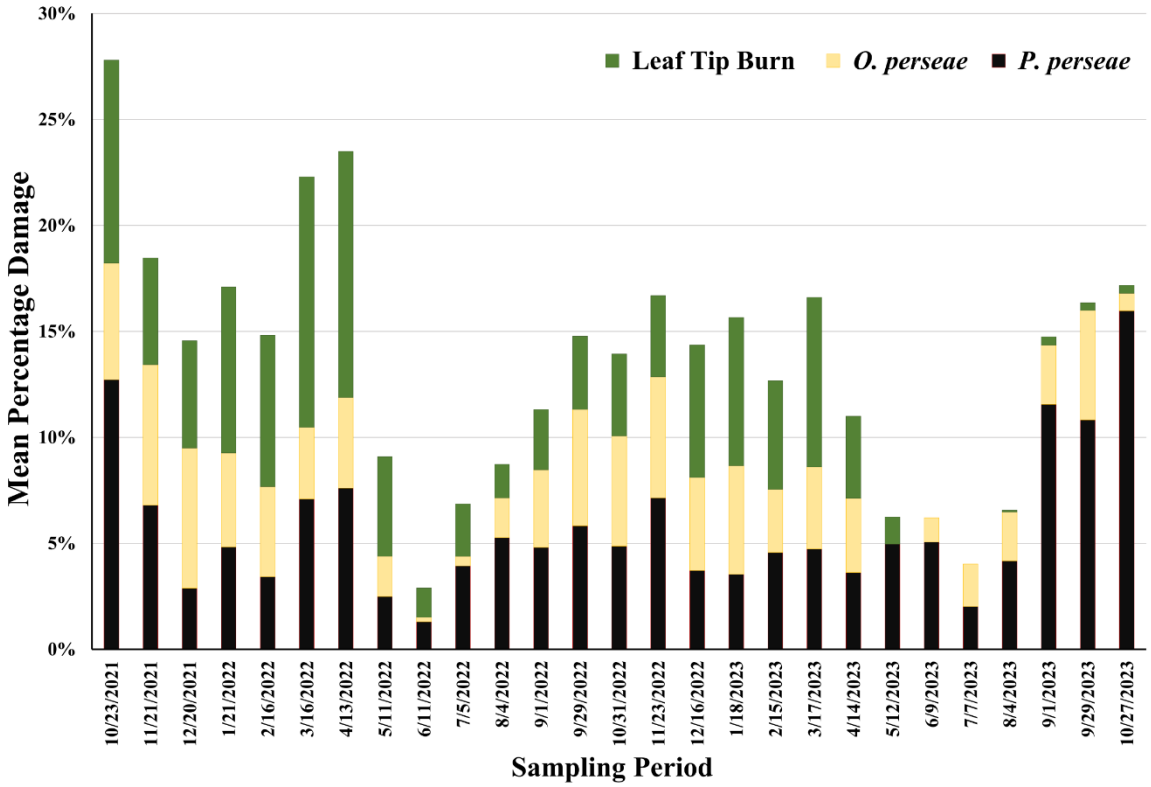

Figure 2.13 Percent leaf area damage caused by *Pseudacysta perseae* and *Oligonychus perseae* feeding, and leaf tip burn across four commercial Hass avocado orchards over a two-year sampling period (November 2021- October 2023).

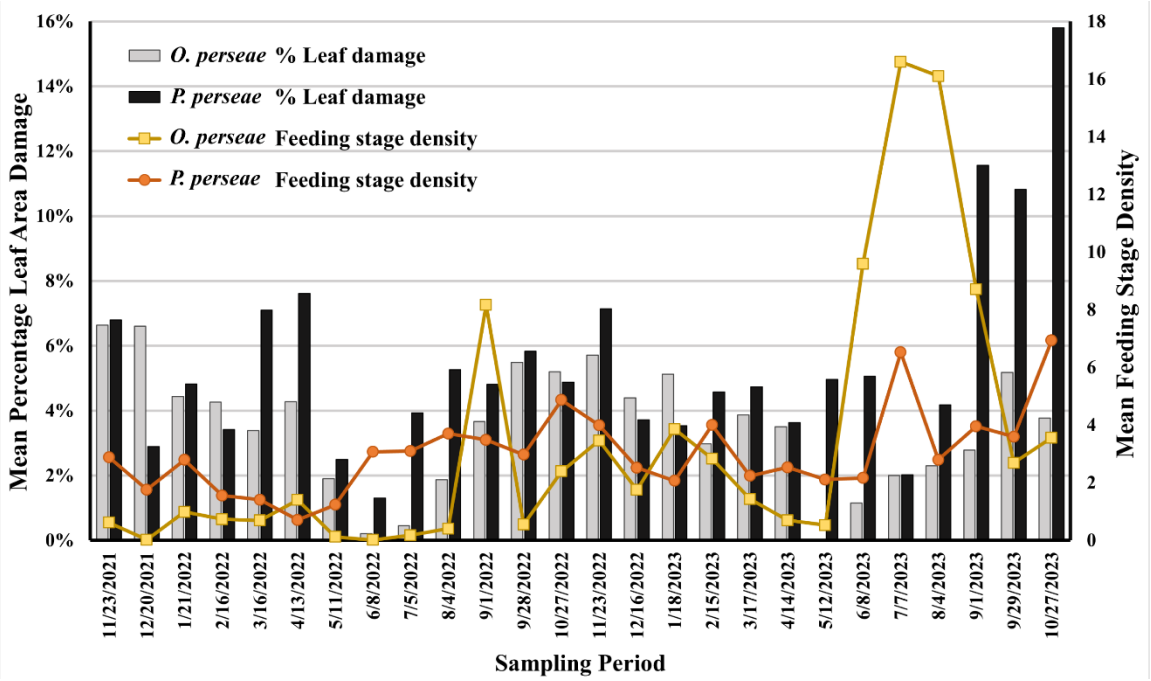

Figure 2.14 Relationship between mean densities of feeding life stages and percentage leaf area damage of *Pseudacysta perseae* and *Oligonychus perseae* across four commercial Hass avocado orchards over a two-year sampling period (November 2021- October 2023).

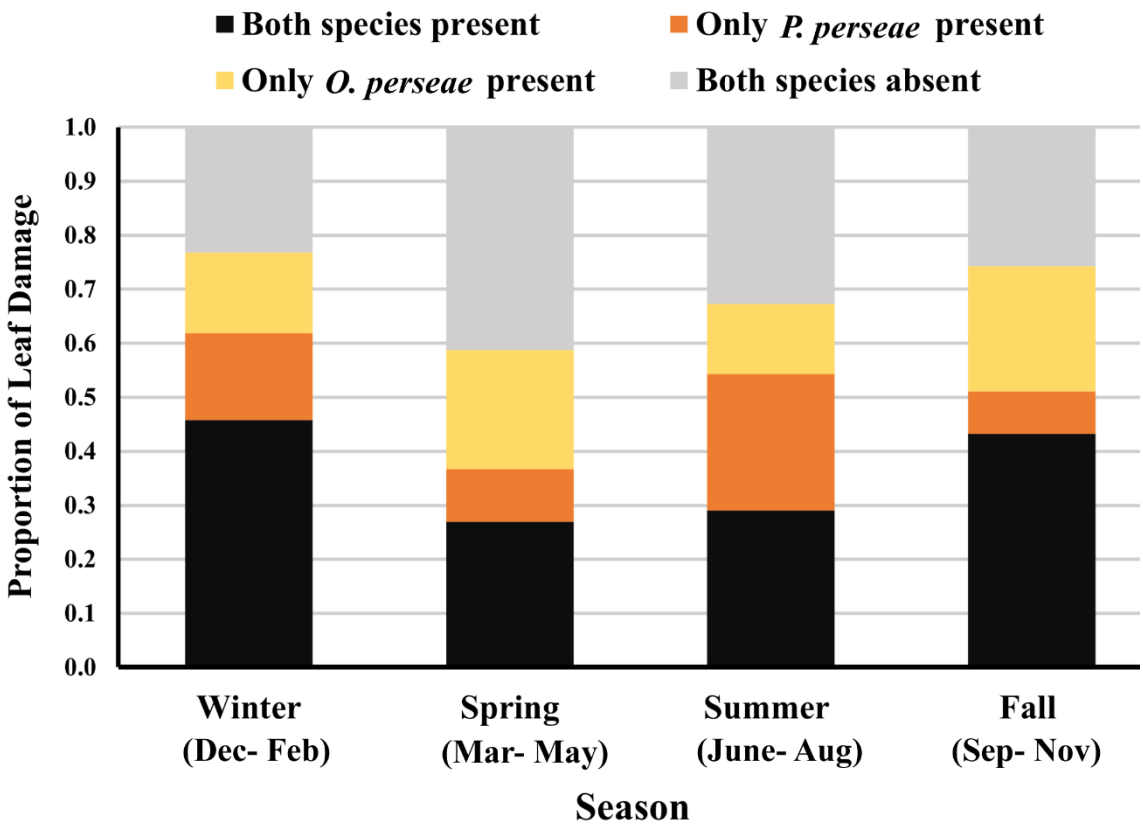

Figure 2.15 Proportion of leaves with *Pseudacysta perseae* and *Oligonychus perseae* feeding damage by season across four commercial Hass avocado orchards over a two-year sampling period (November 2021- October 2023).

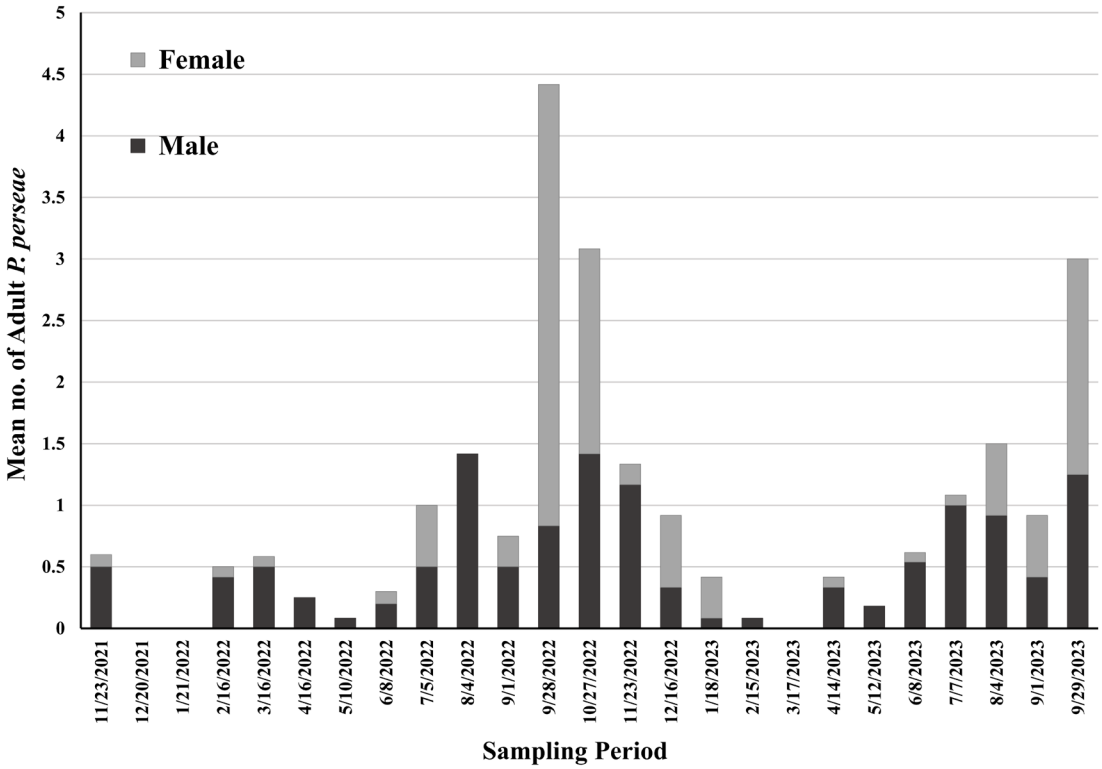

Figure 2.16 Mean number of adult (male and female) *Pseudacysta perseae* captured on yellow sticky cards across four commercial Hass avocado orchards over a two-year sampling period (November 2021- October 2023).

Chapter 3. Genetic Profiling and Laboratory Hybridization between Haplotypes of the Invasive Avocado Lace Bug, *Pseudacysta perseae* (Hemiptera: Tingidae)

INTRODUCTION

The avocado lace bug, *Pseudacysta perseae* (Heidemann), is native to Mexico and assumed to be native to the Caribbean, and southeastern United States. This leaf feeding pest poses a threat to avocados, *Persea americana* Miller (Lauraceae), by occasionally reaching economically damaging levels (Peña, 2003; Hoddle et al., 2005). The feeding damage inflicted by *P. perseae* on the undersides of leaves causes chlorotic spots on foliage, which commonly advances to necrosis, leading to defoliation and reduced fruit yields (Hoddle et al., 2005). Among avocado-producing states in the U.S., California leads in avocado production, contributing 90% of the total output across 48,000 acres, valued annually at $487 million (CAC, 2023). Florida follows with roughly 9% of the production volume, while Hawai'i accounts for less than 1% of total U.S. production (USDA/ERS, 2022a).

Pseudacysta perseae was first discovered in California in 2004, on backyard avocado trees, of the Bacon cultivar, in the Chula Vista and National City areas of southern San Diego Count, California (Hoddle, 2022). Extensive foreign exploration efforts at that time, followed by genetic population profiling, first based on variation in the DNA sequences of a mitochondrial gene (COI), and subsequently, incorporating eight nuclear markers, revealed evidence of very strong population structure among *P. perseae* populations (Rugman-Jones et al., 2012). These studies indicated that the invasive population in California likely originated from Nayarit, a state on the west coast of Mexico (Rugman-Jones et al., 2012). Molecular analysis also revealed substantial genetic diversity between *P. perseae* populations in western Mexico, and populations in other parts of the presumed native range that included the southeastern U.S., Caribbean, and

eastern Mexico (Rugman-Jones et al., 2012). Molecular analyses suggested that the actual native range of *P. perseae* may be situated in western Mexico and that populations were translocated from this region and established in eastern parts of Mexico, the Caribbean and southeastern United States (Rugman-Jones et al., 2012), including Florida, from where the original specimens of *P. perseae* were collected and described (Heidemann 1908).

For approximately thirteen years, *P. perseae* populations in California remained confined primarily to non-Hass avocado trees in residential properties in southern San Diego County. Beginning in 2017, there were increasing reports of *P. perseae* infesting Hass avocados outside of the original infestation zones in Chula Vista and National City. Infested commercial Hass avocado groves occurred in Oceanside and Bonsall in northern San Diego County and Temecula and Riverside in Riverside County (CAC, 2017; Hoddle, 2022). Additionally, residential trees in Los Angeles County (2019) and Orange County (2022) were infested (CAC, 2017). In 2023, *P. perseae* was discovered in commercial Hass orchards in Santa Barbara County, approximately 150 km north of the closest infestations in Los Angeles County. This range expansion was not confined to California. In 2019, commercial non-Hass avocado groves in Hawai'i reported extensive *P. perseae* infestations, feeding damage, and reduced yields due to *P. perseae* infestations (Hoddle, 2022).

The 2017 occurrence and subsequent spread of a putative more "aggressive" *P. perseae* population with an increased predilection for the Hass cultivar in California and the invasion into Hawai'i prompted uncertainty as to whether the source of these new infestations was the original population previously identified in southern San Diego in 2004 or if these spreading populations resulted from new introduction events into California and Hawai'i. Additionally, it was unknown if the original southern San Diego County population from Nayarit still existed or had been replaced by the more northern spreading population. Further, it was unknown if the Hawaiian

populations differed from those in California and could act as a source area for additional future introductions.

To address these concerns, molecular analyses to genetically profile *P. perseae* populations in the original infestation areas of southern San Diego County, commercial groves located in Oceanside and Bonsall in northern San Diego County, Temecula in Riverside County, residential areas in Los Angeles County, and populations from Hawai'i were conducted. These studies were augmented with additional *P. perseae* specimens collected from Florida, and eastern (i.e., Veracruz and Quintana Roo) and western (i.e., Colima and Baja California) areas in Mexico. These analyses were conducted to determine whether new introductions of *P. perseae* had occurred in California sometime prior to 2017, or if the original 2004 population had undergone a lag phase before undergoing rapid range expansion. These studies were enhanced further with molecular analyses of a maternally inherited endosymbiont, *Wolbachia*, which can strongly influence reproductive compatibility between populations of the same species (Hurst and Jiggins, 2005). To provide insights into whether there was reproductive incompatibility between different populations of *P. perseae* in California that exhibit substantially different levels of pestiferousness, a second set of laboratory experiments comprised of controlled intra-haplotype and inter-haplotype mating trials were conducted. The purpose of these experiments was to investigate the reproductive compatibility between *P. perseae* populations in the original infestation zone in San Diego County (i.e., the 2004 populations) and those from commercial Hass orchards in northern San Diego County (i.e., the 2017 populations). The results of these molecular and mating studies are presented here.

MATERIALS AND METHODS

Specimen Collection

Between 2017 and 2023, adult specimens of *P. perseae* were collected from various avocado cultivars in parts of the U.S. and Mexico (see Table 3.1 for collecting details). Specimens were preserved in 5 ml screw cap vials containing 95% ethanol, labelled by locality, and stored at -20°C until molecular analyses were conducted.

DNA Extraction

Adult *P. perseae* were removed from labeled vials and individually homogenized using a 2010 Geno/Grinder® (SPEX™ SamplePrep) in 2-ml Eppendorf Safe- Lock tubes with two 4-mm stainless steel grinding balls (Spex Sample Prep 2150) at 1,100 rpm for 1.5 minutes. The DNeasy® Blood & Tissue Kit (Qiagen Inc., USA) was utilized to extract DNA, following the manufacturer's handbook protocol (Qiagen, 2023). The quality and concentration of the extracted DNA were assessed using the NanoDrop 2000 instrument (Thermo Fisher Scientific).

COI Mitochondrial DNA Sequencing

A set of primers specific to *P. perseae* (Rugman-Jones et al., 2012) were used to amplify the cytochrome C oxidase subunit I (COI) of mitochondrial DNA (mtDNA). The forward and reverse primers were combined with the OneTaq 2X Master Mix with Standard Buffer (New England Biolabs, USA) in a 25-µL reaction volume. PCR was performed in a Bio-Rad thermocycler (Bio-Rad, Hercules, CA, USA) and followed the cycle outlined by Rugman-Jones et al. (2012). A *P. perseae* DNA sample that had been amplified previously with the same primer pair was used as a positive control. Double distilled water was used as a negative control. Electrophoresis using a 1% agarose gel stained with SYBR Safe DNA gel stain (Invitrogen,

USA) was used to verify PCR amplification and lack of contamination. Magnetic bead-based purification of amplicons was performed using Mag-Bind Total Pure NGS kit (Omega Bio-Tek, USA). NanoDrop 2000 was used to measure the concentration of purified PCR products. The PCR products were dispatched to Retrogen Inc. (San Diego, CA) for Sanger sequencing. DNA sequences then were aligned manually using BioEdit Sequence Alignment Editor version 7.0.5.3 (Hall, 1999). Sequences were submitted to GenBank under GenBank® accessions PP188058–PP188091. Every aligned COI mtDNA sequence was either assigned an existing haplotype letter following the A-I identification scheme outlined in Rugman-Jones et al. (2012) (GenBank® accessions JF838244–838277), or a new letter was issued when a different haplotype was identified.

Haplotype Network Analyses

Haplotypes were analyzed by differentiating sequence alignments based on Single Nucleotide Polymorphisms (SNPs) using DnaSP v6.12.03 (Rozas et al., 2017). Median Joining Network analysis was performed using PopART v1.7 (Leigh and Bryant, 2015) to create a haplotype network, which was then annotated in Adobe Illustrator v27.3.1 (Adobe Inc., DE, USA). A geographic distribution map of haplotypes was generated using ArcGIS v10.8 (Environmental Systems Research Institute, Inc., ESRI; Redlands, CA, USA) and Adobe Illustrator to plot results for the 20 collection localities in California, Florida, Hawai'i, and Mexico (see Table 3.1 for locality details).

Genetic Diversity Analysis

DnaSP v6.12.03 (Rozas et al., 2017) was used to calculate haplotype diversity (Hd) and nucleotide diversity (π) for each sampled locality (Table 3.3).

Wolbachia Endosymbiont Screening

At least one specimen for each COI haplotype recovered from *P. perseae* collection locations (Table 3.3) underwent screening for the presence of *Wolbachia.* Screening specifically targeted the *wsp* aliquot gene, utilizing the *wsp*-81F and *wsp*-691R primers which amplified 555 base pairs of the *wsp* gene (Braig et al. 1998). To validate the screening process, a positive control consisting of a *Trichogramma* sp. (Hymenoptera: Trichogrammatidae) known to be infected with *Wolbachia* was used. *Wolbachia* sequences were submitted to GenBank under GenBank® accessions PP278551 – PP278582 (Table 3.3).

Geographic Distribution of *P. perseae*

A summary table of the ten *P. perseae* haplotypes found in various locations to date was constructed using data from Rugman-Jones et al. (2012) and this study. (Table 3.4)

Intra- and Inter-Haplotype Crossing Experiments

Pseudacysta perseae used for cross-mating studies were reared and mated on Hass avocado leaves in climate-controlled cabinets (Darwin Chambers, St. Louis, MO, USA) under a fluctuating temperature regimen that averaged 25 ± 1°C, with an average relative humidity of 60 ± 5% and a 14:10 h light: dark photoperiod at a light intensity of 100 µE m^{-2} s^{-1}. Temperature cycles and humidity were verified using HOBO Pro V2 Temperature/RH loggers (Onset Computer Corp., Bourne, MA, USA). To set the climate-controlled cabinets to an average temperature of 25°C, the hourly temperatures were programmed using an average of five years of daily temperature data (2017-2021) from the CIMIS weather station, Escondido SPV #153, in San Diego County, California, U.S., a locality within 20 km of active *P. perseae* infestations (Table 3.2).

Hass avocado leaves used for cross-mating studies were collected from unsprayed avocado trees at the University of California, Riverside. An observational arena was constructed on individual avocado leaves using Munger cells (Munger, 1942). QuakeHold!™ museum putty (Ready America™, San Marcos, CA, USA) was used to adhere Munger cells to avocado leaves so that leaf undersides were exposed as feeding and oviposition substrates. Munger cells, together with attached leaves, were placed on water-saturated foam pads that were maintained in stainless-steel pans (25 cm x 22 cm x 4 cm) to retain water (set up as in Chapter 1, Fig. 1.1). Clear plexiglass panels were placed over the top of Munger cells to contain motile feeding *P. perseae* life stages inside the feeding arena. Assays with egg-bearing leaves were left uncovered to prevent condensation and excessive fungal growth. As leaves deteriorated, *P. perseae* nymphs and adults were transferred to new Munger cells with new clean (i.e., washed and dried) Hass avocado leaves using a 0.5 mm camel-hair paintbrush.

Source of Unmated Adults for Mating Studies

To obtain unmated adults for cross-mating tests, third and fourth instar *P. perseae* nymphs were collected from Hass avocado trees in Oceanside (site of the 2017 invasion) and infested non-Hass avocado trees in Chula Vista (site of the 2004 invasion) in San Diego County. Nymphs from these two locations were reared to adulthood, sexed under a microscope, and sorted into Munger cells containing same sex individuals from the same location.

Cross-Mating Treatments

Based on the haplotypes obtained from limited mtCOI sequencing of specimens collected in 2021 from Oceanside (designated as haplotype G based on preliminary studies) and Chula Vista (haplotype A [Rugman-Jones et al. 2012]) (Hoddle 2022), four cross-mating treatments were established. Intra-haplotype (control) crosses: Oceanside (haplotype G), Chula Vista

(haplotype A) and inter-haplotype crosses: Chula Vista-male x Oceanside-female (i.e., haplotypes A x G), Oceanside-male x Chula Vista-female (i.e., haplotypes G x A). Ten mating pairs of each of the four crosses were prepared for a total of 40 cross-mating replicates. Each replicate in each mating cross treatment contained one male and one female and was maintained in the Munger cell arena with Hass avocado leaves as described above. The total number of eggs laid, and the number of eggs that hatched, were recorded daily for each mating pair from their 6th day of adulthood to their 24th day of adulthood. On the 25th day of adulthood, *P. perseae* mating pairs were preserved in 95% ethanol in labeled 5 ml screw cap vials and stored at -20^{o}C until sequenced. This egg laying record was started on the 6th day of adulthood because preliminary *P. perseae* fecundity experiments indicated that eggs laid on the 7th day of adulthood began hatching and fertility peaked on the 12th day of adulthood. The egg-laying record was concluded on the 25th day of adulthood as preliminary observations indicated that mated adults, under a fluctuating average temperature of 25°C, had an average lifespan of 27 days and egg-laying decreased significantly by the 25th day. Eggs laid by mating pairs were monitored for nymph emergence for a duration of 14 consecutive days. Preliminary studies indicated that the maximum developmental time from egg to nymph at a fluctuating average temperature of 25°C was 12 days. The number of F_1 progeny nymphs that reached adulthood and their sex was recorded.

F_2 Progeny Production

Unmated adult progeny resulting from the F_1 generation for each cross-mating combination were subjected to additional cross-mating studies to determine effects of parental cross-mating on F_2 progeny production. For each cross-mating combination (see above) eight mating pairs were established and maintained for a period of 25 days as described above. To prevent potential deleterious effects from inbreeding, no siblings were used as mating partners.

The number of eggs laid, and the number of eggs hatched, were recorded for each mating pair from day 6 to day 24. After the 25-day mating period, all the F_1 mating pairs, and an additional four unmated 24-hour old adults (consisting of two males and two females), were preserved in 95% ethanol in labeled 5 ml screw cap vials at -20ºC for sequencing. The number of F_2 nymphs that successfully reached adulthood were recorded and sexed.

Statistical Analyses

The parameters analyzed to assess the viability of offspring resulting from the four cross-mating combinations used for the F_1 and F_2 generations included: fertility (i.e., proportion of mating pairs that laid at least one fertile egg), fecundity (i.e., mean number of eggs laid by each female in each mating pair replicate over a 20-day period), egg hatching rates (i.e., proportion of eggs that produced nymphs) and adult emergence rates (i.e., proportion of progeny that reached adulthood). Statistical analyses for these data were done in R (R Core Team, 2021). Fecundity of different crosses were compared using one-way analysis of variance (ANOVA) using the function '*lm*', checking normality and heteroscedasticty of the model residuals. Tukey posthoc tests at the 0.05 level of significance were used for multiple comparisons of means facilitated by the '*multcomp*' package which tested for differences between cross-mating combinations. Significant differences were visualized using the '*multcompview*' package. Egg hatching and adult emergence rate proportion data were analyzed by using the function '*glm*' and were fitted using a logistic regression model ('*logit*' link function) with a binomial distribution.

RESULTS

COI Mitochondrial DNA Sequencing and Haplotype Network Analyses

A total of 375 specimens from 20 localities that spanned three U.S. states (i.e., California, Florida, and Hawai'i) and four Mexican States (i.e., Veracruz, Colima, Quintana Roo, and Baja

California) (Table 3.1) were analyzed. Four polymorphic sites and five distinct COI haplotypes were identified (Fig. 3.1). Three of the four polymorphic sites were the result of synonymous substitutions. A new haplotype, designated as L (Fig. 3.1), which displayed a single non-synonymous substitution, was identified and represented by four specimens.

The haplotype distribution across the U.S. (three states) and Mexico (four states) indicated that in 6 out of the 7 states sampled, more than one haplotype was observed (Fig. 3.2). Haplotype D, E and G differed from haplotype A by a single nucleotide. Haplotype G (Fig. 3.1; Table 3.3) was the most frequent haplotype encountered comprising approximately 49% of all individuals analyzed. Importantly, haplotype G was the only haplotype recovered from four different islands in Hawai'i (U.S.). Haplotype G comprised 100% of individuals analyzed in Riverside County, 75% of material from northern San Diego County (both California, U.S.), and 94% of specimens sampled from Florida (U.S.). Haplotype A (Fig. 3.1; Table 3.3) was the second most frequent haplotype encountered, accounting for approximately 38% of sampled individuals. This haplotype accounted for 100% of individuals from Los Angeles, California (U.S.) and Baja California (western Mexico), 93% of individuals from southern San Diego County (U.S.), California and 79% of individuals from Quintana Roo (eastern Mexico). Haplotype D (Fig. 3.1; Table 3.3) was found predominantly in *P. perseae* populations sampled in Colima (western Mexico). Haplotype E (Fig. 3.1; Table 3.3) was found predominantly in material collected from Veracruz (eastern Mexico). The most divergent haplotype, L, differed from its nearest haplotype E by a single nucleotide and only included individuals from Veracruz (eastern Mexico).

Wolbachia Endosymbiont Screening

Out of 78 specimens examined for *Wolbachia* endosymbiont infection, 65 (i.e., 83%) were infected (Table 3.3). No nucleotide differences were detected among *Wolbachia* infecting individuals carrying the 5 mtDNA haplotypes.

Intra- and Inter-Haplotype Crossing Experiments

Each F_0 mating pair of each cross-mating combination laid viable eggs (Table 3.5). The F_0 intra-haplotype (i.e., control cross), between G haplotype males and females, G_M x G_F produced a significantly higher number of eggs ($F_{3,36} = 5.58$, $P = 0.003$) than any other cross. One of the inter-haplotype crosses, A_M x G_F, showed a significantly lower F_1 hatching rate ($z = -2.17$, $P = 0.03$) when compared to the control crosses. The logistic regression model for F_1 adult emergence rate showed no statistically significant differences ($P > 0.05$) across the four different cross-mating combinations.

The F_1 mating pairs of all the cross-mating combinations, except one of the mating pairs of the inter-haplotype cross type, G_M x A_F, did not produce viable eggs (% F_1 Fertility= 87.5). The F_1 control cross, G_M x G_F exhibited significantly higher fecundity ($F_{3,28} = 9.63$, $P = 0.0002$). Cross-mating combination type that produced the F_1 generation significantly influenced egg hatch rates ($X^2 = 33.38$, $df = 3$, $P < 0.001$). Inter-haplotype crosses, A_M x G_F ($P = 0.008$) and G_M x A_F ($P < 0.001$), had significantly higher hatching rates when compared to control crosses. The logistic regression model for F_2 adult emergence rate showed no statistically significant differences across the four different cross-mating combinations. These results suggest that the two predominant *P. perseae* haplotypes in southern California, haplotype A and haplotype G, are highly reproductively compatible.

DISCUSSION

Analyses of relatively conserved mtDNA for evaluating the genetic diversity of *P. perseae* populations in the native range (i.e., the Pacific coastal regions of Mexico [haplotypes A, B, D, F, G H, I]), putative non-native regions (i.e., eastern coastal regions of Mexico [haplotypes A, C, D, E, G, I, L]), the Caribbean [haplotype G], and the southeast U.S. haplotypes [haplotypes G, A, E]), and definitively invaded regions (i.e., California [haplotypes A and G] and Hawai'i [haplotype G]), suggest that California has been invaded twice by two different *P. perseae* haplotypes, A and G. The first invasion into California in 2004 that established in National City and Chula Vista in southern San Diego County was by haplotype A and the source area was identified as the state of Nayarit in Mexico (Rugman-Jones et al., 2012). The irruption of damaging *P. perseae* populations in northern San Diego County and Riverside County in 2017, and subsequent spread to Los Angeles (2019) and Santa Barbara (2023) Counties was by haplotype G, the same haplotype that invaded Hawai'i in 2019.

Haplotype G was originally identified from Florida, the Caribbean, and the Atlantic coast of Mexico (Rugman-Jones et al., 2012). As part of this current study, analyses of *P. perseae* collected from Florida, and from the eastern coastal areas (i.e., Veracruz and Quintana Roo) of Mexico, contained haplotype G. Importantly, 94% of material collected from Florida (i.e., 66 out of 70 samples analyzed) were comprised of haplotype G. Therefore, the most parsimonious source for *P. perseae* haplotype G into California sometime around 2017 is Florida considering the high frequency of this haplotype in this state and its location within the contiguous U.S. Similarly, a plausible hypothesis for the source population of *P. perseae* in Hawai'i, which is comprised 100% of haplotype G, may be California rather than Florida, given the closer geographic proximity between Hawai'i and California when compared to Florida.

The original 2004 infestation areas of South San Diego County (i.e., Chula Vista and National City), *P. perseae* populations are still predominantly of haplotype A originally identified from the Pacific Coast of Mexico (i.e., Nayarit) (Rugman-Jones et al., 2012), but a small percentage of two other haplotypes, D (4%) and E (4%), were detected. These two haplotypes, D and E, have been detected in other sampled areas outside of California. For example, haplotype D was recorded from the states of Colima (this study), Jalisco, and Michoacán (Rugman-Jones et al., 2012) in Mexico. Haplotype E was originally identified from material collected in eastern areas of Mexico (i.e., Chiapas, Tabasco, Veracruz, Yucatan) (Rugman-Jones et al., 2012). However, results from this study detected a single sample (i.e., 1.4% of samples) of haplotype E in Florida. The significance of these findings with respect to haplotypes D and E are uncertain, but may tentatively suggest that additional invasion events have occurred in California, or that insufficient sampling was done in California when the original *P. perseae* population was detected in 2004. Understanding of the invasion dynamics of haplotypes D and E would be enhanced with additional sampling in Mexico, especially in regions in the western part of the country, to determine if additional populations in previously unsampled areas with these two haplotypes exist.

In northern San Diego County, haplotype G is predominant (i.e., the area of the 2017 invasion), which is in contrast to the southern part of the county where haplotype A continues to prevail (i.e., the area of the 2004 invasion). Notably, sampling in northern San Diego in 2017 showed a 70% prevalence of haplotype G and 30% of haplotype A, whereas in 2021, all samples were identified as haplotype G. This shift tentatively suggests that haplotype G, a problematic variant causing severe infestations in Florida, Hawai'i, and parts of the Caribbean, may be replacing haplotype A, the original haplotype that invaded from the Pacific coast of Mexico. If this suggestion is correct, it is unknown as to why haplotype G has failed to displace haplotype A

in southern San Diego County, the area of original establishment by this haplotype in 2004. With respect to haplotype G, cultivar preferences seem unlikely, as haplotype G, which was originally detected on Hass avocados, has flourished on Hass, and non-Hass varieties in invaded areas of California and non-Hass avocados in Hawai'i.

Rugman-Jones et al. (2012) identified the state of Nayarit on the Pacific coast of Mexico as the origin of the 2004 southern San Diego County invasion. However, results from this current study may now challenge this conclusion. The first-time collection of *P. perseae* from avocados in Tijuana, Baja California Mexico, approximately 20 km south of Chula Vista in southern San Diego County, revealed the presence of haplotype G, the same haplotype as the 2004 invasive population. Notably, the distance between the initial invasion site in Chula Vista, San Diego County and Nayarit Mexico is approximately 2000 km, compared to the significantly shorter distance (i.e., 20 km) to Tijuana in Baja California. This closer proximity suggests a potential invasion bridgehead for *P. perseae* may have been northern Baja California (e.g., Tijuana), rather than Nayarit Mexico, as a likely source of the invasion into southern San Diego County in 2004. However, if the Rugman-Jones et al. (2012) hypothesis is correct, and Nayarit is the source of the *P. perseae* invasion into southern San Diego County, then the possibility exists that the haplotype A population in Baja California population may have originated from San Diego.

Nine haplotypes (A-I) of *P. perseae* were originally identified by Rugman-Jones et al. (2012). Haplotype L, a newly discovered haplotype in Veracruz, differs from the predominant haplotype E in the Veracruz population, by a single nucleotide. In the Rugman-Jones et al. (2012) study, haplotype I was found to differ from haplotype E by eight nucleotides. Given that haplotype divergence typically occurs gradually through single nucleotide substitutions over time (Harrison, 1991), it is probable that haplotype L has always existed in this region but was not detected during previous sampling efforts.

The *Wolbachia* sequences (*wsp* gene of 555 base pairs) of the five COI haplotypes recovered across the collection locations were identical. These finding are consistent with Rugman- Jones et al. (2012), which determined that the distribution of mitochondrial haplotypes in *P. perseae* is unlikely to be a consequence of mitochondrial sweeps due to cytoplasmic incompatibility that arise from Wolbachia infections.

The findings from the mating cross experiments revealed high levels of reproductive compatibility and fecundity among the two predominant haplotypes (i.e., haplotypes A and G) of *P. perseae* in southern California. The F_0 generation demonstrated that all cross-mating pairs were reproductively compatible and produced viable offspring, with control crosses between G haplotype individuals from Oceanside yielding a notably higher quantity of eggs. However, this observation could have been influenced by the experimental setup, which utilized Hass avocado leaves, which aligned with the G haplotype's strong preference for Hass avocados. Conversely, the A haplotype, originating from Chula Vista is primarily found on non-Hass varieties such as Bacon. This difference in host plant preference could account for the variability in fecundity and egg hatch rates, leading to the diminished fitness observed in the A haplotype control cross. One of the inter-haplotype pairings, A_M x G_F exhibited a diminished hatching rate, suggesting some level of reproductive incompatibility may exist between these two haplotypes. However, the emergence rates of F_1 adults did not vary significantly between cross-mating set ups, indicating that, once hatched, the survivability of offspring is not dependent on the haplotype combinations of the parents.

In the F_1 generation, all but one inter-haplotype (i.e., G_M x A_F) mating pair failed to produce viable eggs, suggesting a decrease in reproductive success when different haplotypes are cross mated. Additionally, the F_1 control crosses (i.e., G_M x G_F) showed significantly enhanced fecundity (Table 3.5 [F_1 and F_2 Eggs Laid]), further emphasizing the observation of enhanced

reproductive output when the same haplotypes mate together. Interestingly, egg hatch rate in the F_2 generation was significantly influenced by mating-cross type in the F1 generation, with two inter-haplotype (i.e., A_M x G_F and G_M x A_F) crosses showing higher hatching rates when compared to control crossed (i.e., G_M x G_F and A_M x A_F). This finding challenges the initial assumption of reduced viability resulting from inter-haplotype crossings and under the prevailing experimental conditions in the laboratory, results presented here suggest that increased vigor could result from inter-haplotype crosses. The persistent existence of Haplotype A in San Diego County, despite evidence of increased vigor from inter-haplotype crossings, raises questions. It seems that preferences for certain avocado varieties, like Haplotype A's inclination towards the Bacon variety found in southern San Diego's residential areas, might explain its lack of integration with Haplotype G in the north, where the Hass avocado variety is more prevalent. The Hass variety might not offer the same level of suitability for Haplotype A, leading to its localized distribution in urban areas in southern San Diego County. This possibility, if correct, suggests that the compatibility between specific haplotypes and avocado cultivars could influence the distribution and evolution of these haplotypes in the region.

The egg hatch rate for both intra- and inter-haplotype crosses in the F_1 generation was comparable, with the inter-haplotype crosses exhibiting a slightly lower hatch rate overall, while in the F_2 generation, the inter-haplotype crosses demonstrated a significantly higher hatch rate compared to the intra-haplotype crosses. The consistent lack of significant differences in adult emergence rates across F_1 and F_2 generations for all cross-mating combinations indicates that once *P. perseae* eggs hatch, the likelihood of reaching adulthood is similar, regardless of parental haplotype combinations. These results suggest that these California-dominant haplotypes, A and G, are fully capable of interbreeding and producing viable offspring when reared in the laboratory on Hass avocado leaves. These findings indicate that the capacity for genetic exchange between

haplotypes A and G remains intact, potentially influencing the genetic diversity and evolutionary trajectory of *P. perseae* populations in invaded avocado production regions like southern California.

REFERENCES

Braig H. R., W. Zhou, S. Dobson, S. L. O'Neill. 1998. Cloning and characterization of a gene encoding the major surface protein of the bacterial endosymbiont *Wolbachia*. *J Bacteriol* 180: 2373–2378.

CAC. 2017. Green Sheet – California Avocado Industry News, Volume 33, Issue 19.

CAC. 2020. *The History of California Avocados*. California Avocados. Available online: https://californiaavocado.com/avocado101/the-history-of-california-avocados/

CAC. 2023. California Avocado Commission Annual Report 2022. Available online: https://www.californiaavocadogrowers.com/sites/default/files/2022-CAC-Annual-Report-Final.pdf

Cariou, M., L. Duret and S. Charlat. 2017. The global impact of *Wolbachia* on mitochondrial diversity and evolution. *Journal of Evolutionary Biology* 30(12): 2204-2210.

Hall, T. A. 1999. BioEdit: a user-friendly biological sequence alignment and analysis program from Windows 95/98/NT. *Nucleic Acids Symp* 41: 95–98.

Harrison, R. G. 1991. Molecular changes at speciation. *Annual Review of Ecology and Systematics* 22(1): 281-308.

Heidemann O. 1908. Two new species of North American Tingidae. *Proc. Entomol. Soc. Washington* 10: 103-108.

Hoddle, M. S. 2022. Avocado Lace Bug is Continuing to Spread in California. *From the Grove* 12(2): 22-25.

Hoddle, M. S., J. Morse, R. Stouthamer, E. Humeres, G. Jeong, W. Roltsch, G. S. Bender, P. Phillips, D. Kellum, R. Dowell, G. W. Witney. 2005. Avocado lace bug in California. *Calif. Avocado Society Yearbook* 88: 67–79.

Hurst, G. D., and F. M. Jiggins. 2005. Problems with mitochondrial DNA as a marker in population, phylogeographic and phylogenetic studies: the effects of inherited symbionts. *Proceedings of the Royal Society B: Biological Sciences* 272(1572): 1525-1534.

Leigh, J. W., D. Bryant. 2015. POPART: full-feature software for haplotype network construction. *Methods in Ecology and Evolution* 6(9): 1110-1116.

Morse, J. G., B. A. Faber, M. S. Hoddle. 2016. *Avocado Lace Bug*. Avocado Pest Management Guidelines. Available online: https://ipm.ucanr.edu/agriculture/avocado/avocado-lace-bug/

Munger, F. A. 1942. A method for rearing citrus thrips in the laboratory. *J. Economic Entomology* 35: 373-375.

Peña, J. E. 2003. Pests of avocado in Florida. In *Proceedings of V World Avocado Congress*, pp. 487–494. Tropical Research and Education Center, University of Florida, Homestead, FL, USA.

Qiagen, DNeasy® Blood & Tissue Handbook. 2023. Available: https://www.qiagen.com/us/resources/download.aspx?id=68f29296-5a9f-40fa-8b3d-1c148d0b3030&lang=en

R Core Team. 2021. R: A language and environment for statistical computing." R Foundation for Statistical Computing, Vienna, Austria. Available at http://www.R-project.org/.

Rozas J., A. Ferrer-Mata, J.C. Sánchez-Del Barrio, S. Guirao-Rico, P. Librado, S. E. Ramos-Onsins, A. Sánchez-Gracia. 2017. DnaSP 6: DNA sequence polymorphism analysis of large data sets. *Molecular Biology and Evolution* 34 (12): 3299-3302.

Rugman-Jones, P. F., M. S. Hoddle, P. A. Phillips, G. S. Jeong, R. Stouthamer. 2012. Strong genetic structure among populations of the invasive avocado pest *Pseudacysta perseae* (Heidemann) (Hemiptera: Tingidae) reveals the source of introduced populations. *Biological Invasions* 14(6): 1079-1100.

USDA/ERS. 2022. Avocados: Production, season-average grower price, and value, by state, 1980/81 to date. United States Department of Agriculture, Economic Research Service, Washington, D.C.

Zug, R., and P. Hammerstein. 2012. Still a host of hosts for *Wolbachia*: analysis of recent data suggests that 40% of terrestrial arthropod species are infected. *PloS one* 7(6): e38544.

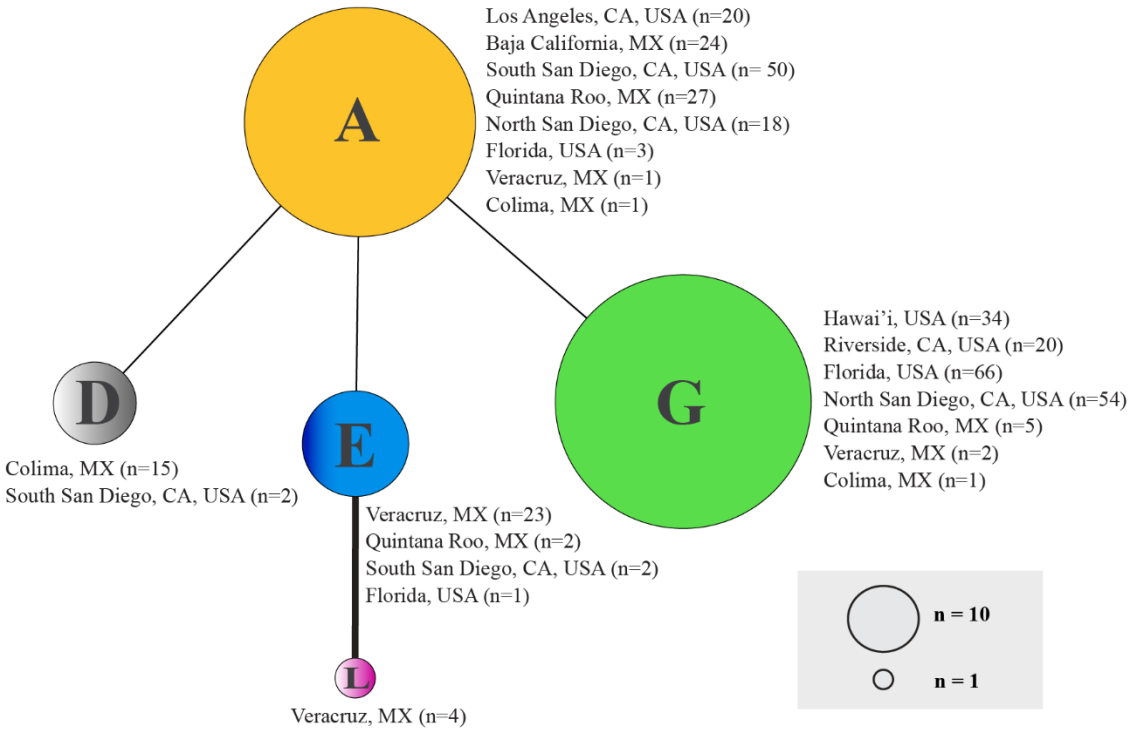

Figure 3.1 Mitochondrial haplotype network for *Pseudacysta perseae* constructed from 375 sequences of the COI gene. Connecting lines indicate single nucleotide substitutions. Connecting line in bold represents a non-synonymous substitution.

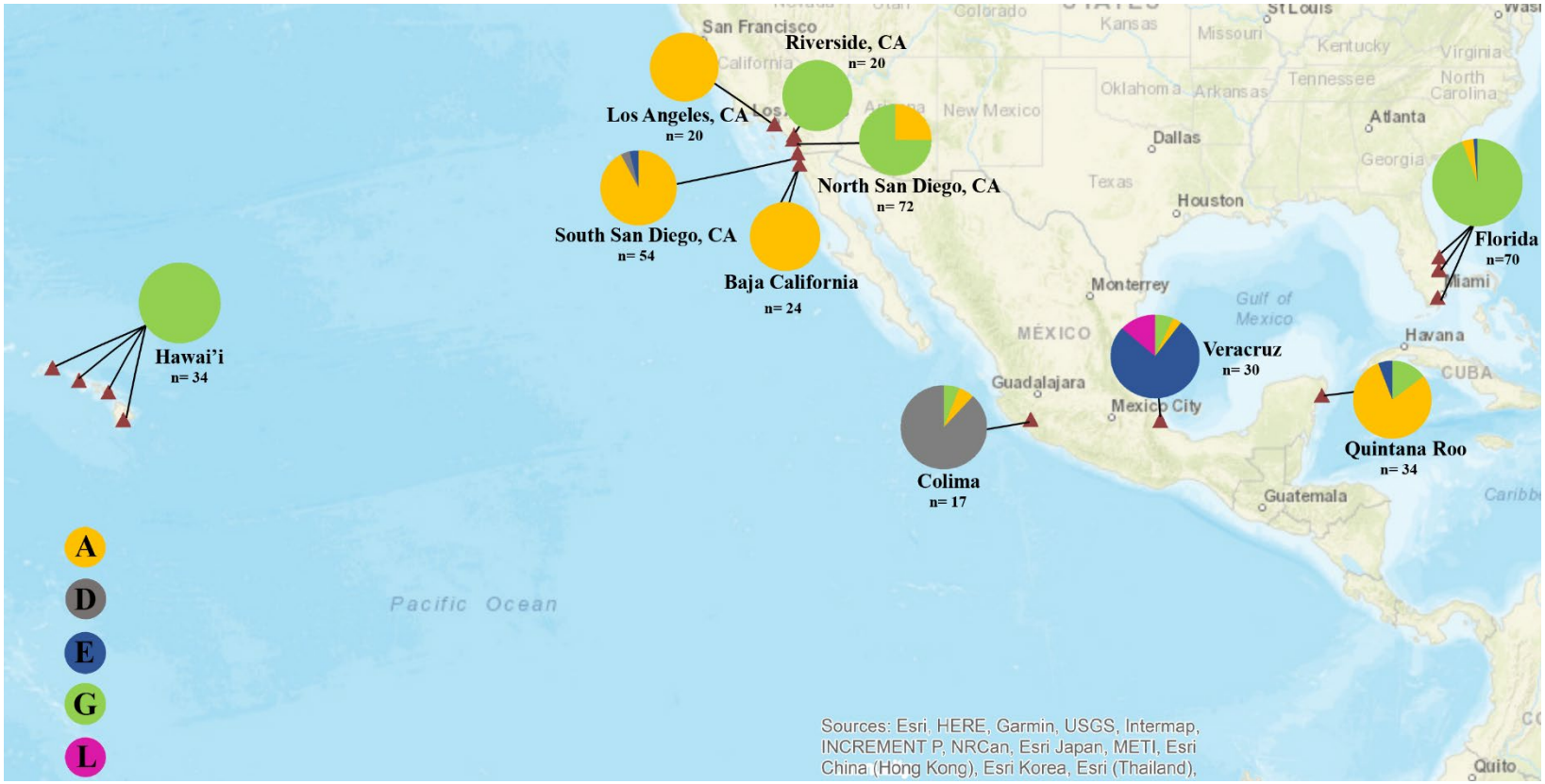

Figure 3.2 Geographic distribution of five haplotypes (A, D, E, G, L) across twenty localities in seven sampled states in the U.S. and Mexico. Each pie chart represents a state or locality. California [southern San Diego County (n=54), northern San Diego County (n=72), Riverside (n=20) and Los Angeles (n=20) Counties]; Florida (n=70); Hawai'i (n=34); Baja California (n=24); Colima (n=17); Veracruz (n=30); Quintana Roo (n=34). For additional collection information see Table 3.1.

Table 3.1 Collection details for specimens of *Pseudacysta perseae* used for molecular analyses.

Ctry.	State	Locality	Seq ID	Cultivar	Spec.	Date	Latitude	Longitude	Elev. (m)	Collector
USA	California	Chula Vista, San Diego	CV	Bacon	18	03-Aug-21	32.64707	-117.0135		M. Hoddle
			SD	-	10	08-Feb-22				
		National City, San Diego	NC	Bacon	12	03-Aug-21	33.274536	-117.26184	90	M. Hoddle
		Encanto Area, San Diego	66S	Bacon	12	03-Aug-21	32.71174	-117.05557		M. Hoddle
		Bonsall, San Diego	BON	Hass	20	07-Dec-17	33.261319	-117.20549	120	M. Hoddle & L. P. Dadlani
			CAM	Hass	8	29-Oct-21	33.264065	-117.16373	205	
			BR	Hass	8	29-Oct-21	33.258775	-117.16359	312	
		Oceanside, San Diego	OCE	Hass	20	09-Oct-17	33.274726	-117.26177	90	M. Hoddle & L. P. Dadlani
			MOR	Hass	8	29-Oct-21	33.285084	-117.26823	152	
			PASO	Hass	8	29-Oct-21	33.2793491	-117.25014	122	
		Temecula, Riverside	TEM	Hass	20	09-Oct-17	33.455552	-117.22676	364	M. Hoddle
		Los Angeles	LA	Fuerte	20	06-Ju l-18	33.997381	-118.3258	43	M. Hoddle
	Hawai'i	Oahu	OaPc5	Hass	2	16-Jul-21	21.394104	-157.97772		J. N. Matsunaga & J. Ocenar
			OaPo	Greengold	4	16-Jul-21	21.542274	-158.08854		
			OaWa	Chang	10	16-Jul-21	21.334982	-157.71208		
		Kauai	KaMo	-	4	28-Jul-21	22.182196	-159.33313		E. J. Garcia
		Hawai'i	HaKu	Otani	3	02-Aug-21	19.59362	-155.05542		S. Chun
			HaWa	McDonald	4	02-Aug-21	19.64702	-155.08034		
		Maui	MaLa	Murashige	3	02-Aug-21	20.905245	-156.68497		M. Fukada & A. Fleming
			MaPu	Malama	4	02-Aug-21	20.79648	-156.36727		
	Florida	Miami-Dade Co.	Si	Simmonds	9	26-Jan-22				D. Carrillo
			Don	Donnie	3	26-Jan-22				
			Mig	Miguel	4	26-Jan-22				
			Mon	Monroe	11	26-Jan-22				
			EG	Donnie	3	26-Jan-22				
			Buck	Buck 3	3	26-Jan-22				

Ctry.	State	Locality	Seq ID	Cultivar	Spec.	Date	Latitude	Longitude	Elev. (m)	Collector
			Sand	Donnie	2	26-Jan-22				
			AG	Donnie	5	26-Jan-22				
			BTG	Donnie	8	26-Jan-22				
		Fort Pierce, St. Lucie Co.	FL1	-	8	31-May-23	27.4330104	-80.41811	8	M. Hoddle
			FL2	-	6	31-May-23	27.4330104	-80.41811	8	
		Vero Beach, Indian River	FL3	-	10	01-Jun-23	27.6387163	-80.39754	6	M. Hoddle
Mexico (West)	Baja California	Ensenada	B1	-	6	01-Aug-23	31.87459	-116.62478	27	M. Hoddle
			B2	-	6	01-Aug-23	31.87459	-116.62478	27	
		Tijuana	B3	-	6	02-Aug-23	32.51357	-117.09731	162	M. Hoddle
			B4	-	6	02-Aug-23	32.51357	-117.09731	162	
	Colima	Coquimatlana	Col13	Non-Hass	1	25-Jul-22	19.21122	-103.8056	368	M. Hoddle
		Comala	Col12	Non-Hass	3	26-Jul-22	19.37593	-103.7168	1035	M. Hoddle
			Col12	Non-Hass	13	26-Jul-22	19.41002	-103.69601	1260	
Mexico (East)	Quintana Roo	Playa del Carmen	H12	Non-Hass	11	13-Jun-22	20.63515	-87.0814	23	M. Hoddle
			H13	Non-Hass	7	13-Jun-22	20.63515	-87.0814	23	
			H14	Non-Hass	10	13-Jun-22	20.63326	-87.0892	22	
			H15	Non-Hass	6	13-Jun-22	20.64313	-87.09499	20	
	Veracruz	La Antigua	H10	Non-Hass	15	03-Jun-22	19.32309	-96.32076	10	M. Hoddle
			H11	Non-Hass	15	03-Jun-22	19.32145	-96.32047	14	

Spec., number of DNA source specimens of *P. perseae*; Cultivar, avocado host cultivar; Elev., Elevation (in meters [m])

Table 3.2 Average hourly temperature parameters utilized in climate-controlled cabinets for rearing *Pseudacysta perseae* at a fluctuating average temperature that averaged 25°C over a 24-hour period.

Hour	25°C Mean	Photoperiod
1:00 AM	19.5	Dark
2:00 AM	19.2	
3:00 AM	18.8	
4:00 AM	18.4	
5:00 AM	18.0	
6:00 AM	17.8	Light
7:00 AM	19.2	
8:00 AM	21.5	
9:00 AM	24.6	
10:00 AM	28.0	
11:00 AM	30.6	
12:00 PM	32.8	
1:00 PM	33.9	
2:00 PM	33.6	
3:00 PM	32.6	
4:00 PM	31.5	
5:00 PM	30.0	
6:00 PM	28.2	
7:00 PM	26.0	
8:00 PM	23.8	Dark
9:00 PM	22.9	
10:00 PM	22.0	
11:00 PM	21.3	
12:00 AM	20.4	

Table 3.3 Haplotype distribution and genetic diversity, and GenBank accessions for COI and *Wolbachia*, *wsp* sampled populations grouped according to geographical origin (2 countries, 7 states and 20 localities).

Ctry.	State	Locality	N COI	h	Haplotype dist.	Hd	π	*N wsp*	% *wsp* infection	GENBANK ACC. COI	*wsp*
USA	California	Chula Vista, S SD	28	3	A(24) D(2) E(2)	0.26455	0.00053	A(2) D(1) E(1)	A(0) D(100) E(100)	PP188058-PP188060	PP278551-PP278553
		National City, S SD	12	1	A(12)	0	0	1	100	PP188062	PP278554
		Encanto Area, S SD	12	1	A(12)	0	0	2	0	PP188061	PP278555
		Bonsall, N SD	36	1	G(36)	0	0	2	100	PP188063-PP188064	PP278556
		Oceanside, N SD	36	2	G(18) A(18)	0.51429	0.001	G(3) A(8)	G(100) A(0)	PP188065-PP188067	PP278557-PP278558
		Riverside	20	1	G(20)	0	0	10	100	PP188068	PP278559
		Los Angeles	20	1	A(20)	0	0	20	95	PP188069	PP278560
	Hawai'i	Oahu	16	1	G(16)	0	0	1	100	PP188070	PP278561
		Kauai	4	1	G(4)	0	0	1	100	PP188071	PP278564
		Hawai'i	7	1	G(7)	0	0	1	100	PP188072	PP278563
		Maui	7	1	G(7)	0	0	1	100	PP188073	PP278562
	Florida	Miami-Dade Co.	48	3	G(44) A(3) E(1)	0.15869	0.00038	G(3) A(2) E(1)	G(100) A(100) E(100)	PP188074-PP188076	PP278565-PP278567
		St. Lucie Co.	14	1	G(14)	0	0	1	100	PP188077	PP278568
		Indian River Co.	10	1	G(10)	0	0	1	100	PP188078	PP278569
MX (W)	Baja California	Ensenada	12	1	A(12)	0	0	1	100	PP188079	PP278570
		Tijuana	12	1	A(12)	0	0	1	100	PP188080	PP278571
	Colima	Coquimatlna	1	1	D(1)	0	0	1	100	PP188081	PP278572
		Comala	16	3	D(14) A(1) G(1)	0.24167	0.0007	D(2) A(1) G(1)	D(100) A(100) G(100)	PP188082-PP188084	PP278573-PP278575
MX (E)	Quintana Roo	Playa del Carmen	34	3	A(27) G(5) E(2)	0.35472	0.00072	A(2) G(1) E(1)	A(100) G(100) E(100)	PP188085-PP188087	PP278576-PP278578
	Veracruz	La Antigua	30	4	E(23) L(4) G(2) A(1)	0.4023	0.00108	E(2) L(1) G(1) A(1)	E(100) L(100) G(100) A(100)	PP188088-PP188091	PP278579-PP278582

N COI, number of individuals sampled for COI; h, number of haplotypes; Hd, haplotype diversity; π, nucleotide diversity; N *wsp*, number of individuals sampled for *wsp*

Table 3.4 Geographic Distribution of ten *Pseudacysta perseae* haplotypes.

Country	State	Locality	HAPLOTYPE									
			A	**B**	**C**	**D**	**E**	**F**	**G**	**H**	**I**	**L**
North America	California	South San Diego Co.	✓			✓	✓					
		North San Diego Co.	✓						✓			
		Riverside Co.							✓			
		Los Angeles Co.	✓									
	Florida	Miami-Dade Co., St. Lucie Co., Indian River Co.	✓				✓		✓			
	Hawai'i	Oahu, Kauai, Hawai'i, Maui							✓			
	Texas	Weslaco	✓									
	Caribbean	Dominican Republic, Jamaica, Puerto Rico, St. Thomas, St. John, St. Lucia, St. Kitts							✓			
Mexico (West)	Baja California	Ensenada, Tijuana	✓									
	Colima	Coquimatlana, Comala, Manzanillo, Puertocita de Lajas	✓			✓			✓	✓		
	Michoacan	Cuamio, Las Penas	✓			✓					✓	
	Nayarit	Las Vivosas, San Blas, Xalisco	✓			✓		✓				
	Jalisco	Puerto Vallarta	✓	✓		✓						
	Guerrero	Tierra Colorada	✓									
	Guanajuato	Guanajuato									✓	
Mexico (East)	Quintana Roo	Playa del Carmen	✓				✓		✓			
	Veracruz	La Antigua, Jaltipan, La Tinaja	✓		✓	✓	✓		✓			✓
	Yucatan	Oxkutcab, Hunucma, Merida							✓			
	Tabasco	La Venta	✓									
	Chiapas	Palenque	✓									
Central America	Guatemala	Santa Maria, Escuintla				✓						
South America	French Guyana								✓			

Table 3.5 Parameters assessed in the Intra-Haplotype and Inter-Haplotype Crossing-Mating Experiments.

Cross	N F_0	% F0 Fertil.	F_1 Eggs Laid (SE)	% F_1 Hatch Rate (SE)	% F_1 Adults	N F_1	% F_1 Fertil.	F_2 Eggs Laid (SE)	% F_2 Hatch Rate	% F_2 Adults
G_M x G_F	10	100	50 (4.86) ** b	16.8 (1.9) a	92.86 (2.94) a	8	100	50.88 (3.88) * b	20.15 (2.59)	97.56 (2.27) a
A_M x A_F	10	100	32.6 (1.66) a	17.79 (2.43) a	98.28 (2.5) a	8	100	32.38 (1.36) a	22.39 (1.62)	100 (0) a
A_M x G_F	10	100	43.6 (5.22) ab	12.16 (4.66) * a	88.68 (2.98) a	8	100	35.25 (4.35) a	32.62 (4.78) **	98.91 (0.9) a
G_M x A_F	10	100	30.6 (2.64) a	14.05 (3.23) a	88.37 (10.5) a	8	87.5	27.62 (2.51) a	39.37 (8.69) ***	98.85 (1.2) a

G = Haplotype G (Oceanside, north San Diego County); A = Haplotype A (Chula Vista, south San Diego County); M = male, F = female; N = number of mating pair replicates; % F_0 and % F_1 Fertility represent the proportion of F_0 and F_1 mating pairs laying fertile eggs; % F_1 and % F_2 Adults represent the proportion of F_1 and F_2 progeny reaching adult stage

Eggs laid, % Hatch Rate, and % Adults of F_1 and F_2 generations are reported as means (± SE); Statistically significant differences denoted by letters from post hoc analysis.

*P < 0.05, **P < 0.01, ***P < 0.001